

N
P
**JOURNAL
OF
FOOD
PROCESS
ENGINEERING**

**D.R. HELDMAN
and
R.P. SINGH
COEDITORS**

**FOOD & NUTRITION
PRESS, INC.**

VOLUME 18, NUMBER 4

QUARTERLY

Annual
Index
Vol. 18(4)
1995

JOURNAL OF FOOD PROCESS ENGINEERING

Editor: **D.R. HELDMAN**, Food Science/Engineering Unit, University of Missouri, Columbia, Missouri
R.P. SINGH, Agricultural Engineering Department, University of California, Davis, California

Editorial

Board: **M.O. BALABAN**, Gainesville, Florida (1996)
S. BRUIN, Vlaardingen, The Netherlands (1995)
M. CHERYAN, Urbana, Illinois (1996)
J.P. CLARK, Chicago, Illinois (1995)
A. CLELAND, Palmerston North, New Zealand (1995)
K.H. HSU, E. Hanover, New Jersey (1996)
J.L. KOKINI, New Brunswick, New Jersey (1996)
E.R. KOLBE, Corvallis, Oregon (1996)
J. KROCHTA, Davis, California (1995)
L. LEVINE, Plymouth, Minnesota (1996)
S. MULVANEY, Ithaca, New York (1996)
M.A. RAO, Geneva, New York (1995)
S.S.H. RIZVI, Ithaca, New York (1995)
E. ROTSTEIN, Minneapolis, Minnesota (1995)
T. RUMSEY, Davis, California (1995)
S.K. SASTRY, Columbus, Ohio (1995)
J.F. STEFFE, East Lansing, Michigan (1995)
K.R. SWARTZEL, Raleigh, North Carolina (1995)
A.A. TEIXEIRA, Gainesville, Florida (1995)
G.R. THORPE, Victoria, Australia (1995)
H. WEISSER, Freising-Weihenstephan, Germany (1995)

All articles for publication and inquiries regarding publication should be sent to DR. D.R. HELDMAN, COEDITOR, *Journal of Food Process Engineering*, Food Science/Engineering Unit, University of Missouri-Columbia, 235 Agricultural/Engineering Bldg., Columbia, MO 65211 USA; or DR. R.P. SINGH, COEDITOR, *Journal of Food Process Engineering*, University of California, Davis, Department of Agricultural Engineering, Davis, CA 95616 USA.

All subscriptions and inquiries regarding subscriptions should be sent to Food & Nutrition Press, Inc., 6527 Main Street, P.O. Box 374, Trumbull, CT 06611 USA.

One volume of four issues will be published annually. The price for Volume 18 is \$142.00, which includes postage to U.S., Canada, and Mexico. Subscriptions to other countries are \$162.00 per year via surface mail, and \$173.00 per year via airmail.

Subscriptions for individuals for their own personal use are \$112.00 for Volume 18, which includes postage to U.S., Canada and Mexico. Personal subscriptions to other countries are \$132.00 per year via surface mail, and \$143.00 per year via airmail. Subscriptions for individuals should be sent directly to the publisher and marked for personal use.

The *Journal of Food Process Engineering* (ISSN:0145-8876) is published quarterly (March, June, September and December) by Food & Nutrition Press, Inc.—Office of Publication is 6527 Main Street, P.O. Box 374, Trumbull, Connecticut 06611 USA. Current issue is December 1995.

Second class postage paid at Bridgeport, CT 06602.

POSTMASTER: Send address changes to Food & Nutrition Press, Inc., 6527 Main Street, P.O. Box 374, Trumbull, Connecticut 06611 USA.

JOURNAL OF FOOD PROCESS ENGINEERING

JOURNAL OF FOOD PROCESS ENGINEERING

Editor: **D.R. HELDMAN**, Food Science/Engineering Unit, University of Missouri, Columbia, Missouri
R.P. SINGH, Agricultural Engineering Department, University of California, Davis, California

Editorial Board:

M.O. BALABAN, Department of Food Science and Human Nutrition, University of Florida, Gainesville, Florida
S. BRUIN, Unilever Research Laboratory, Vlaardingen, The Netherlands
M. CHERYAN, Department of Food Science, University of Illinois, Urbana, Illinois
J.P. CLARK, Epstein Process Engineering, Inc., Chicago, Illinois
A. CLELAND, Department of Biotechnology, Massey University, Palmerston North, New Zealand
K.H. HSU, RJR Nabisco, Inc., E. Hanover, New Jersey
J.L. KOKINI, Department of Food Science, Rutgers University, New Brunswick, New Jersey
E.R. KOLBE, Department of Bioresource Engineering, Oregon State University, Corvallis, Oregon
J. KROCHTA, Agricultural Engineering Department, University of California, Davis, California
L. LEVINE, Leon Levine & Associates, Plymouth, Minnesota
S. MULVANEY, Department of Food Science, Cornell University, Ithaca, New York
M.A. RAO, Department of Food Science and Technology, Institute for Food Science, New York State Agricultural Experiment Station, Geneva, New York
S.S.H. RIZVI, Department of Food Science, Cornell University, Ithaca, New York
E. ROTSTEIN, The Pillsbury Co., Minneapolis, Minnesota
T. RUMSEY, Agricultural Engineering Department, University of California, Davis, California
S.K. SASTRY, Agricultural Engineering Department, Ohio State University, Columbus, Ohio
J.F. STEFFE, Department of Agricultural Engineering, Michigan State University, East Lansing, Michigan
K.R. SWARTZEL, Department of Food Science, North Carolina State University, Raleigh, North Carolina
A.A. TEIXEIRA, Agricultural Engineering Department, University of Florida, Gainesville, Florida
G.R. THORPE, Department of Civil and Building Engineering, Victoria University of Technology, Melbourne, Victoria, Australia
H. WEISSER, University of Munich, Inst. of Brewery Plant and Food Packaging, Freising-Weihenstephan, Germany

Journal of FOOD PROCESS ENGINEERING

**VOLUME 18
NUMBER 4**

**Coeditors: D.R. HELDMAN
R.P. SINGH**

**FOOD & NUTRITION PRESS, INC.
TRUMBULL, CONNECTICUT 06611 USA**

© Copyright 1996 by
Food & Nutrition Press, Inc.
Trumbull, Connecticut 06611 USA

All rights reserved. No part of this publication may be reproduced, stored in a retrieval system or transmitted in any form or by any means: electronic, electrostatic, magnetic tape, mechanical, photocopying, recording or otherwise, without permission in writing from the publisher.

ISSN 0145-8876

Printed in the United States of America

CONTENTS

Characterization of Single Particle Tube-Flow Behavior at Elevated Temperatures S. GRABOWSKI and H.S. RAMASWAMY	343
Residence Time Distribution of Cylindrical Particles in a Curved Section of a Holding Tube: The Effect of Particle Size and Flow Rate S. SALENGKE and S.K. SASTRY	363
Method for Measuring CO ₂ Absorption in CO ₂ and N ₂ Packaged Fresh Meat Y. ZHAO and J.H. WELLS	383
Modeling the Power Consumption During Sheeting of Doughs for Traditional Indian Foods C.V. RAGHAVAN, N. CHAND, R.S. BABU and P.N.S. RAO	397
Effect of Plasticizer Level and Temperature on Water Vapor Transmission of Cellulose-Based Edible Films M.S. CHINNAN and H.J. PARK	417
Heat Transfer to and Transport Properties of Wheat Gluten in a Tubular Reactor T.D. STRECKER, R.P. CAVALIERI and R. ZOLLARS . . .	431
Author Index	449
Subject Index	453

CHARACTERIZATION OF SINGLE PARTICLE TUBE-FLOW BEHAVIOR AT ELEVATED TEMPERATURES

S. GRABOWSKI¹ and H.S. RAMASWAMY²

*Department of Food Science and Agricultural Chemistry
Macdonald Campus of McGill University, Box 187
Ste Anne de Bellevue, PQ, H9X 3V9
Canada*

Accepted for Publication September 30, 1994

ABSTRACT

The single particle flow behavior of food (carrot, parsnip and potato cubes) and Nylon spheres was investigated in simulated holding tubes at different temperatures under pressurized (110C) and nonpressurized (80 and 100C) flow conditions using different carrier fluids (water and 2, 3 and 4% starch suspensions). It was found that the particle to fluid velocity ratio (u_p/u) was a function of carrier fluid effective viscosity, temperature and flow rate, and particle relative size, density and shape. The maximum value of u_p/u ranged from 0.4-1.9 which increased almost linearly with temperature showing no specific deviations in the flow behavior of particles as conditions changed from the nonpressurized (< 100C) to pressurized (110C) flow. In dimensionless form, the particle to fluid velocity ratio (mean and maximum) as well as particle Reynolds number were found to be functions of generalized fluid Reynolds number, particle Archimedes number, particle to tube diameter ratio and particle sphericity.

INTRODUCTION

Aseptic processing of low acid liquid foods containing solid particles is currently being evaluated with considerable interest following its success with liquid foods. Two main parameters viewed as critical for such a process are: particle residence time distribution and a conservative value of heat transfer coefficient (h_p) between the liquid and particle. Both these depend on the flow behavior of the fluid characterized usually by its Reynolds number. For example, the widely utilized Froessling equation (Eq. 1) or several of its modifications (presented recently by Maesmans *et al.* 1992; Sastry 1992, 1993; Zuritz *et al.* 1990) contain Reynolds number (Re_p) defined for a single particle with the velocity term used in the form u_p-u (relative velocity) instead than u_p :

¹ On Leave from Dept. of Chemical Engineering, Lodz Technical University, Lodz, Poland.

² To whom correspondence should be addressed.

$$\text{Nu} = 2 + 0.6 \text{Re}_r^{0.5} \text{Pr}^{0.5} \quad (1)$$

Data available for the flow behavior of particulate liquid foods in aseptic processing system (contrary to the minerals, grains or chemicals in hydrotransport) are not consistent and, especially under pressurized processing conditions, no accurate informations for holding tube flow exist in the literature.

In light of above, the specific objectives of the present study were: (1) to investigate the effect of different parameters (flow rate, temperature, density and viscosity of the fluid, size, shape and density of particles and holding tube diameter) on mean and maximum velocity of solid food particles in a holding tube, and (2) to answer the question if the transition from nonpressurized to pressurized flow conditions changes the two-phase flow behavior in the holding tube. The study was undertaken using the particles introduced one at a time (single particle flow behavior) in order to avoid uncertainty related to particle to particle interactions while assessing the influence of potential factors. Particle to particle interactions can only be expected to reduce the maximum velocity of the fastest traveling particle (small or big). Thus, processes established based on the maximum velocity derived from single particles would generally be conservative and desirable from the view point of aseptic processing.

Literature Review

The majority of fluid foods contain several constituents, solid or semi-solid particles, agglomerate, etc., dispersed in a liquid which forms a continuous phase. Considering the full spectrum of particle sizes, the following general characteristics of the two-phase flow behavior have been recognized (Bain and Bonnington 1970; Govier and Aziz 1972; Jacobs 1991):

- (1) Ultrafine particles ($d_p < 40 \mu\text{m}$) which are almost always carried in a fully suspended, homogeneous state without any gravitational effects.
- (2) Fine particles ($40 < d_p < 150 \mu\text{m}$) which are usually carried in a fully suspended state with uniform solid concentration distribution across the tube (pseudo-homogenous state), but sometimes concentration gradients due to gravitational effect may be encountered.
- (3) Medium-sized particles ($0.15 < d_p < 1.5 \text{ mm}$) which may form a heterogeneous type of mixture resulting in solid concentration gradients over the depth of the tube while some particles may be sliding along the bed. A fully suspended type of flow may be expected for particles when particle densities are relatively close to the density of fluid.
- (4) Coarse particles ($d_p > 1.5 \text{ mm}$) which are seldom fully suspended (unless they are very light or the fluid is flowing very fast) often leading to stratification of particles.

Particulate liquid foods may contain particles of different type, size and shape. As follows from the above classification, the solid particles of group 1 to 3 move within the liquid as a single phase. The prevailing heat transfer mechanism in this case will be conduction of heat from the liquid to solid particles. The movement of larger solid particles (group 4) has been considered to be critical in designing of aseptic processing. From public health safety point of view, the minimal lethality criterion is established with respect to the fastest moving large (often the largest) particle. The prevailing heat transfer mechanism in this case is convection from carrier fluid to food particle.

The relative velocity between the fluid and particle depends on several parameters. Generalized differential equations describing the flow of solid particles in a liquid stream has been given much attention in the fluid mechanics involving mineral slurries (Lawler and Lu 1971; Smoldyrev 1982; Darby 1986; Shook and Roco 1991). Basic theory of this phenomena was developed for hydro- and pneumo-transport of different solid materials, mostly minerals. With reference to the aseptic processing, Sastry and Zuritz (1987) developed a mathematical model for prediction of single particle trajectories and velocities in holding tube flow. The authors concluded that the model was capable of providing some qualitative understanding of the phenomena and it remains to be verified quantitatively. More recently, Dutta and Sastry (1990a,b) made a detailed analysis of the flow of solid particles in a model holding tube. The authors analyzed two situations: particle initially at the pipe center and particle initially at the tube bottom. Because of the complicated flow pattern in comparison to the simplified mathematical description, they found that their simulation described some of the trends observed only in a qualitative way. In the light of poor agreement between mathematical models and experimental results, extrapolation of the results may not be valid.

Experimental results of particle to liquid relative velocity or particle residence time distribution (RTD) have been presented in several publications (Chandarana 1992; Ramaswamy *et al.* 1992; Sancho and Rao 1992; Singh and Lee 1992; Yang and Swartzel 1991 and 1992; Sastry 1993; Abdelrahim *et al.* 1993). The results of these studies generally indicate that the major factors influencing particle velocity in a stream of the carrier fluid are: viscosity, temperature and flow rate of the liquid, relative (particle to fluid) density of solids, relative (particle to tube) particle size, particle shape and concentration of the solid phase in the fluid.

Some regression equations describing the above relationships have been published. For example, Dutta and Sastry (1990a) proposed the following experimental regression equation for mean particle velocity ratio (polystyrene spheres in CMC solutions):

$$u_p/u = 0.748 + 0.0136 Fr_p' + 6.725 \mu_{nd} + 0.392 Fr_p' \mu_{nd} \quad (2)$$

The authors found that the particle to fluid velocity ratio was a stronger function of nondimensional viscosity μ_{nd} than the particle Froude number Fr_p' . More recently, Yang and Swartzel (1992) obtained the following empirical equation for mean particle velocity ratio:

$$u_p/u = 0.5 Fr_p'^{0.11} \quad (3)$$

and Eq.(4) for the maximum particle velocity ratio:

$$u_{p \max}/u = 0.4 Fr_p'^{0.14} \quad (4)$$

Equation (3) is similar to that proposed by Zhang *et al.* (1993):

$$u_p/u = Fr_p'^{0.5}/(0.462 Fr_p'^{0.5} + 0.219) - 0.969 \quad (5)$$

and Okuda (1981):

$$u_p/u = 1 - \exp[-a (d_p/D)Fr_p'^{0.5} + b] \quad (6)$$

Equations 3-6 emphasize the importance of density effect on velocity ratio only. As follows from our previous studies on incipient (start-up) velocity (Grabowski and Ramaswamy 1995), the viscosity of the carrier fluid strongly damped the density effect. For low viscosity fluids, the predominant factor was density ratio, while for high viscosity fluids it was viscosity.

MATERIALS AND METHODS

A recirculating fluid flow system (Fig. 1) was designed and built (Ramaswamy *et al.* 1992) which consisted of exchangeable 1.25 m long Pyrex tube (internal diameters of 29.5, 41.2 or 54.6 mm), a feed tank (steam kettle), variable speed pump, flow meter and a specially designed by-pass system for particle injection. In accordance with FDA regulations, the model holding tube was inclined upwards at an angle of 1.19°.

The carrier fluid used in the studies were water and pregelatinized solutions of starch (Therm-flo™, National Starch and Chemical Corp., Bridgewater, NJ) of 2, 3 and 4% concentration. The temperature of fluid was maintained at either 80, 100 and 110C. The starch solutions were prepared by heating the suspension by recirculating in the system for 90 min at approximately 100C for gelatinization and allowing the solution to cool in the kettle for 1 h to set the gel formation. Detailed rheological characteristics of starch were studied and described elsewhere (Abdelrahim *et al.* 1991) from which consistency factor, K and the flow behavior index, n were obtained for 2, 3 and 4% starch at

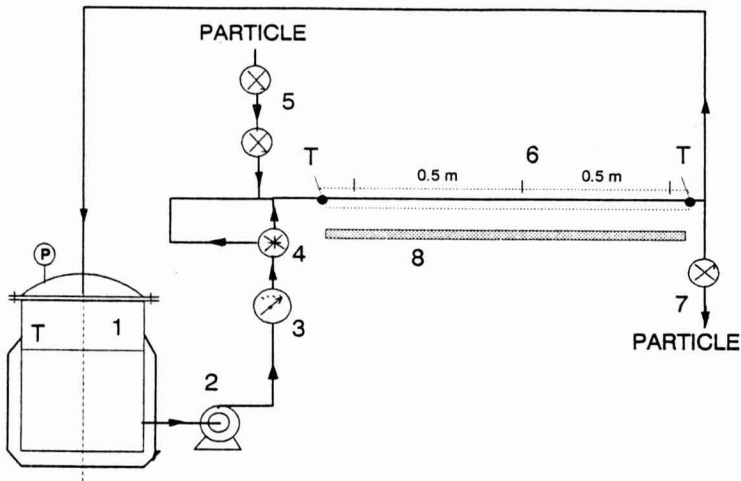


FIG. 1. SCHEMATIC DIAGRAM OF THE EXPERIMENTAL SET-UP

- 1-Steam kettle, 2-Variable-speed pump, 3-Flowmeter, 4-3-Way valve of by-pass system, 5-Port for particle entry, 6-Glass holding tube, 7-Port for particle exit, 8-Source of the light, T-Thermocouple locations and P-pressure gauge.

temperatures of 80, 100 and 110C. The apparent viscosity of the solution was also measured before and after each test at 20C as a ratio of shear stress and shear rate (100 s^{-1}) using a Haake RV-20 rotational viscometer (Haake, Germany). It was noted that during the experiments the apparent viscosity of starch solution remained unchanged up to about 3 h of circulation in the system. After this time, a fresh starch solution was used.

Food particles used in this study were carrot, parsnip and potato cubes (density 1020 ± 25 , 980 ± 20 and $1080 \pm 25 \text{ kg/m}^3$, respectively) of 3 different sizes. Additionally Nylon (density 1140 kg/m^3) spheres of 4 different diameters were used as model food particles. Details of the experimental parameters are given in Tables 1 and 2.

Experimental Procedure

Vegetables (carrot, parsnip and potato) obtained from a local market were cut using a knife to proper size and blanched for 1 min in boiling water. The carrier fluid was circulated in the system (by-passing the particle entrance port) until a steady condition (preselected flow rate and temperature) was achieved. A single particle was introduced in to the system through the entrance port and by changing the position of the 3-way ball valve, the particle was set to move.

TABLE 1.
MEASUREMENT SYSTEM

No.	Parameter	Symbol	Measurement Equipment	Accuracy
1.	Temperature	T [C]	Thermocouples (T-Type)	0.1C
2.	Flow Rate	V [m ³ /s]	1) OMEGA FTB 4015-Flowmeter 2) Direct measurement (Volume/Time)	1% 1%
3.	Time	t [s]	Direct measurement	0.1 s
4.	Effective Viscosity	η [Pas]	HAAKE RV-20 (MSOSC-head & MV1-rotor)	1%

TABLE 2.
RANGE OF EXPERIMENTS

No.	Parameter	Symbol	Experimental Range
1.	Temperature	T	80, 100 and 110 degC
2.	Pressure	P	10 ⁵ - 1.43 10 ⁵ Pa
3.	Diameter of holding tube	D	0.0546, 0.0413 and 0.0295 m
4.	Carrier fluid		Water Starch Solution 2, 3 & 4%
5.	Particle size		
	Nylon Spheres (density 1140 kg/m ³)	d_p	0.019, 0.0127, 0.00953 & 0.00635 m
	Food particles: cubes	1	carrot, parsnip, potato 1 = 0.0127, 0.01 and 0.0076 m
6.	Tube inclination	β	upwards 1.19°
7.	Tube flow Reynolds number GRe		0 - 30,000

Prior to movement, the particles remained at the bottom of the tube except for parsnip, the radial position of which depended on the type of fluid used (generally on the top with water and randomly distributed when using starch solution). On the transparent glass tube, three marks were made to give two consecutive 0.5 m traveling distances (at 0.1, 0.6 and 1.1 m from the entrance side of the glass tube). The first, second and the third marks represented a distance of about 0.3, 0.8 and 1.3 m, respectively, from the entrance port. The time taken for the particle to travel 0.50 and 1.0 m in the glass tube were measured visually (under brightly illuminated conditions) with the aid of a stopwatch. For each test condition, the measurements were repeated a minimum of 10 times to get the maximum and mean velocities as well as standard deviations (STD) in particle velocities. Generally, the time taken by the particles for traveling the total 1.0 m distance was about twice that for traveling the first 0.5 m which indicated the entrance effect to be negligible.

Density of vegetables was determined before and after blanching using a volume displacement technique. Generally, blanching increased the density by about 10-20 kg/m³ for each type of vegetable tested.

Dimensionless Correlations

As a first step in the interpretation of our experimental results, an analysis was made to determine the nature of relationship between the relative particle to fluid velocity ratio and some dimensionless numbers describing the flow system. Considering the theory of similarity for an analogous case (Smoldyrev 1982), the relative particle velocity ratio was evaluated as a function of the following dimensionless numbers:

- (1) tube flow Reynolds number, Re ,
- (2) tube flow Froude number, Fr ,
- (3) particle Archimedes number, Ar_p ,
- (4) dimensionless particle size, (d_p/D) and,
- (5) sphericity of the particle, Ψ .

These dimensionless variables covered all major parameters influencing the flow of particle in a carrier fluid, i.e., density of the food particle and the fluid (included in Ar_p), viscosity of the carrier fluid (in Re , Ar_p), fluid flow rate (Re , Fr), particle size (d_p/D) , shape of the particle (Ψ), temperature of the mixture (indirect effect on density and viscosity) and velocity profile in the tube (Re). The non-Newtonian character of starch solutions required the use of generalized Reynolds numbers (GRe) with power law effective viscosity defined as follows (Zandi 1971; Harrod 1989):

$$\eta = 2^{(n-3)} K [(3n+1)/n]^n / [u^{(1-n)} D^{(n-1)}] \quad (7)$$

RESULTS AND DISCUSSION

Particle Mean Velocity

A stepwise multiple regression analysis of experimental data (over 500 points, each point an average for a minimum of 10 measurements) on various factors, represented in dimensionless form, indicated that the tube flow Froude number was nonsignificant ($p > 0.05$) in comparison with the other parameters. The following was the best correlation obtained for the particle to fluid mean velocity ratio (u_p/u) ($R^2 = 0.71$):

$$u_p/u = 1.35 \text{ GRe}^{0.2} \text{ Ar}_p^{-0.09} (d_p/D)^{0.6} \Psi^{0.2} \quad (8)$$

The validity of this equation is limited to tube flow Reynolds number up to 30,000, Archimedes number up to 2×10^8 , relative particle size (d_p/D) in range, 0.12-0.65, particle sphericity Ψ in range 0.8-1.0 and density simplex (a) other than zero. Figure 2 shows the comparison of the experimental u_p/u and that calculated using Eq. (8).

Multiplying the dimensionless velocity (u_p/u) by the tube generalized Reynolds number ($\text{GRe} = D u \rho / \eta$) and particle to tube diameter ratio, one can get the particle generalized Reynolds number:

$$(u_p/u) (D u \rho / \eta) (d_p/D) = (u_p d_p \rho) / \eta = \text{GRe}_p \quad (9)$$

Reevaluating the previous correlations using experimental GRe_p as the dependent variable, the following dimensionless equation was obtained for the mean GRe_p :

$$\text{GRe}_p = 1.35 \text{ GRe}^{1.2} \text{ Ar}_p^{-0.09} (d_p/D)^{1.6} \Psi^{0.2} \quad (10)$$

It is important to note that experimental data gave a much better fit ($R^2 = 0.93$) for this relationship than for the previous Eq. (8). This indicates that generalized particle Reynolds number may be a more appropriate dependent variable describing particle flow in the holding tube than the dimensionless particle velocity ratio (u_p/u). Figure 3 shows a comparison of experimental and calculated (Eq. 10) data for GRe_p . There were 2 distinct groups of points: one for water as a carrier fluid, part A, and a second one for starch suspensions, part B.

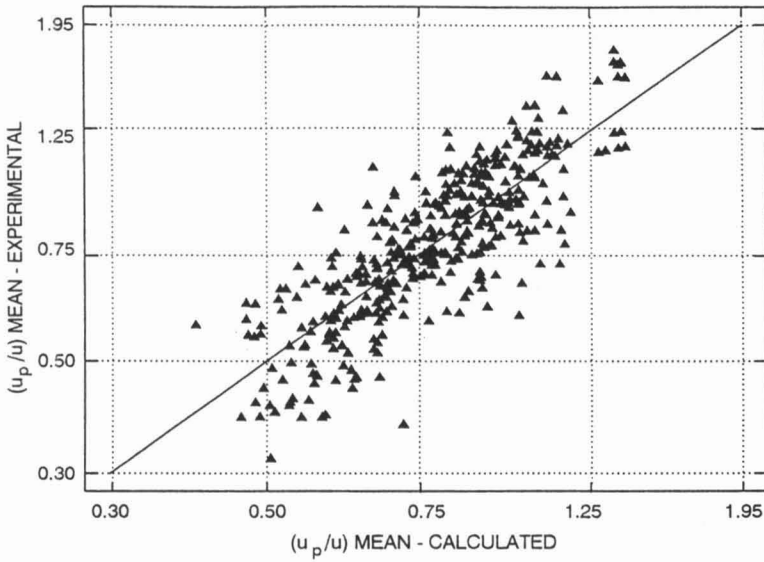


FIG. 2. COMPARISON OF CALCULATED (EQ. 8) AND EXPERIMENTAL MEAN VELOCITY RATIO

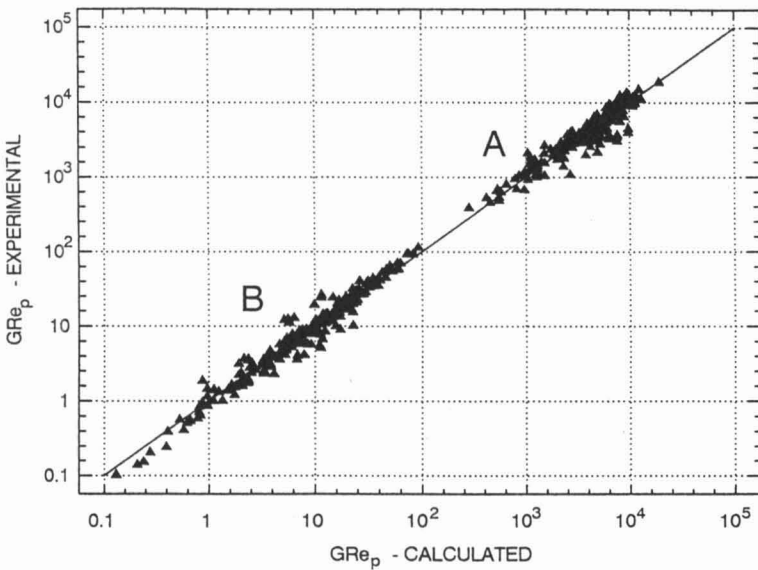


FIG. 3. COMPARISON OF CALCULATED (EQ. 10) AND EXPERIMENTAL PARTICLE Gr_{e_p} DATA

In heat transfer correlations (Eq. 1), the generalized particle Reynolds number, $GR_{e,r}$ based upon difference of particle and fluid velocity ($u_p - u$) is more appropriate. Therefore, the following form of regression equation was also obtained ($R^2 = 0.89$):

$$GR_{e,r} = 0.046 GR_e^{0.75} Ar_p^{0.15} (d_p/D)^{-0.17} \Psi^{1.1} \quad (11)$$

Particle Maximum Velocity

Taking into account the maximum value of particle velocity rather than the mean, the following dimensionless correlation ($R^2 = 0.70$) was obtained by a stepwise multiple regression analysis:

$$U_{p,max}/u = 1.5 GR_e^{0.12} Ar_p^{-0.06} (d_p/D)^{0.33} \Psi^{0.08} \quad (12)$$

Figure 4 shows the relationship between experimental and calculated values of maximum particle relative velocity. Again, transforming ($U_{p,max}/u$) into maximum particle Reynolds number ($GR_{e,p,max}$) as in Eq. (9), a significantly improved regression equation was obtained ($R^2 = 0.87$):

$$GR_{e,p,max} = 1.5 GR_e^{1.12} Ar_p^{-0.06} (d_p/D)^{1.35} \Psi^{0.08} \quad (13)$$

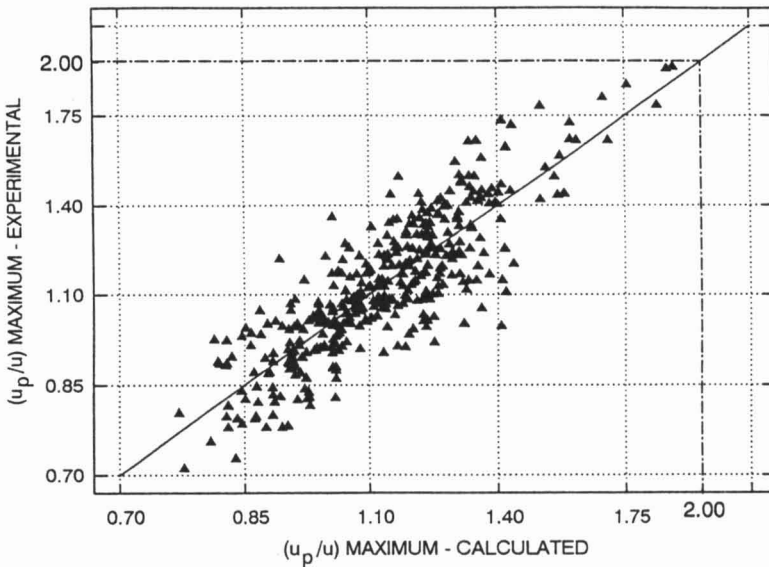


FIG. 4. COMPARISON OF CALCULATED (EQ. 12) AND EXPERIMENTAL MAXIMUM VELOCITY RATIO.

Equations (10)-(13) have the same validity limits as Eq. (8).

Occurring in Eq. (8)-(13), the Archimedes number indicates a special role of drag coefficient during flow of solid/fluid mixture in holding tubes. This has been implicated in the study of settling and fluidization behavior of particles in slurry flow (Smoldyrev 1982; Darby 1986). Considering the results of the present study, Archimedes number appears to be a more useful parameter in correlation of particle flow velocity in holding tube than the more widely used Froude number.

Transition from Nonpressurized to Pressurized Flow

Commercial aseptic processing is carried out under pressurized, high temperature flow conditions, while most literature gathered data deal with the nonpressurized, low temperature conditions with few exceptions (for example, Chandarana *et al.* 1991). In the present study, an attempt has been made to evaluate the temperature effect on the particle flow behavior in the holding tube. Especially for the study of this effect, investigations were extended to lower temperatures of 20, 40 and 60C while the rest of the data were collected in 80, 100 and 110C. Typical relationship between particle to fluid velocity ratio (u_p/u) and temperature is demonstrated in Fig. 5. The figure, as well as the rest of data (for starch suspensions as a carrier fluid), indicated a general linear increase in the velocity ratio with increasing temperatures. Further, the data points represented a smooth continuum with no major deviations during the transition from the nonpressurized to pressurized flow conditions (100C). This suggests that the approach of two-phase nonpressurized flow in holding tube can be extended to pressurized flow simply by taking into consideration the temperature effect which has influence on fluid viscosity and hence the flow behavior. A similar conclusion was presented by Wilson and Brebner (1971) for slurry flow in open channels.

Density and Viscosity Effects

General trends with respect to density and viscosity effects on particle Reynolds number or particle velocity are indicated by Eq. (8)-(11), with the Archimedes number calculated as an absolute value. Results indicate that density and viscosity have a major influence on particle flow characteristics. Similar to the approach suggested by Dutta and Sastry (1990b), the analysis of results was extended to the standard deviation in particle velocities under each conditions tested. Figure 6 shows the distribution of the coefficient of variation in particle velocity ($100 \times \text{STD}/u_p$) as a function of density simplex a , where $a = (\rho_p - \rho)/\rho$, for 2% starch suspension. The distribution showed a characteristic peak in standard deviations at the density simplex equal to zero confirming the existence of generally randomized flow under such flow conditions. The behavior was

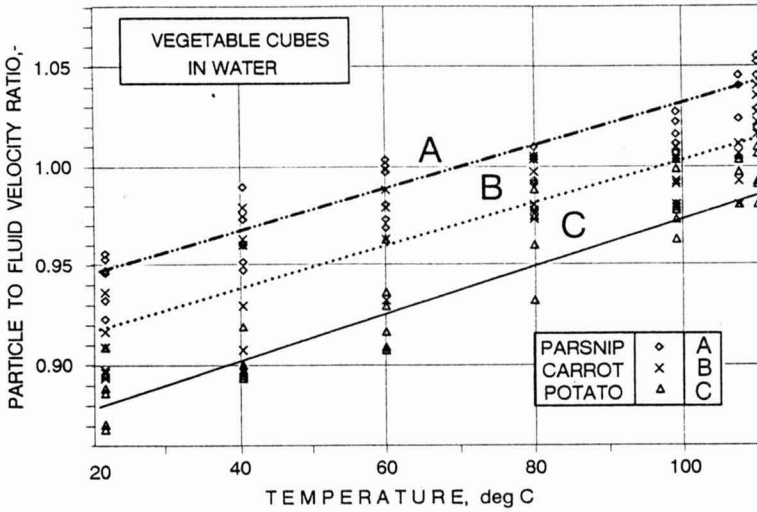
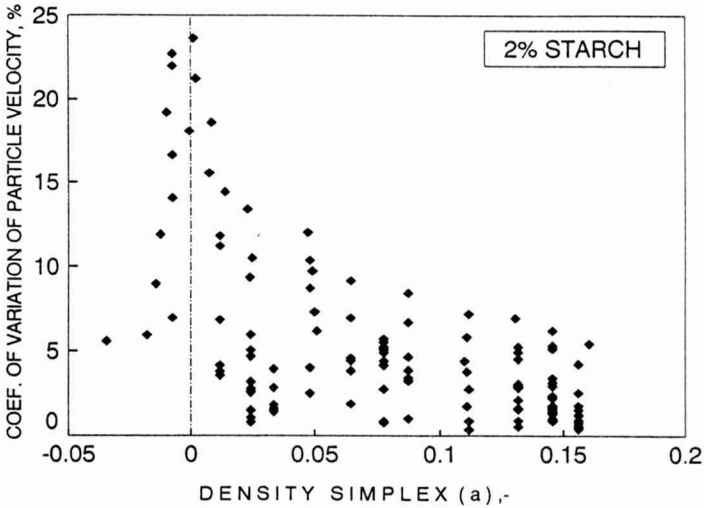


FIG. 5. TEMPERATURE EFFECT ON THE RELATIVE PARTICLE VELOCITY OF VEGETABLE CUBES IN WATER STREAM



1. COEFFICIENT OF VARIATION IN PARTICLE VELOCITY AS INFLUENCED BY DENSITY SIMPLEX (a) FOR 2% STARCH SOLUTION

typical for all carrier fluids tested (water and 2, 3 and 4% starch solutions) as shown in Fig. 7. The coefficient of variation generally reached a maximum at $a = 0$. It also increased with the starch concentration (i.e. with viscosity of carrier fluid). For 4% starch suspension and density simplex $a = 0$ (parsnip cubes), the coefficient of variation was as high as 45%. Such large variations in particle velocities make their evaluation less precise. Hence, when density of particles is nearly equal to density of carrier fluid, it would be better to assume the velocity of the fastest particle to be equal to the maximum fluid velocity in the tube flow profile (usually along the axis of the tube) rather than rely on experimental data. For laminar flow conditions, the assumption for the particle to liquid velocity ratio (u_{pmax}/u) equal to 2 appears to be reasonable. The maximum value of the velocity ratio of parsnip cubes to carrier fluid found in this study was 1.92 (at density simplex, a , close to zero and starch concentration = 4%) while the minimum was 0.4.

Effect of Flow Rate

Increasing the flow rate of the carrier fluid results in an increase in the particle to carrier fluid velocity ratio (u_p/u). This trend is directly evident from Eq. (8)-(11) with typical data shown in Fig. 8. Such an effect could result from differences in the fluid flow velocity profile in the holding tube leading toward turbulence as the fluid flow rate increased. Similar trends in experimental data have been reported in other studies (Ramaswamy *et al.* 1992; Dutta and Sastry 1990b).

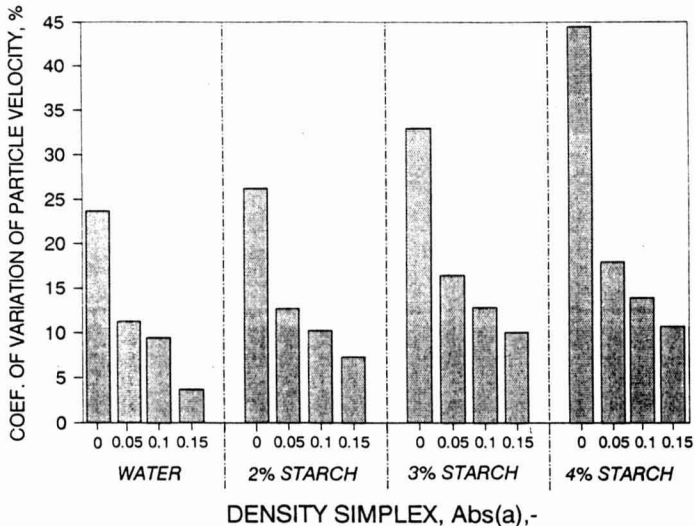


FIG. 7. COEFFICIENT OF VARIATION IN PARTICLE VELOCITY AS INFLUENCED BY CARRIER FLUID TYPE AND DENSITY SIMPLEX (a)

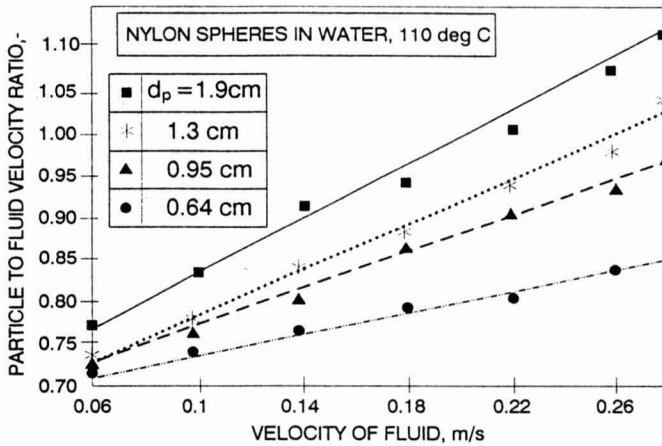


FIG. 8. TYPICAL RELATIONSHIP BETWEEN RELATIVE PARTICLE VELOCITY AND CARRIER FLUID VELOCITY

Particle Size Effect

Literature data (Ramaswamy *et al.* 1992; McKay *et al.* 1992; Smoldyrev 1982; Okuda 1981) suggest a significant influence of the particle size on particle velocity in the tube flow. This effect arises from the position occupied by the particle in the cross-sectional area of the tube entrapping carrier fluid with different velocity profiles. The velocity profile of moving liquid being lower along the tube wall and higher along the central axis, larger particles are affected by a liquid stream of higher overall velocity. Hence, the particle to fluid velocity ratio (u_p/u) can be expected to increase with increase in particle size. This tendency is confirmed from the correlation equations (Eq. 8-11). From sterilization safety point of view, this would mean that the critical particle is the largest one because it will be the fastest to travel and slowest to heat. Only when $a = 0$, the particle size may not have any special significance.

Shape Effect

It is well recognized that the shape of the particle moving in a carrier fluid in the holding tube has a significant influence on its flow behavior. The following are some illustrative examples (except for $a = 0$): (1) a spherical particle tends to roll, unless the tube surface is entirely frictionless; (2) other regularly shaped particles (for example, a cube) may slide if the surface is smooth or may tumble if it is rough or when there is a deposit of other particles at the surface, and (3) a rough or irregular shaped particle is likely to move in succession of jumps or "bounces" (so called "saltation flow"). Typical effect of

shape on particle Reynolds number is shown in Fig. 9 (for water and for 3% starch as a carrier fluid). Data presented shows a significant influence ($p \leq 0.05$) of particle sphericity ($\Psi = 1$ for spheres and $\Psi = 0.805$ for cubes) on the flow behavior. The shape effect decreases as the fluid viscosity increases (3% starch vs water). This damping effect was observed with all starch concentrations (2-4%) tested. However, because experimental data were obtained for particles of spherical and cubical form only, the applicability of this analysis is limited

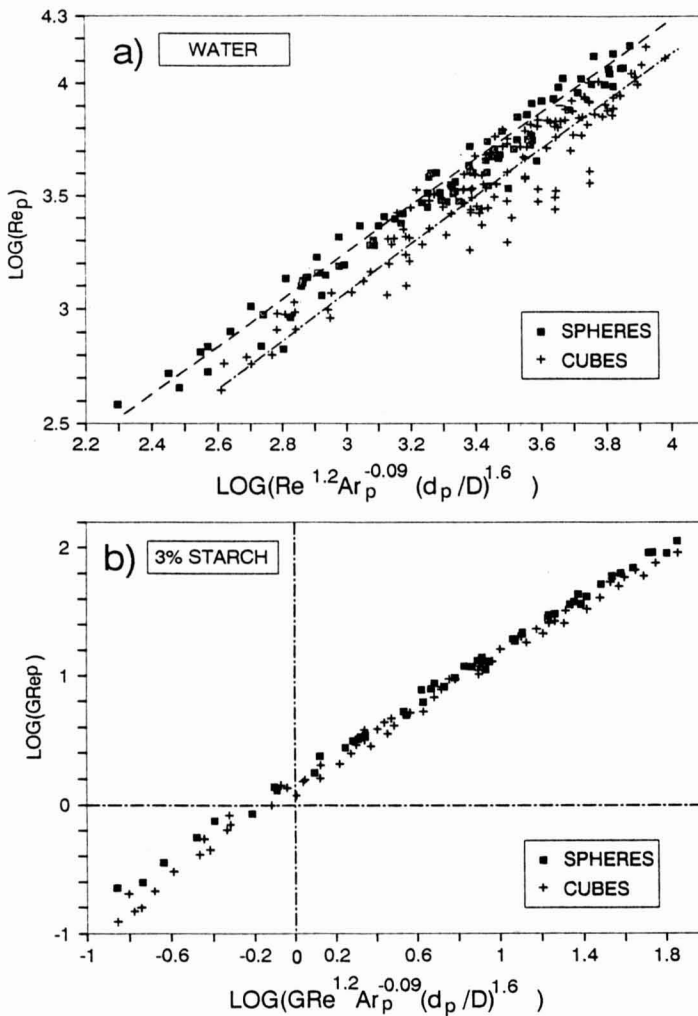


FIG. 9. PARTICLE SHAPE EFFECT ON PARTICLE REYNOLDS NUMBER a) FOR WATER AND b) FOR 3% STARCH SOLUTION AS A CARRIER FLUID

to sphericity of particles between 0.8 and 1.0. Typical particle shapes for this range of sphericity have been presented elsewhere (Grabowski and Ramaswamy 1995).

CONCLUSIONS

- (1) Particle velocity in the holding tube of aseptic processing system is a function of carrier fluid viscosity, flow rate and relative particle size, density and shape.
- (2) In dimensionless form, both mean and maximum particle to fluid velocity ratio as well as their generalized particle Reynolds number (GRe_p) are a function of generalized Reynolds number of the liquid in the tube (GRe), particle Archimedes number (Ar_p), particle to tube diameter ratio (d_p/D) and particle sphericity (Ψ).
- (3) Particle Reynolds number (GRe_p) can be similarly correlated, for use in heat transfer correlations, using particle to fluid differential velocity in GRe calculations.
- (4) Validity of the developed single particle correlations is limited to GRe up to 30,000, Ar_p up to 2×10^8 , (d_p/D) in range 0.12 - 0.65, sphericity Ψ from 0.8 to 1 and density simplex a not equal to 0.
- (5) Predictability of food particle velocity is poor (i.e., standard deviations are high) when the difference in density between the food particle and the carrier fluid is small.
- (6) When operating temperatures change from nonpressurized flow conditions (temperature $< 100C$) to pressurized flow (temperature $\geq 100C$), no specific change is observed in the flow behavior.

NOMENCLATURE

a, b	Constants in Eq.(6) (-)
A_p	Surface area of the particle (m^2)
A_{sph}	Surface area of an equivalent sphere (diameter d_p), respectively (m^2)
D	Tube diameter (m)
d_p	Particle diameter (equivalent) [$d_p = (6V_p/\pi)^{0.33}$](m)
g	Acceleration due to gravity (m/s^2)
h	Heat transfer coefficient ($W/(m^2K)$)
K	Consistency coefficient ($Pa \cdot s^n$)
k	Thermal conductivity ($W/(m \cdot K)$)
l	Cube edge length (m)
n	Flow behavior index (-)
T	Temperature (C)
u	Linear, average velocity of carrier fluid [$u=4V/(\pi D^2)$] (m/s)

u_p	Particle velocity, mean of 10 replicates (m/s)
$u_{p,max}$	Particle velocity, maximum of 10 replicates (m/s)
V	Carrier fluid volumetric flow rate (m ³ /s)
V_p	Volume of the particle (m ³)
α	Thermal diffusivity of fluid (m ² /s)
β	Slope of the holding tube (angle, degree)
η	Dynamic, effective viscosity (Pa s)
μ_{nd}	Nondimensional viscosity after Dutta and Sastry (1990a) [$Ku^{n-2}/(\rho d_p^n)$]
γ	Kinematic viscosity [$\gamma = \eta/\rho$] (m ² /s)
Ψ	Sphericity of the particle [$\Psi = A_{sph}/A_p$] (-)
ρ, ρ_s	Density of fluid and solid particles, respectively (kg/m ³)

Dimensionless Parameters

a	Density simplex [$(\rho_s - \rho)/\rho$]
Ar_p	Particle Archimedes number, Abs [$g d_p^3 a/\gamma^2$]
Fr	Froude number for tube flow [$u^2/(g D)$]
Fr_p	Modified Froude number [$u^2/(g d_p a^{0.5})$]
Fr_{p^*}	Modified Froude number [$u^2/(g d_p a)$]
Nu	Nusselt number [$h d_p/k$]
Pr	Prandtl number [γ/α]
GRE	Generalized tube flow Reynolds number [$u D \rho/\eta$]
GRE_p	Generalized particle Reynolds number [$u_p d_p \rho/\eta$]
GRE_r	Generalized particle Reynolds number based upon relative particle velocity [$(u_p - u) d_p \rho/\eta$]
Re_p	Particle Reynolds number (for Newtonian fluid) [$u_p d_p \rho/\eta$]
Re_r	Particle Reynolds number (for Newtonian fluid) based upon relative particle velocity [$(u_p - u) d_p \rho/\eta$]

ACKNOWLEDGMENTS

The authors wish to acknowledge the financial support for the research from the Natural Sciences and Engineering Research Council of Canada (NSERC) Operating and Strategic Grants Program.

REFERENCES

- ABDELRAHIM, K.A., RAMASWAMY, H.S., M. MARCOTTE and TOUPIN, C. 1993. Residence time distribution of carrot cubes in starch solutions in a pilot scale aseptic processing system. *Food Res. Int.* 26, 431-442.

- ABDELRAHIM, K.A., RAMASWAMY, H.S. and VAN DE VOORT, F.R. 1991. Rheological properties of Therm-flo™ starch at high temperatures evaluated using a high pressure viscometer. pp. 17–20. Paper presented at ASAE '91 Int. Winter Meeting, Chicago, IL.
- BAIN, A.G. and BONNINGTON, S.T. 1970. *The Hydraulic Transport of Solids by Pipeline*, Pergamon Press, Oxford.
- CHANDARANA, D.J. 1992. Acceptance procedures for aseptically processed particulate foods. In *Advances in Aseptic Processing Technologies*, (R.K. Singh and P.E. Nelson, eds.) Elsevier Appl. Sci., London.
- CHANDARANA, D.J., UNVERFERTH, I.A., STOFOROS, N.G., GAUVIN III, A. and KOSHUTE, K.A. 1991. Particle RTD of aseptically processed low-acid foods. Paper No. 534. 1991 Annual Meeting of the Inst. Food Technologists, Dallas.
- DARBY, R. 1986. Hydrodynamics of slurries and suspensions. In *Encyclopedia of Fluid Mechanics. Vol. 5, Slurry Flow Technology*, (N.P. Cheremisinoff, ed.) Gulf Publ., Houston, TX.
- DUTTA B. and SASTRY S.K. 1990a. Velocity distribution of food particle suspension in holding tube flow: experimental and modelling studies on average particle velocities. *J. Food Sci.* 55, 1448–1453.
- DUTTA, B. and SASTRY, S.K. 1990b. Velocity distribution of food particle suspension in holding tube flow: distribution characteristics and fastest particle velocities. *J. Food Sci.* 55, 1703–1710.
- GOVIER, G.W. and AZIZ, K. 1972. *The Flow of Complex Mixtures in Pipes*, Van Nostrand Reinhold, New York.
- GRABOWSKI, S. and RAMASWAMY, H.S. 1995. Incipient carrier fluid velocity for particulate flow in a holding tube. *J. Food Eng.* 24, 123–136.
- HARROD, M. 1989. Modelling of flow properties of starch pastes prepared by different procedure. *J. Food Process Engineering* 11, 257–275.
- JACOBS, B.E.A. 1991. *Design of Slurry Transport System*, Elsevier Sci. Publ., New York.
- LAWLER, M.T. and LU, P.C. 1971. The role of lift in the radial migration of particles in a pipe flow. In *Advances in Solid-liquid Flow in Pipes and its Application*, (I. Zandi, ed.) pp. 39–58, Pergamon Press, Oxford.
- MAESMANS, G., HENDRICKX, M., DECORDT, S.D., FRANSIS, A. and TOBBACK, P. 1992. Fluid-to-particle heat transfer coefficient determination of heterogeneous foods: a review. *J. Food Processing and Preservation*, 16, 26–69.
- McKAY, G., MURPHY, W.R. and JODERI-DABBAGHZADDEH, S. 1992. Settling characteristics of carrot particles in vertical pipelines. *J. Food Process Engineering*, 15, 81–97.
- OKUDA, K. 1981. Trajectory and diffusion of particles in liquid-solid flow of a slurry pipeline. *J. Pipelines*, 3, 211–223.

- RAMASWAMY, H.S., PANNU, K., SIMPSON, B.K. and SMITH, J.P. 1992. An apparatus for particle-to-fluid relative velocity measurement in tube flow at various temperatures under nonpressurized flow conditions. *Food Res. Int.* 25, 277-284.
- SANCHO, M.F. and RAO, M.A. 1992. Residence time distribution in a holding tube. *J. Food Eng.*, 15, 1-19.
- SASTRY, S.K. 1992. Liquid-to-particle heat transfer coefficient in aseptic processing. In *Advances in Aseptic Processing Technologies*, (R.K. Singh and P.E. Nelson, eds.) Elsevier Appl. Sci. Publ., London.
- SASTRY, S.K. 1993. Momentum and heat transfer in particulate sterilization. Paper No B.2.3 presented at Third Conference of Food Engineering, CoFE'93, Chicago, IL.
- SASTRY, S.K. and ZURITZ, C.A. 1987. A review of particle behavior in tube flow: applications to aseptic processing. *J. Food Process Engineering* 10, 27-52.
- SHOCK, C.A. and ROCO, M.C. 1991. *Slurry Flow*, Butterworth-Heinemann, Boston.
- SINGH, R.K and LEE, J.H. 1992. Residence time distribution of foods with/without particulates in aseptic processing systems. In *Advances in Aseptic Processing Technologies* (R.K. Singh and P.E. Nelson, eds.) Elsevier Appl. Sci. Publ., London.
- SMOLDYREV, A.Y. 1982. *Pipeline Transport - Principles of Design*, Publ. Terraspace Inc., Rockville, MD.
- WILSON, K.C. and BREBNER, A. 1971. On two phase pressurized and nonpressurized flow: behavior near deposition point. In *Advances in Solid-liquid Flow in Pipes and Its Applications*, (I. Zandi, ed.) pp. 175-186, Pergamon Press, Oxford.
- YANG, B.B. and SWARTZEL, K.R. 1991. Photo-sensor methodology for determining residence time distribution of particles in continuous flow in thermal processing systems. *J. Food Sci.* 56, 1076-1081, 1086.
- YANG, B.B. and SWARTZEL, K.R. 1992. Particle residence time distribution in two-phase flow in straight round conduit. *J. Food Sci.* 57, 497-502.
- ZANDI, I. 1971. Hydraulic transport of bulky material. In *Advances in Solid-liquid Flow in Pipes and its Applications*, (I. Zandi, ed.) pp. 1-37, Pergamon Press, Oxford.
- ZHANG, L., LIU, S., PAIN J-P. and FRYER, P.J. 1993. Heat transfer and flow in solid-liquid food mixtures. IChEME Symp. Series No. 126, 79-88.
- ZURITZ, C.A., McCOY, S.C. and SASTRY, S.K. 1990. Convective heat transfer coefficients for irregular particles immersed in non-Newtonian fluid during tube flow. *J. Food Eng.*, 11, 159-174.

RESIDENCE TIME DISTRIBUTION OF CYLINDRICAL PARTICLES IN A CURVED SECTION OF A HOLDING TUBE: THE EFFECT OF PARTICLE SIZE AND FLOW RATE¹

S. SALENGKE and S.K. SASTRY²

*Department of Agricultural Engineering
The Ohio State University
590 Woody Hayes Drive
Columbus, OH 43210*

Accepted for Publication November 23, 1994

ABSTRACT

The residence time and the residence time distributions of cylindrical particles (density 1130 kg/m³ and particle concentration 20% v/v) in a U-bend of 22 cm radius of curvature were studied. All experiments were conducted at room temperature and with an aqueous solution of sodium carboxymethylcellulose (0.5% CMC) as the carrier medium. Two levels of particle size (11 and 20 mm) and three levels of product flow rates (0.66×10⁻³, 0.81×10⁻³, and 0.97×10⁻³ m³/s) were used. The results obtained from this study showed that the mean and the standard deviation of the normalized residence time of particles decreased as either particle size or flow rate was increased. The E(Θ) and F(Θ) curves indicated that flow profile of particles approached the plug flow profile as the particle size or the flow rate was increased. Results obtained from regression analyses revealed that the mean and the standard deviation of the normalized residence time were significantly influenced by particle Froude number and most strongly by particle-to-tube diameter ratio.

INTRODUCTION

For the proper design of aseptic processing systems, studies concerning critical processing parameters are of paramount importance. Two major parameters, namely the residence time distributions (RTDs) of food particles and

¹ Salaries and research support provided by State and Federal Funds appropriated to the Ohio Agricultural Research and Development Center, The Ohio State University. Reference to commercial products and trade names is made with the understanding that no discrimination and no endorsement by The Ohio State University is implied.

² Author to whom correspondence is to be addressed.

the fluid-to-particle heat transfer coefficient (h_p), greatly influence lethality achieved during aseptic processing (Sastry 1989) and in general, numerical values of these parameters remain unknown.

Studies on flow behavior, residence time, and residence time distribution of particles suspended in liquid flowing at a certain flow rate in tubes and heat exchangers have been reported by many researchers (Toda *et al.* 1973; Maruyama *et al.* 1979; Richardson and Gaze 1986; McCoy *et al.* 1987; Sastry and Zuritz 1987a; Berry 1989; Dutta and Sastry 1990a,b; Alcairo and Zuritz, 1990; Pannu *et al.* 1991; Yang and Swartzel 1991, 1992; Lee and Singh, 1990, 1991, 1993; Hong *et al.* 1991; and Palmieri *et al.* 1992). Sastry and Zuritz (1987b) and Rao and Loncin (1974a,b) respectively, presented a critical review of flow behaviors of particles in tube flow and published models for predicting the residence time distribution in a pasteurizer.

From the results of the previous studies, it was evident that the flow behavior and the residence time of the suspended particles were influenced by process conditions such as pipe orientation, carrier fluid viscosity and flow rate, particle size, concentration, shape, and density. The effects of pipe orientation (horizontal or vertical) on the particle velocity in straight pipes and radius of curvature of bend on the particle velocity in the bend were reported by Toda *et al.* (1973). However, the results reported in their study are not applicable to aseptic processing of particulate food since the size and the density of the particles that they used were extremely different from those of real food particles. The effects of carrier viscosity (Dutta and Sastry 1990a,b and McCoy *et al.* 1987), flow rate (Berry 1989; Yang and Swartzel 1991; Palmieri *et al.* 1992; and Tucker and Richardson 1993), particle size (Pannu *et al.* 1991; McCoy *et al.* 1987), and particle concentration (Palmieri *et al.* 1992; Tucker and Richardson 1993) on the particle residence time were found to exist.

In spite of the considerable amount of research on the particle residence time that have been reported, all of the previous research concentrated on the study of the particle residence time in either complete holding tubes, straight sections of holding tubes, or scraped surface heat exchangers. Currently, no residence time data are available specifically for the curved sections (bends) of aseptic processing systems.

The objectives of this study were to investigate the residence time and the residence time distribution of simulated food particles in the curved section of a holding tube as affected by particle size and pump speed. A separate study (Salengke and Sastry 1994) has been conducted on the effects of particle concentration and bend radius of curvature.

MATERIALS AND METHODS

Experimental Apparatus

Figure 1 shows the schematic diagram of the apparatus used in the experiment. The major parts of the apparatus are a reservoir (0.12 m³ tank), a positive displacement progressive cavity pump (Sine pump, Div. of Kontro Co., Orange, MA), 2 transparent straight pipes (4.7 cm inside diameter and 3.048 m length), and a transparent U-bend (4.7 cm inside diameter and 22 cm radius of curvature). The pipes were inclined upward with a slope of 2.1 cm per linear meter. The bend (the measurement section) was oriented horizontally. A video camera equipped with a built-in digital stopwatch (Panasonic 8AF, Panasonic Co., Japan) was mounted directly above the bend to record particle motions and register the time elapsed during the experiment. To reduce the volume of the system, a small space near the outlet of the tank was isolated from the rest of the tank. The volume of this isolated space was 0.006 m³. The effective volume of the whole system was 0.0226 m³.

Material Preparation

The test particles used in the experiment were made of agar gel whose density was made comparable to that of potato (1130 kg/m³). The shape of the particles were cylindrical with the length and the diameter being the same.

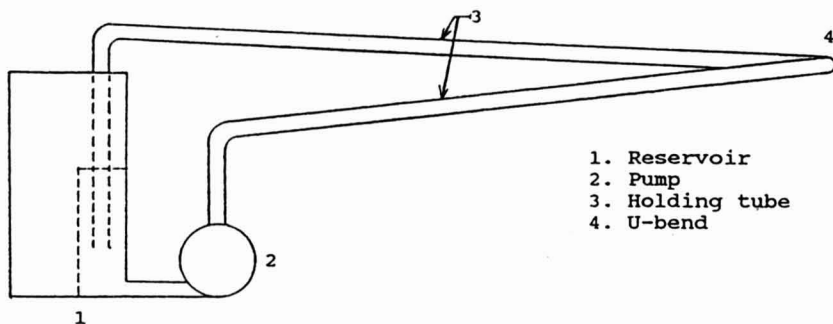


FIG. 1. SCHEMATIC OF EXPERIMENTAL APPARATUS

The carrier fluids used were aqueous solutions of sodium carboxymethylcellulose (CMC) containing 0.5 percent CMC (CMC, 7HF; Aqualon Company, Wilmington, DE). The fluid was prepared by slowly dispensing 600 grams of CMC powder into 0.12 m³ of hot water in a 0.2 m³ mixing tank with a mixing blade turned on. The solution was stirred for 30 min to accelerate the mixing process and to break up the flocculated powder. The solution was left in the mixing tank for 24 h to allow further dispersion. The density of the CMC solution was measured by measuring the weight of 250 ml CMC solution in a Pyrex graduated cylinder (250 ml \pm 2 ml). The density of the CMC solution was 1001 kg/m³. Rheological characteristics of the carrier fluid were determined by measuring shear stress (τ) at various shear rates ($\dot{\gamma}$) using a rotational viscometer (Rheomat model 115, Contraves AG, Zurich, Switzerland). The data obtained were fitted to the Ostwald-de Waele power law model (Eq. 1) to determine the consistency coefficient (K) and the flow behavior index (n) of the carrier fluid.

$$\tau = K\dot{\gamma}^n \quad (1)$$

The values obtained for the two rheological property indices were 0.297 Pa.sⁿ for K and 0.7025 for n.

Experimental Operation

All the experiments were conducted at room temperature at 2 levels of particle diameter (11 and 20 mm) and 3 levels of flow rate (0.66×10^{-3} , 0.81×10^{-3} , and 0.97×10^{-3} m³/s), corresponding to pump speeds 100, 120, and 140 rpm. For each combination of variables, residence time data were collected at least 100 consecutive tracer particles resulting in a total of 600 data points.

At the beginning of each run, the carrier fluid was circulated in the system for about 5 to 8 min to remove all air bubbles from the system. Pump speeds were regulated by an A-C variable speed drive (Reliance Electric Co., Cleveland, OH) and the pump rpm was measured using a Digital Tachometer (Shimpo Co., Kyoto, Japan).

Test particles (20% of the effective volume of the system) were introduced into the system through the isolated space in the tank. A total of 20 tracer particles (in five different colors) were later introduced into the system after a more uniform distribution of particles in the system was achieved.

Particle movements in the bend were recorded using the video camera and the residence times of the tracer particles were obtained from the readings of the built-in digital stopwatch. All experiments were run for 5 min. The overall product flow rate was measured using a bucket and a digital stopwatch at the end of each experimental run.

Data Analyses

To rule out any effect of small variabilities of flow rate at the same pump speed, the residence times of particles were normalized with respect to their respective average overall product flow rate. Statistical analyses were performed using the General Linear Model procedure of SAS (SAS 1988) to test the influence of each factor included in the experiment on the mean and the standard deviation of the normalized residence time (NRT) of particles. Duncan's multiple range test was used to test for significant differences among means at the 5% level. Multiple regression analyses were performed using stepwise regression procedures of SAS (SAS 1988) to correlate between various regressor variables (particle Froude number, dimensionless viscosity, and particle to tube diameter ratio) and the mean and the standard deviation of the NRT. The values of the particle Froude number were calculated using the equation proposed by Nesaratnam and Gaze (1987) and values of dimensionless viscosity were determined using the equation proposed by Dutta and Sastry (1990b).

$$\mu_{ND} = \frac{KV_f^{n-2}}{\rho_f D_t^n} \quad (2)$$

$$Fr_p = \frac{V_f}{gD_p \left(\frac{\rho_p}{\rho_f} - 1 \right)^{0.5}} \quad (3)$$

where V_f is the estimated fluid velocity, D_p is particle diameter, D_t is tube diameter, ρ_p is particle density, ρ_f is fluid density, K and n are the rheological indices of the carrier fluid. The carrier fluid velocities (V_f) were estimated using the following equation (Ohashi *et al.* 1980).

$$V_f = \frac{V_s - C \cdot V_p}{1 - C} \quad (4)$$

where V_s is average overall product (slurry) velocity, V_p is average particle velocity, C is volume fraction of the particle.

For illustration purposes, the plots to illustrate magnitude of the spread of the normalized particle residence time were presented in the forms of the normalized residence time distribution function, $E(\Theta)$, and the cumulative normalized residence time function, $F(\Theta)$. The normalized residence time distribution function is expressed in the following equation as defined by Brown and Fogler (1986).

$$E(\theta) = \frac{\Delta N/N_o}{\Delta t} \quad (5)$$

where ΔN is the number of particles having normalized residence times between time t and $t+\Delta t$, N_o is total number of replicates in the run. The normalized residence time of particles were obtained by dividing the particle residence time by their corresponding average product residence time. The $E(\Theta)$ and the $F(\Theta)$ curves were also used to characterize the distribution of the normalized residence time and the type of flow profile to which they may belong or at least approximate.

RESULTS AND DISCUSSION

Effects of Experimental Parameters on Mean NRT

Analysis of variance of mean normalized residence time (NRT) is summarized in Table 1. The results show that the effects of experimental parameters included in the study were significant ($P < 0.01$). However, the effects of the interactions between the two parameters were not significant ($P > 0.1$). Table 2 summarizes the results of Duncan's multiple range test for the normalized residence time. A typical plot, featuring the means and the 95% confidence interval of the means, for each main effect summarized in Table 2 is also presented for a better representation of the trends observed. It is worth noting that the data sets used in constructing the plots were exactly the same as those used by the General Linear Model of the SAS (SAS 1988) in analyzing the significant difference of the mean of the normalized residence time of each group in Duncan's grouping.

TABLE 1.
ANALYSIS OF VARIANCE TABLE FOR THE MEAN NORMALIZED RESIDENCE TIME

Source	DF	Sum of square	Mean square	F
Particle size (S)	1	0.3490	0.3490	33.93*
Flow rate (Q)	2	0.0971	0.0486	4.72*
S * Q	2	0.0316	0.0158	1.53 ^{NS}

*Highly significant at 1% level ($P < 0.01$)

^{NS}Not significant at 5% level ($P > 0.05$).

TABLE 2.
MEAN NORMALIZED RESIDENCE TIME AS INFLUENCED BY
EXPERIMENTAL PARAMETERS

Parameters	Levels	Mean NRT	SD NRT
Particle Size (mm)	11	0.9435 ^a	0.1318
	20	0.8952 ^b	0.0461
Flow rate (m ³ /s)	0.66 × 10 ⁻³	0.9370 ^c	0.1092
	0.81 × 10 ⁻³	0.9137 ^d	0.0912
	0.97 × 10 ⁻³	0.9074 ^d	0.0665

^{a-d} Means within the same parameter with at least one superscript in common are not significantly different at 5%-level.

Data on the effects of particle Froude number and particle-to-tube diameter ratio on the means and the standard deviations of the normalized residence time are presented in Table 3. In Fig. 2 and 3, the mean and the standard deviation of the normalized residence time of particles were plotted against particle Froude number and particle-to-tube diameter ratio. The relationships between the dependent variables (the mean and the standard deviation of NRT) and the regressor variables (particle Froude number and particle-to-tube diameter ratio) are well fitted by the empirical correlations presented in Eq. 6 and 7. The coefficients of determination (R^2) yielded from Eq. 6 and 7 were 0.9119 and 0.9631, respectively.

$$\text{Mean} = 1.0121(\text{Fr}_p)^{-0.0376}(\text{D}_r)^{-0.1086} \quad (6)$$

$$\text{SD} = 0.1081(\text{Fr}_p)^{-0.4408}(\text{D}_r)^{-1.9561} \quad (7)$$

TABLE 3.
NUMERICAL VALUES OF VARIABLES USED IN REGRESSION ANALYSES

Fr_p	μ_{ND}	D_r	Mean NRT	SD NRT
210.7	0.00087	0.425	0.912	0.0467
313.0	0.00068	0.425	0.881	0.0509
446.2	0.00054	0.425	0.892	0.0407
310.2	0.001	0.234	0.954	0.1579
463.3	0.00077	0.234	0.946	0.1314
672.5	0.00061	0.234	0.922	0.0923

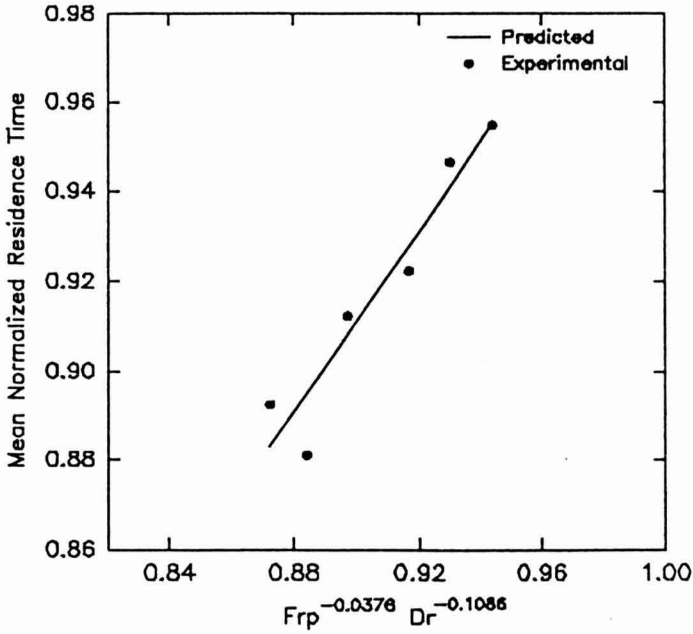


FIG. 2. MEAN NORMALIZED RESIDENCE TIME OF PARTICLES AS AFFECTED BY PARTICLE AND FROUDE NUMBER (Fr_p) AND PARTICLE-TO-TUBE DIAMETER RATIO (D_r)

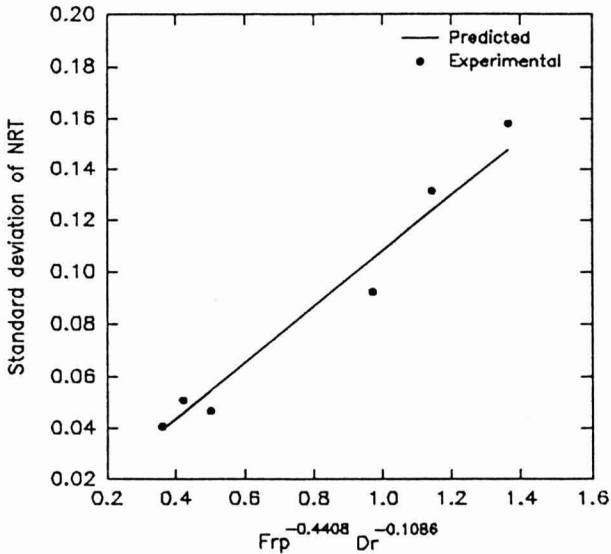


FIG. 3. STANDARD DEVIATION OF THE NORMALIZED RESIDENCE TIME OF PARTICLES AS AFFECTED BY PARTICLE FROUDE NUMBER (Fr_p) AND PARTICLE-TO-TUBE DIAMETER RATIO (D_r)

Effect of Particle Size

The effect of particle size on the mean normalized residence time was significant ($P < 0.05$). The means of the NRT decreased significantly as the particle size was increased from 11 to 20 mm (Table 2). A typical relationship between particle size and mean normalized residence time is illustrated in Fig. 4. This trend indicates that large particles tend to move faster than their smaller counterparts. Table 2 also indicates that the average velocities of both the small and the large particles exceeded that of the overall product (slurry). Similar trends have been reported by McCoy *et al.* (1987); Berry (1989); and Pannu *et al.* (1991). However, direct comparison between the results obtained in this study with those obtained by these investigators cannot be made because of differences in experimental conditions.

The above phenomenon can be explained by the observation that the average flow rates employed in this experiment were relatively high (ranging from 0.66×10^{-3} to 0.97×10^{-3} m³/s). In this range of flow rates, the carrier fluid appears to have enough momentum to lift the particles off the bottom of the tube. In addition, viscous forces may, to some extent, magnify the effect. This possibility was speculated based on previous findings by McCoy *et al.* (1987) which suggested the existence of combined effects of carrier viscosity and particle size on the particle residence time and its distribution. Moreover, an

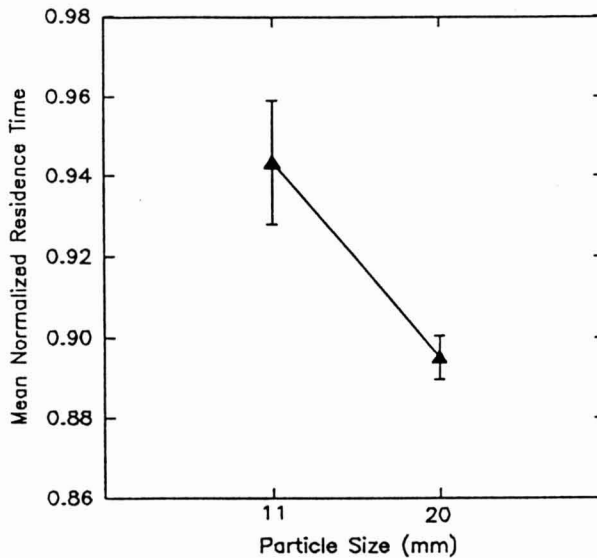


FIG. 4. THE MEANS AND 95% CONFIDENCE INTERVALS OF THE NORMALIZED RESIDENCE TIMES OF PARTICLES AS INFLUENCED BY PARTICLE SIZE

explanation proposed by Alcairo and Zuritz (1990) may also be used: when particles move along or near the tube wall, a large particle would tend to move faster than a small particle because some part of its mass would likely occupy the higher velocity region of the tube cross section.

The effect of particle size on the standard deviations of the normalized residence time is presented in Table 2. It can be seen from the table that the standard deviations or the spreads of the normalized residence time were highly particle size dependent. In particular, the magnitude of the standard deviation was much lower for the large particles than for the small particles. Typical plots for $E(\Theta)$ and $F(\Theta)$ as influenced by particle size are illustrated in Fig. 5 through 7. The shapes of the distribution curves were far from being normal. For the small particles, the $E(\Theta)$ curves were positively skewed and their distributions were much wider than the normal curve. On the other hand, the $E(\Theta)$ curves for the large particles were very much narrower than the normal curves. It was evident from the curves that the distributions of residence time for small particles were very much wider than those for large particles. Their corresponding $F(\Theta)$ curves showed that the curves for the large particle were steeper than those for the small particle. These trends suggest that the flow profile of particles in a bend approached a plug flow profile as the particle size increased. In order to explain the trend observed, it was appropriate to presume that some of the small particles were easily channelled with the high velocity carrier medium at or near the bend axis while some others lagged behind as they moved with the low velocity carrier at or near the bend wall, yielding a long tail on the right.

Effect of Flow Rate

The means of the normalized residence time as affected by flow rate (corresponding to pump speeds) are shown in Table 2. A typical plot for the relationship between flow rate and the mean of the normalized residence time is illustrated in Fig. 8.

The trend of the data shows that there was a tendency for the normalized residence time to decrease with increasing flow rate. The result is comparable with previous findings of Dutta and Sastry (1990) and Berry (1989) for flow in straight section of a holding tube. A closer examination to the data reveals that the change of flow rate from 0.66×10^{-3} to 0.81×10^{-3} m³/s or from 0.81×10^{-3} to 0.97×10^{-3} m³/s had no appreciable effect on the normalized residence time of particles. However, the mean of the normalized residence time at flow rate 0.97×10^{-3} m³/s was significantly lower than that at flow rate 0.66×10^{-3} m³/s. This trend may suggest that increasing flow rate to the highest level in the experiment may have significantly altered the inertial force of the particles to a higher value, causing the particles to move faster than the carrier medium.

The effect of changing flow rate (corresponding to pump speed) on the standard deviation of the normalized residence time as shown in Table 2 indicates that there is a clear tendency of the standard deviation to decrease as the flow rate increased. The normalized residence time distribution curves along

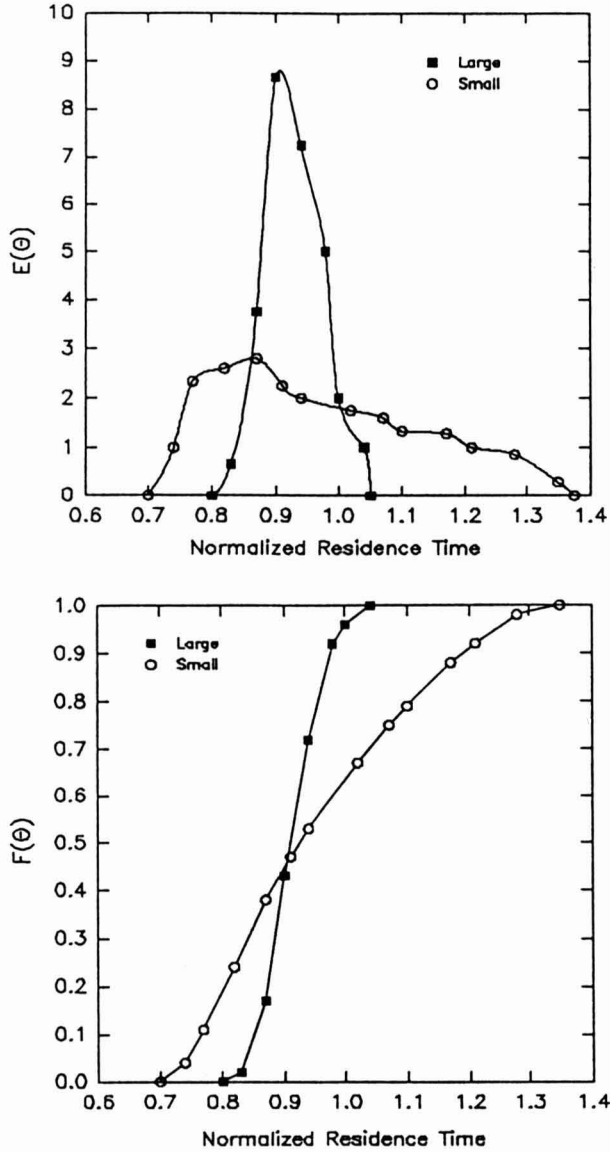


FIG. 5. $E(\theta)$ AND $F(\theta)$ CURVES OF THE NORMALIZED RESIDENCE TIMES OF PARTICLES AT FLOW RATE $0.66 \times 10^{-3} \text{ M}^3/\text{S}$ AS INFLUENCED BY PARTICLE SIZE

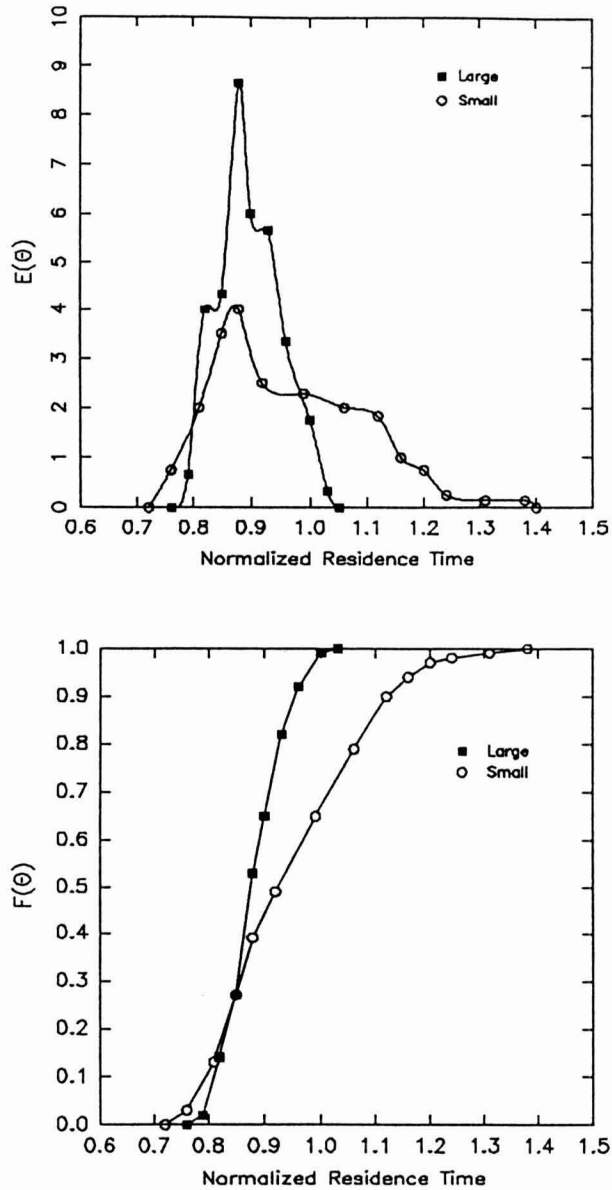


FIG. 6. $E(\theta)$ AND $F(\theta)$ CURVES OF THE NORMALIZED RESIDENCE TIMES OF PARTICLES AT FLOW RATE 0.81×10^{-3} M³/S AS INFLUENCED BY PARTICLE SIZE

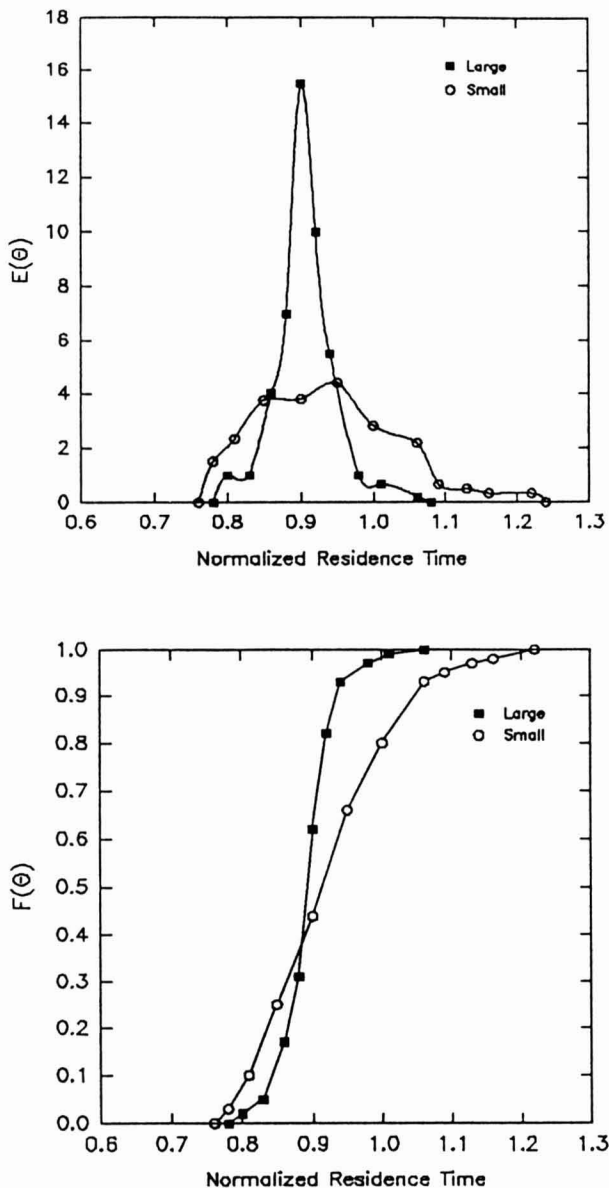


FIG. 7. $E(\theta)$ AND $F(\theta)$ CURVES OF THE NORMALIZED RESIDENCE TIMES OF PARTICLES AT FLOW RATE $0.97 \times 10^{-3} \text{ M}^3/\text{S}$ AS INFLUENCED BY PARTICLE SIZE

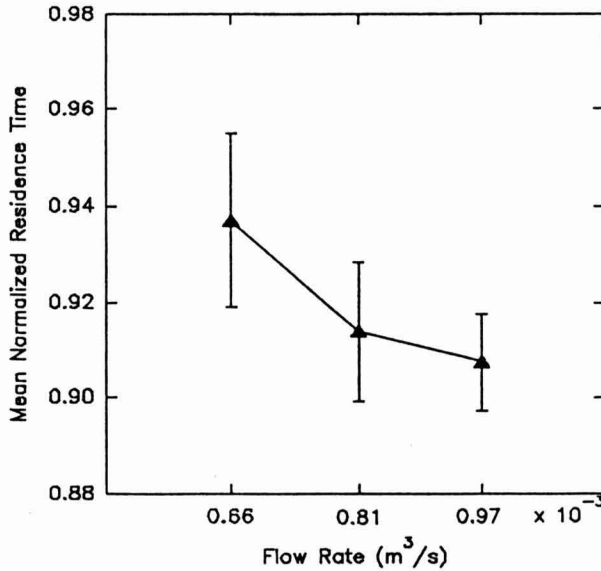


FIG. 8. THE MEANS AND 95% CONFIDENCE INTERVALS OF THE NORMALIZED RESIDENCE TIMES OF PARTICLES AS INFLUENCED BY FLOW RATE

with their cumulative normalized residence time curves for the small and the large particles as influenced by flow rate are presented in Fig. 9 and 10. The figures reveal that the spreads of the distribution curves tended to decrease and the steepness of the cumulative distribution curves increased as the flow rate increased. These trends indicated that the residence time of particles became more uniform (approached the plug flow profile) as the flow rate increased. Reverse trends have been reported by Alcairo and Zuritz (1990) for flow of a single particle in a scraped surface heat exchanger. In order to explain the above trend, it was presumed that the radial mixing and erratic motions of particles, which is most likely the case at relatively high particle concentration as in this experiment, became more severe as the flow rate increased. As a result, the majority of the particles would be expected to have spent approximately the same amount of time in the bend.

CONCLUSION

The overall trend observed for the effect of changing flow rate showed that the mean of the normalized residence time tends to decrease as the flow rate increases. A similar trend was observed for the standard deviation or the spread of the normalized residence time. The trends obtained from the $E(\Theta)$ and $F(\Theta)$ curves indicated that the flow profile of particles approached the ideal plug flow profile as the flow rate increased.

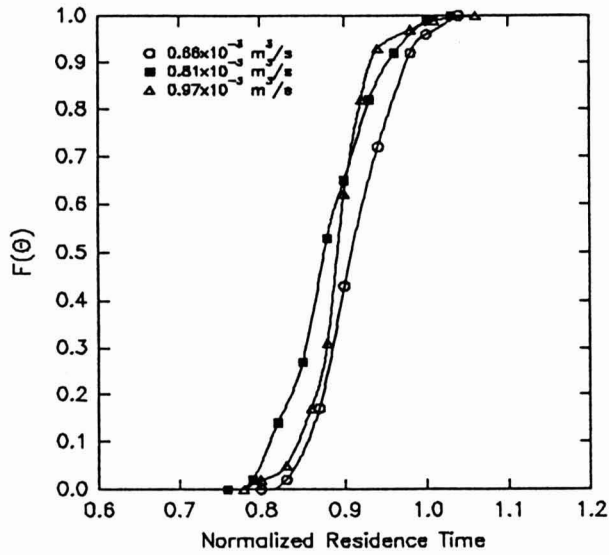
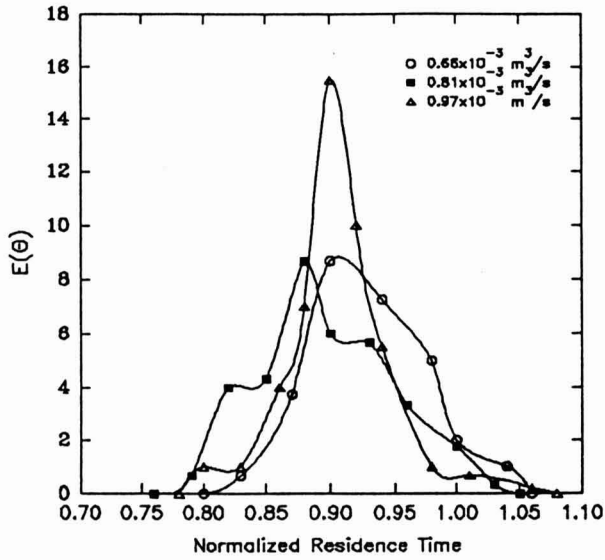


FIG. 9. $E(\theta)$ AND $F(\theta)$ CURVES OF THE NORMALIZED RESIDENCE TIMES OF LARGE PARTICLES AS INFLUENCED BY FLOW RATE

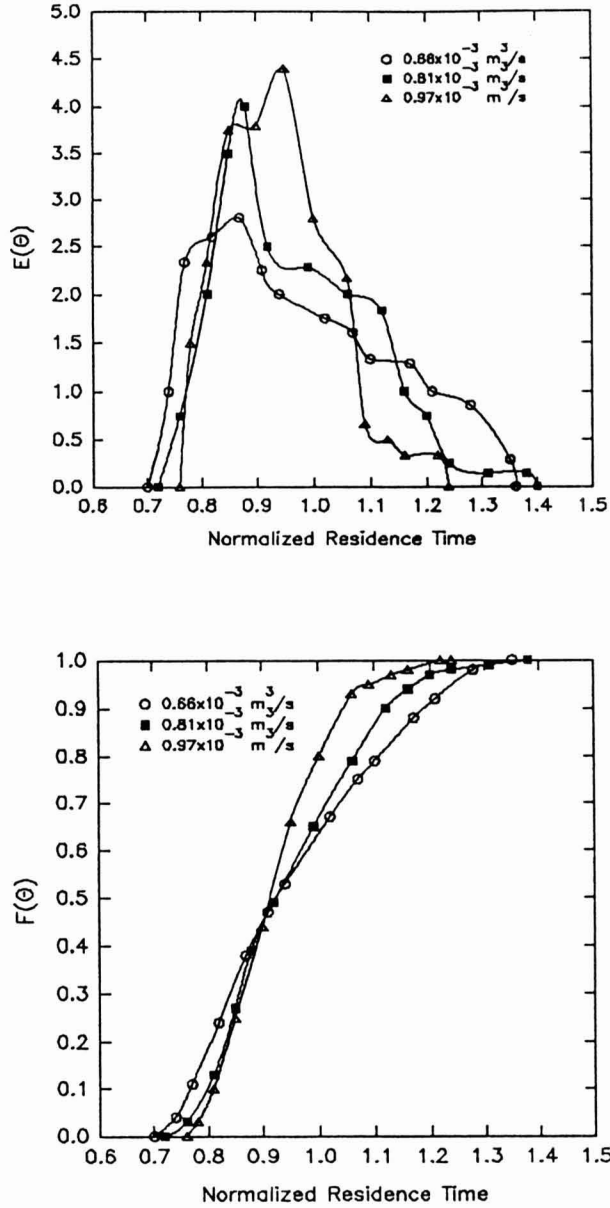


FIG. 10. $E(\theta)$ AND $F(\theta)$ CURVES OF THE NORMALIZED RESIDENCE TIMES OF SMALL PARTICLES AS INFLUENCED BY FLOW RATE

The mean and the standard deviation of the normalized residence time were significantly lower for the large particles. This trend was most likely due to the high flow rates employed in this study. The $E(\Theta)$ curves for large particles were much narrower than those for the small particles and their corresponding $F(\Theta)$ curves were steeper for the large particles. These trends indicated that the flow profile of particles approaches the ideal plug flow as the particle size increases.

NOMENCLATURE

Symbols

C	Particle concentration
D_p	Particle diameter, cm
D_r	Particle-to-tube diameter ratio
D_t	Tube inside diameter, cm
$E(\Theta)$	Normalized residence time function
$F(\Theta)$	Cumulative normalized distribution function
Fr_p	Particle Froude number
g	Acceleration due to gravity, m/s^2
K	Coefficient of consistency, $Pa \cdot s^n$
n	Flow behavior index
ΔN	Number of particles having residence time within certain time interval
N_o	Total number of replicates in a data set
NRT	Normalized residence time of particles
Q	Overall product flow rate, m^3/s
SD	Standard deviation of NRT
Δt	Time interval, s
V_f	Fluid velocity, m/s
V_p	Particle velocity, m/s
V_s	Average slurry velocity, m/s

Greek letters

$\dot{\gamma}$	Shear rate, s^{-1}
ρ_f	Fluid density g/cm^3
ρ_p	Particle density g/cm^3
μ_{ND}	Dimensionless viscosity
τ	Shear stress, Pa

REFERENCES

- ALCAIRO, E.R. and ZURITZ, C.A. 1990. Residence time distributions of spherical particles suspended in non-Newtonian flow in a scraped surface heat exchanger. *Trans. of the ASAE*. 33(5), 1621–28.

- BERRY, M.R. 1989. Predicting fastest particle residence time. First International Congress on Aseptic Processing Technologies. Indianapolis, IN.
- BROWN, L.F. and FOGLER, H.S. 1986. Distributions of residence time for chemical reactors. In *Elements of Chemical Reaction Engineering*. (H.S. Fogler, ed.) pp. 629-79, Prentice-Hall, Englewood Cliffs, NJ.
- DUTTA, B. and SASTRY, S.K. 1990a. Velocity distributions of food particle suspensions in holding tube flow: distribution characteristics and fastest-particle velocities. *J. Food Sci.* 55(6), 1703-10.
- DUTTA, B. and SASTRY, S.K. 1990b. Velocity distributions of food particle suspensions in holding tube flow: experimental and modelling studies on average particle velocities. *J. Food Sci.* 55(5), 1448-53.
- HONG, C.W., PAN, B.S., TOLEDO, R.T. and CHIOU, K.M. 1991. Measurement of residence time distribution of fluid and particles in turbulent flow. *J. Food Sci.* 56(1), 255-9.
- LEE, J.H. and SINGH, R.K. 1990. Particle residence time distribution in a scraped surface heat exchanger. ASAE Paper No. 90-6522. American Society of Agricultural Engineers, St. Joseph, MI.
- LEE, J.H. and SINGH, R.K. 1991. Particle residence time distribution in a model horizontal scraped surface heat exchanger. *J. of Food Process Engineering* 14, 125-46.
- LEE, J.H. and SINGH, R.K. 1993. Residence time distribution characteristics of particle flow in a vertical scraped surface heat exchanger. *J. of Food Eng.* 18, 413-24.
- MARUYAMA, T., KOJIMA, K. and MIZUSHINA, T. 1979. The flow structure of slurries in horizontal pipes. *J. of Chem. Eng. of Japan.* 12(3), 177-82.
- MCCOY, S.C., ZURITZ, C.A. and SASTRY, S.K. 1987. Residence time distribution of simulated food particles in a holding tube. ASAE Paper No. 87-6536, American Society of Agricultural Engineers, St. Joseph, MI.
- NESARATNAM, R. and GAZE, J.E. 1987. Application of a particulate technique to the study of particle sterilization under dynamic flow. Technical Memorandum No. 461. Campden Food Preservation Research Association, Chipping Campden, UK.
- OHASHI, H., SUGAWARA, T., KIKUCHI, K. and ISE, M. 1980. Average particle velocity in solid-liquid two-phase flow through vertical and horizontal tubes. *J. of Chem. Eng. of Japan.* 13(5), 343-49.
- PALMIERI, L., CACACE, D., DIPOLLINA, G. and DALL'AGLIO, G. 1992. Residence time distribution of food suspensions containing large particles when flowing in tubular systems. *J. of Food Eng.* 17 225-39.

- PANNU, K., RAMASWAMY, H.S., SIMPSON, B.K. and SMITH, J.P. 1991. Apparatus for evaluating particle/fluid flow at elevated temperatures. ASAE Paper No. 91-6600, American Society of Agricultural Engineers, St. Joseph, MI.
- RAO, M.A. and LONCIN, M. 1974a. Residence time distribution and its role in continuous pasteurization. (Part I). *Lebensm.-Wiss. u. Technol.* 7(1), 5-13.
- RAO, M.A. and LONCIN, M. 1974b. Residence time distribution and its role in continuous pasteurization. (Part II). *Lebensm.-Wiss. u. Technol.* 7(1), 14-17.
- RICHARDSON, P. and GAZE, J. 1986. Application of an alginate particle technique to the study of particle sterilization under dynamic flow. Technical Memorandum No. 429. Campden Food Pres. Res. Assoc., Chipping Campden, UK.
- SALENGKE, S. and SASTRY, S.K. 1994. Residence time distribution of cylindrical particles in the curved section of a holding tube: the effect of particle concentration and bend radius of curvature. *J. Food Engr.* (submitted).
- SAS. 1988. *SAS/STATTM User's Guide*, Release 6.04. SAS Inst. Inc. Cary, NC.
- SASTRY, S.K. 1989. Aseptic technology for particulate foods: problems, issues and some potential solutions. First International Congress on Aseptic Processing Technologies. Indianapolis, IN.
- SASTRY, S.K. and ZURITZ, C.A. 1987a. A review of particle behavior in tube flow: application to aseptic processing. *J. Food Process Engineering* 10, 27-52.
- SASTRY, S.K. and ZURITZ, C.A. 1987b. A model for particle suspension flow in a tube. ASAE Paper No. 87-6537, American Society of Agricultural Engineers, St. Joseph, MI.
- TODA, M., ISHIKAWA, T., SAITO, S. and MAEDA, S. 1973. On the particle velocities in solid-liquid two-phase flow through straight pipes and bends. *J. of Chem. Eng. of Japan*, 6(2), 140-6.
- TUCKER, G.S. and RICHARDSON, P.S. 1993. Residence time distribution and flow behavior of food containing particles in Aseptic Processing. Poster Paper, AIChE Conference of Food Engineering. Chicago, IL.
- YANG, B.B. and SWARTZEL, K.R. 1991. Photo-sensor methodology for determining residence time distributions of particles in continuous flow thermal processing systems. *J. Food Sci.* 56(4), 1076-81, 1086.
- YANG, B.B. and SWARTZEL, K.R. 1992. Particle residence time distributions in two-phase flow in straight round conduit. *J. Food Sci.* 57(2), 497-502.

METHOD FOR MEASURING CO₂ ABSORPTION IN CO₂ AND N₂ PACKAGED FRESH MEAT¹

YANYUN ZHAO² and JOHN HENRY WELLS³

*Department of Biological and Agricultural Engineering
Louisiana Agricultural Experimental Station
Louisiana State University Agricultural Center
Baton Rouge, LA 70803*

ABSTRACT

Headspace gas composition of meat stored in modified atmosphere packaging (MAP) undergoes dynamic changes as a result of packaging film permeability, postmortem metabolic activity, CO₂ absorption in water and lipid, and bacteria growth and respiration. A combined analytical and experimental method was developed to investigate CO₂ absorption by packaged fresh meat in a gas-impermeable environment and during isothermal storage. The ideal gas law was used as a theoretical basis and a gas-impermeable and constant-volume chamber was constructed to evaluate the theoretical derivation. Changes in headspace pressure caused by dynamic interactions between beef and MAP atmospheres were monitored to predict concentration changes of CO₂ within the chamber. The proposed methodology for measuring CO₂ concentration changes was confirmed by gas analysis and proved valid for prediction of headspace CO₂ concentration changes in MAP gas-impermeable systems within the range of initial gas composition 20% to 100% CO₂ balanced with N₂, at temperatures ranging from 3 to 13C, and an initial headspace pressure of 155 kPa.

INTRODUCTION

Carbon dioxide-enriched atmospheres have been used to extend the shelf-life of packaged fresh meat because of their effect on the growth inhibition of gram negative microorganisms (Enfors and Molin 1978; Zhao *et al.* 1994). Carbon dioxide is highly soluble in water and lipid (Gill 1988). As CO₂ is absorbed by meat packaged in a high CO₂ concentration modified atmosphere packaging (MAP) system, package shrinkage or collapse may occur. Package collapse has

¹ Approved for Publication by the Director of the Louisiana Agricultural Experiment Station as Manuscript No. 93-07-7360

² Author Zhao is now affiliated with the Department of Animal Science, Iowa State University, 215 Meat Laboratory, Ames, Iowa 50011.

³ Author to whom correspondence should be addressed.

been given as a limiting factor to wider usage of MAP with fresh meat (Gill 1988; Bush 1991). To overcome this problem, the absorptive capacity of the meat for CO₂ must be taken into account when designing a MAP systems.

Few methods for measuring CO₂ absorption in fresh meat have been reported. Gill (1988) measured the solubility of CO₂ in beef, pork and lamb by saturating the meat tissue with CO₂, then absorbing the gas evolved from the tissue in standard 0.05M Ba(OH)₂ solution and titrating the residual Ba(OH)₂ with 0.1M HCl using phenolphthalein as the indicator. Bush (1991) mentioned that the CO₂ absorption diagram (i.e., a plot of CO₂ absorption with respect to time) for meat could be measured using a thermostatic, constant volume or constant pressure chamber. However, the accuracies of methods to measure CO₂ absorption have not been documented.

The overall objective of this work was to develop a method for measuring CO₂ absorption in MAP (CO₂ and N₂) packaged meats. The specific objectives included: (1) derivation of a method to predict CO₂ absorption in packaged fresh meats, and (2) verification of the predicted values of CO₂ absorption by measurements with a gas analyzer. Also suggested are applications of the developed measurement method in a MAP system design.

THEORY

The Ideal Gas Law

The ideal gas law can be stated as:

$$PV = nRT \quad (1)$$

where P is absolute gas pressure (Pa), V is the gas volume (m³), n is the absolute amount of the gas (mole), T is absolute temperature of the gas (K), and R is universal gas constant (8.3144 J/mole·K).

Under normal temperature and pressure conditions, the ideal gas law can be used to describe the behavior of O₂, CO₂ and N₂ (Toledo 1991). For a gas mixture, Dalton's law of partial pressure and Amagat's law of partial volume describe the relationship between total pressure and volume of gas mixture. The partial pressure and partial volume of each individual gas can be expressed respectively as:

$$P = \sum P_j \text{ and } V = \sum V_j \quad (2)$$

where P_j and V_j are partial pressure and volume of individual component gases, respectively. Restated, the ideal gas law can be used to relate the partial pressure of each component gas to the number of moles of that component within the mixture. The partial pressure of a component gas is related to the component amount in a gas mixture by:

$$P_j V = n_j RT \quad (3)$$

where n_j is the absolute amount (moles) of the component gas with partial pressure P_j .

Estimation of CO₂ Absorption

Consider a sealed (gas-impermeable), thermostatic (isothermal), and constant volume chamber, as shown in Fig. 1. Into the chamber, introduce the product under examination and various mixes of CO₂ and N₂, maintaining the product temperature constant. The partial pressures of CO₂ and N₂ in a constant headspace volume and constant temperature are represented by:

$$P_{\text{CO}_2} + P_{\text{N}_2} = \frac{RT}{V_H} (n_{\text{CO}_2} + n_{\text{N}_2}) \quad (4)$$

or

$$n_{\text{CO}_2} = \frac{(P_{\text{CO}_2} + P_{\text{N}_2})}{RT} V_H - n_{\text{N}_2} \quad (5)$$

where P_{CO_2} and P_{N_2} are the partial pressures of CO₂ and N₂, respectively (Pa), V_H is the package headspace volume (m³), and n_{CO_2} and n_{N_2} are the absolute amounts of gaseous CO₂ and N₂ within chamber, respectively (mole). By Dalton's law of partial pressure, Eq. (5) can be rewritten as:

$$n_{\text{CO}_2} = \frac{V_H P}{RT} - n_{\text{N}_2} \quad (6)$$

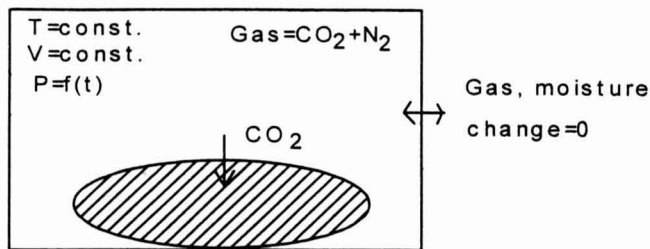


FIG. 1. AN IMITATIVE THERMOSTATIC, CONSTANT VOLUME, AND GAS IMPERMEABLE SYSTEM FOR DERIVATION OF CO₂ ABSORPTION EQUATIONS

Because nitrogen is an inert gas and much less soluble in meat compared with CO₂, the absolute amount of nitrogen is assumed to remain constant in the package (Taylor 1972; Seideman *et al.* 1979; Farber 1991). Differentiating Eq. (6) with respect to time, *t*, yields:

$$\frac{dn_{\text{CO}_2}}{dt} = \frac{V_H}{RT} \frac{dP}{dt} \quad (7)$$

That is, the pressure loss within a constant volume, constant temperature chamber results from CO₂ being absorbed into the meat. Given that total gas volume occupied in the chamber is constant, and assuming the temperature within the chamber remains uniform with no gas permeating through the chamber wall, the amount of CO₂ absorption can be calculated by solving Eq. (7). Solving this differential equation, the amount of CO₂ remaining within the chamber (package) at some final time is:

$$n_{\text{CO}_2f} = n_{\text{CO}_2i} - \frac{V_H}{RT} (P_i - P_f) \quad (8)$$

where n_{CO_2i} and n_{CO_2f} are amounts (moles) of gaseous CO₂ within the chamber initially and at the final time, respectively, and P_i and P_f are the absolute pressure (Pa) of chamber headspace at the initial time and final time, respectively.

The present study is concerned with the absolute amount of CO₂ absorbed by meat during a specified period of time. The term "CO₂ absorption" was used as a gross measure of CO₂ absorbed per unit mass of meat. Other researchers have chosen the terminology "CO₂ solubility" to express a similar concept (Gill 1988). The CO₂ absorption in meats can be calculated as:

$$A_{\text{CO}_2} = \frac{n_{\text{CO}_2i} - n_{\text{CO}_2f}}{M_m} \quad (9)$$

where A_{CO_2} is the accumulative amount of CO₂ absorbed by packaged meats at some final time (mole_{CO₂}/kg_{meat}), and M_m is amount of meat product in the package (kg).

Alternately, the units of CO₂ absorption can be expressed as g_{CO₂}/kg_{meat} by multiplying by the molecular weight of CO₂ (44 g/mole_{CO₂}). Thus CO₂ absorption on a mass/mass basis is expressed as:

$$A_{\text{CO}_2}(\text{g}_{\text{CO}_2}/\text{kg}_{\text{meat}}) = 44A_{\text{CO}_2}(\text{mole}_{\text{CO}_2}/\text{kg}_{\text{meat}}) \quad (10)$$

Combining Eq. (8), (9) and (10), A_{CO_2} is finally expressed as:

$$A_{\text{CO}_2} = \frac{44V_H}{RTM_m} [P_i - P_f] \quad (11)$$

By measuring the headspace gas pressure changes during a specified duration, the headspace CO₂ changes caused by absorption (or evolution) within packaged meat can be determined from Eq. (11). An uncertainty analysis of Eq. (11) is given in the Results and Discussion section. The time selected for measurement of CO₂ absorption in the present study was 12 h. Preliminary research indicated 12 h was a sufficient length of time for meat to absorb CO₂ without influence of other reactions such as microbial growth or lipid oxidation. Also, a time interval of 12 h was previously considered by Gill (1988) as the time needed for fresh beef to reach CO₂ absorption equilibrium.

Estimation of Final CO₂ Concentration in Headspace

Because the volume percentage of CO₂ and N₂ is equal to mole percentage of CO₂ and N₂, according to the ideal gas law, the volume percentage of CO₂ can be calculated as:

$$[\text{CO}_2]_f = \frac{n_{\text{CO}_2f}}{(n_{\text{CO}_2} + n_{\text{N}_2})_f} \quad (12)$$

By analogy of Eq. (12), the initial amount of CO₂ that can be expressed in terms of the initial CO₂ concentration is:

$$n_{\text{CO}_2i} = [\text{CO}_2]_i (n_{\text{CO}_2} + n_{\text{N}_2})_i \quad (13)$$

Since $n_{\text{CO}_2f} = n_{\text{CO}_2i} - \Delta n_{\text{CO}_2}$, and by calculating Δn_{CO_2} from Eq. (8) and the sum of n_{CO_2} and n_{N_2} from Eq. (6), Eq. (12) can be expressed completely in terms of pressure and initial gas concentration:

$$[\text{CO}_2]_f = \frac{[\text{CO}_2]_i P_i - \Delta P}{P_f} \quad (14)$$

where $[\text{CO}_2]_i$ is initial volume percentage of CO₂ in headspace (%) that could be measured by gas analyzer (or assumed from a certified gas mixture used for initial MAP environment), and $\Delta P = P_i - P_f$, is headspace gas pressure change (Pa) with P_i and P_f indicated as the measured initial and final total headspace absolute gas pressure, respectively. Similarly, final calculated volume percentage for N₂, $[\text{N}_2]_f$ can be calculated from:

$$[\text{N}_2]_f = \frac{n_{\text{N}_2f}}{(n_{\text{CO}_2} + n_{\text{N}_2})_f} = \frac{P_{\text{N}_2f}}{P_f} = \frac{P_{\text{N}_2i}}{P_f} = \frac{[\text{N}_2]_i P_i}{P_f} \quad (15)$$

where $[\text{N}_2]_i$ is initial volume percentage of N₂ in headspace (%) that could be measured by gas analyzer (or assumed from a known certified MAP gas mix). Equation (15) is stated assuming that the change in partial pressure of N₂ has a negligible contribution to the overall pressure change ΔP . Equations (14) and

(15) are used to calculate the final volume percentages of N_2 and CO_2 respectively for comparison of results predicted by the pressure measurement method and those observed using a gas analyzer.

MATERIALS AND METHODS

Detailed Construction of Experimental Apparatus

An experimental apparatus used for estimation of CO_2 absorption was constructed as shown in Fig. 2. A sealed aluminum pressure vessel (255 mm diameter by 110 mm high and 10 mm thick) was built as a constant volume chamber. A pressure transducer (Omega Engineering Inc., PX 304-100AV) attached to the lid of the chamber was connected to a strip chart recorder (ABB GOERZ Aktiengeschaft, Austria, Model SE120) to monitor changes of absolute pressure of gases within the chamber. Additionally, temperature inside the chamber was measured with a copper-constantan thermocouple probe (Omega Engineering Inc., Model CPSS-18G-8-RP) connected to the second channel of the strip chart recorder. Two metering valves attached to the chamber (Swagelok Co., Model SS-31RF2) were connected to a premixed gas bottle and vacuum pump (Thomas Industries Inc., Model 607CA32), respectively. The chamber connections allowed for evacuation and gas back flushing to replace the internal chamber atmosphere. A sampling port for withdrawal of gas samples and a pressure release valve to insure the safety of the system were also connected with the chamber.

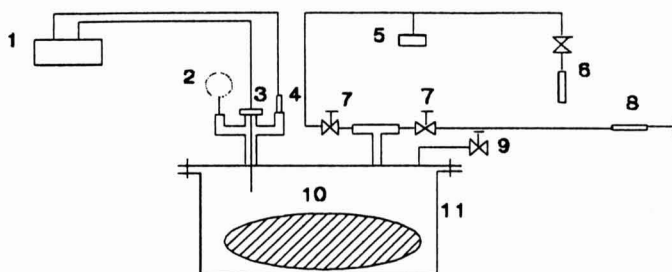


FIG. 2. TEST APPARATUS USED TO MONITOR CHANGE IN GAS PRESSURE

1. strip chart recorder
2. pressure gage
3. thermocouple probe
4. pressure transducer
5. vacuum pump
6. premixed gas tank
7. gas flush valves
8. sampling syringe
9. pressure release valve
10. meat sample
11. test chamber

The composition of headspace gases in the chamber was monitored by removing 30 ml gas at the headspace pressure via a 30 ml gas-tight syringe (Becton Dickinson and Company, Model B-D) through a Shimadzu septum (Chemical Research Supplies, Model 77) attached to the sampling port. The volume percentage of the individual gases present was measured using a CO₂/O₂ gas analyzer (Servomex Co., Model 1450). The gas analyzer was calibrated as per the manufacturer's instructions using N₂, known certified gas mixtures of N₂ and CO₂, and air as calibration gases. The measurements of gas composition were used to confirm the initial and final gas composition within the chamber during CO₂ absorption experiments.

The chamber volume was determined by the total volume of water that could be injected into the chamber, 5.16 l. The seal integrity of the chamber was determined by monitoring the pressure change in nitrogen (initial gas pressure of 207 kPa) during 24 h. The seal integrity was verified periodically throughout the study by holding a desired gas or gas mix within an empty chamber and monitoring gaseous pressure changes over time. In order to achieve isothermal conditions, the test apparatus was located inside a temperature controlled cooler (Master-Bilt, Standex Company, Model D34LCD82) that was adjusted to the desired temperature 12 h before the start of each experiment.

Experimental Validation of CO₂ Absorption Method

A replicated 3 × 3 factorial, complete randomized design (18 sample trials) was conducted to study CO₂ absorption in fresh beef under three different storage temperatures (3, 8, and 13C) and 3 different initial gas compositions (100% CO₂, 50% CO₂/50% N₂, and 20% CO₂/80% N₂). Premixed gases of known CO₂ and N₂ composition were injected into the chamber with repeated vacuum/back-flush cycles. The chamber was evacuated by vacuum pump to approximately 8.0 kPa absolute pressure for 40 min, the desired gas mixture was then admitted into the chamber, then vacuum evacuated and gas back-flushed again. The repeated vacuum/back-flush procedure assured residual O₂ of less than 0.5% as determined by measuring headspace gas composition with a gas analyzer. The headspace to meat volume ratio for all samples was controlled at 2.5, a ratio that was found to provide sufficient absolute amounts of CO₂ for all gas mix combinations (Zhao *et al.* 1995). To validate the CO₂ absorption procedure, pressure changes monitored over the course of each experiment were used to calculate final gas composition within the test chamber headspace. Equation (11) was used to predict amount of CO₂ absorption, and Eq. (14) and (15) were used to calculate final CO₂ and N₂ concentration in headspace, respectively. Predicted headspace gas composition was compared to that observed as measured with the gas analyzer. Correlation and bias analyses

were conducted for observed and predicted percentage concentrations of CO₂ and N₂.

Experimental Validation of N₂ Absorption Assumption

An investigation of N₂ solubility in meat was conducted to verify assumed conditions within the test chamber (i.e., $dn_{N_2}/dt=0$). The N₂ absorption in meat was measured by maintaining 100% N₂ atmosphere in the test chamber and recording absolute pressure changes of N₂ over time. A beef sample was placed into the chamber and held at 8C, and the atmosphere in the chamber was adjusted to 100% N₂ using the previously described vacuum/back-flush treatment. The absolute pressure of headspace gas was monitored to determine N₂ absorption in meat. Pressure reduction would indicate that N₂ is absorbed by meat; otherwise, N₂ absorption in beef could be ignored.

Meat Sample Preparation

Meat composition (e.g., moisture content and fat content), pH and other biological factors can greatly affect CO₂ absorption in packaged meat (Gill 1988). Therefore, care was taken to maintain uniformity among individual beef samples within the experiment. Samples were cut from the inside round semimembranosus muscle obtained from beef carcasses 72 h after slaughter and trimmed free of external fat (Zhao *et al.* 1995). All samples were vacuum packaged in high barrier vacuum bags using a chamber-type, heat-seal vacuum packaging machine (WestGlen Corp., Model VM 200H). Sample bags were stored at 4C for less than seven days until the beginning of each experiment. Care was taken to ensure minimum variability in biological factors among samples. Moisture content, fat content, and pH were measured for all beef samples. Moisture, fat, and pH were measured as $72.0 \pm 2.0\%$, $2.5 \pm 2.0\%$, and 5.5 ± 0.2 , respectively.

RESULTS AND DISCUSSION

Validation of Headspace CO₂ Change Measurement

The comparisons of the predicted volume percentages of CO₂ and N₂ at the end of 12 h storage with the observed values as measured with the gas analyzer are shown in Fig. 3. The deviation of gas composition calculated using Eq. (14) and Eq. (15) from that observed using the gas analyzer was in the range of $\pm 2.0\%$. The R² for regression lines of predicted data and observed data was 0.998. This observation confirmed that the method proposed in this work to estimate headspace CO₂ changes during storage is valid.

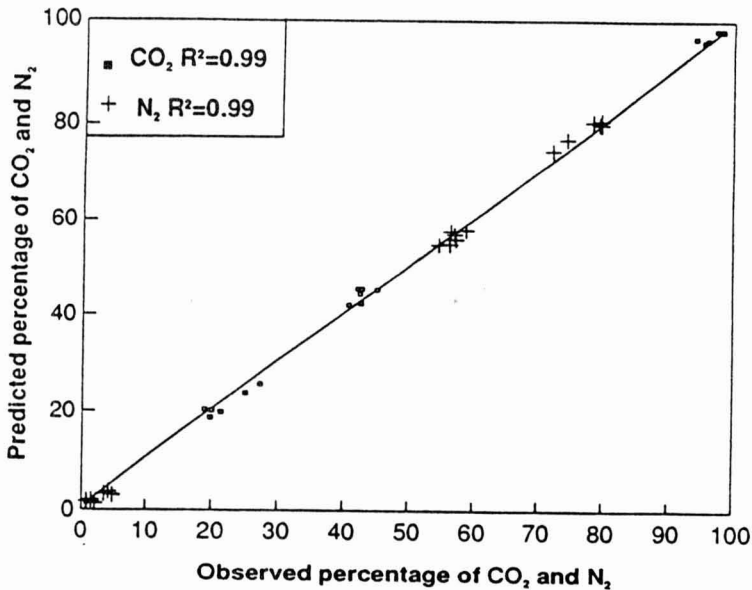


FIG. 3. COMPARISON OF OBSERVED (MEASURED BY GAS ANALYZER) AND PREDICTED (CALCULATED BY ASSUMING THE IDEAL GAS LAW) VOLUME PERCENTAGES OF HEADSPACE CO₂ AND N₂

Validation of N₂ Absorption Assumption

Nitrogen is considered an inert gas in MAP systems and is less soluble in water than CO₂ (Perry and Chilton 1973). Seideman *et al.* (1979) measured the volume and weight percentage changes of N₂ and CO₂ during storage for 100% O₂, 100% N₂, and 100% CO₂ packaged beef. Findings indicated that a significant change in the volume of N₂ did not occur until 14 days of storage. The loss in N₂ after 14 days may have been due to package film permeation or to dissolution of gases into meat tissue (Seideman *et al.* 1979). Enfors and Molin (1984) also reported that CO₂ evolution played an important role in headspace gas behavior for a 100% N₂ packaged beef. The implication was that CO₂ evolution was not due to absorbed O₂, even though it was suggested that it might be due to retained O₂. In the present study, headspace gas pressure increased 14 kPa during 12 h storage for the 100% N₂ packaged beef (Fig. 4). The pressure increase was directly attributed to an increased CO₂ concentration within the headspace as confirmed by analysis of final headspace gas composition. Final CO₂ headspace concentrations ranged from 10% to 13% among replicates. This

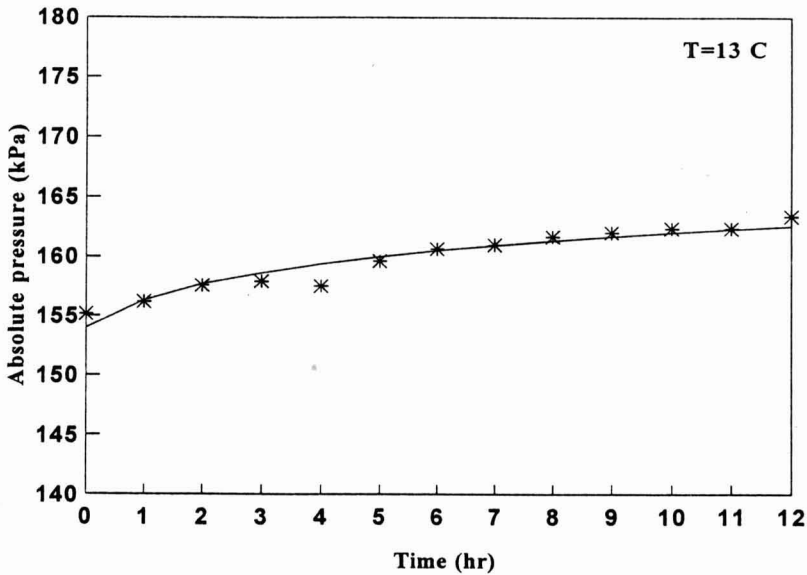


FIG. 4. OBSERVED (SYMBOLS) PRESSURE CHANGES WITH TIME FOR FRESH BEEF PACKAGED WITH 100% N₂ AT 13C

observation further confirmed that N₂ is an inert gas and less soluble compared with CO₂. Thus the assumption to ignore N₂ changes in headspace would appear to be reasonable.

Uncertainty Analysis for Predicted CO₂ absorption

From Eq. (11), CO₂ absorption was calculated by measuring gas pressure, temperature, test chamber volume, and meat sample characteristics. Therefore, a source of error that exists for the predicted CO₂ absorption values is measurement error in the respective variables, propagated within the calculation. The magnitude of the error can be estimated by calculating uncertainty interval for CO₂ absorption. The uncertainty interval for a single sample experiment can be calculated following the procedure by Kline and McClintock (1953). For a function A of n independent variables, v₁, v₂, ..., v_n:

$$A = A(v_1, v_2, \dots, v_n) \quad (16)$$

the uncertainty w_A, is indicated by:

$$w_A^2 = \left(\frac{\partial A}{\partial v_1} w_1\right)^2 + \left(\frac{\partial A}{\partial v_2} w_2\right)^2 + \dots + \left(\frac{\partial A}{\partial v_n} w_n\right)^2 \quad (17)$$

where w₁, w₂, ..., w_n are uncertainty of each independent variable. Since the

CO₂ absorption equation can be expressed as:

$$A_{\text{CO}_2} = \frac{44V_H}{RTM_m} [P_i - P_f] = \frac{44V_H\Delta P}{RTM_m} \quad (18)$$

Evaluating the partial differential terms ($\partial A/\partial v_i$) for Eq. (18) and substituting into Eq. (17) gives:

$$w_{A_{\text{CO}_2}} = 44 \left\{ \left(\frac{\Delta P}{RTM_m} \right)^2 w_{V_H}^2 + 2 \left(\frac{V_H}{RTM_m} \right)^2 w_{\Delta P}^2 + \left(\frac{V_H\Delta P}{RTM_m} \right)^2 \left(\frac{1}{T^2} \right)^2 w_T^2 + \left(\frac{V_H\Delta P}{RT} \right)^2 \left(\frac{1}{M_m} \right)^2 w_{M_m}^2 \right\}^{1/2} \quad (19)$$

where $w_{A_{\text{CO}_2}}$ is the uncertainty of A_{CO_2} , and w_{V_H} , $w_{\Delta P}$, w_T , and w_{M_m} are the uncertainty of V_H , ΔP , T and M_m , respectively. The coefficient 2 for the $w_{\Delta P}$ term is because the uncertainty of ΔP consists of the uncertainty of both P_i and P_f which are the same. Eq. (19) can be greatly simplified by dividing by Eq. (18) to obtain the nondimensionalized form:

$$\left(\frac{w_{A_{\text{CO}_2}}}{A_{\text{CO}_2}} \right)^2 = \left(\frac{w_{V_H}}{V_H} \right)^2 + 2 \left(\frac{w_{\Delta P}}{\Delta P} \right)^2 + \left(\frac{w_T}{T} \right)^2 + \left(\frac{w_{M_m}}{M_m} \right)^2 \quad (20)$$

For typical data observed in this study as an example to calculate the nondimensional uncertainty, a description of the reading might be: $\Delta P = 155 \pm 0.5\% \Delta P$ (kPa), $w_{\Delta P} = 0.775$ (kPa); $V_H = 1.5 \pm 5\% V_H$ (liter), $w_{V_H} = 0.075$ (liter); $T = 286.15 \pm 0.5$ (K), $w_T = 0.5$ (K); $M_m = 650 \pm 2.0$ (gram), $w_{M_m} = 2.0$ (gram).

Substituting above descriptions into Eq. 20 yields

$$w_{A_{\text{CO}_2}}/A_{\text{CO}_2} = 5.06\%$$

Therefore, an uncertainty analysis for A_{CO_2} indicates that the maximum error for A_{CO_2} prediction is approximately 5.1%.

Implications for MAP System Design

The dynamic behavior of CO₂ with respect to initial headspace gas composition, storage temperature, headspace volume of a package, and meat characters is required in establishing design criteria for MAP systems. The measurement methodology is an important tool in advancing an engineering design basis for MAP. The theoretical considerations presented in this work could serve as the basis for developing a MAP design methodology that would predict the amount of headspace CO₂ change based on packaging configuration and storage conditions. The methodology for estimating headspace CO₂ change

is the first step in understanding the influence of packaging configuration and storage conditions on MAP headspace behavior. Zhao *et al.* (1995) developed mathematical equations to relate the amount of CO₂ absorbed by beef during 12 h storage to meat temperature, initial CO₂ concentration, packaging headspace-to-meat volume ratio, and surface area of beef samples. With these equations, processors can predict the minimum amount of CO₂ required to saturate beef at the specific storage and packaging configuration conditions. Therefore, the package collapse observed in the modified atmosphere packaged meat could be avoided. Further, with above calculated amount of CO₂ added to the package, the full effect of CO₂ addition in MAP meat can be achieved since CO₂ quantities in excess of those required for meat saturation could be added to package initially or through a dynamic MAP strategy (Gill and Penney 1988; Zhao *et al.* 1994).

SUMMARY

The combined analytical and experimental method used in this work showed that CO₂ absorption in meat can be estimated directly from observed changes of headspace gas pressure for a gas-impermeable package. Compared with the chemical procedures, this method is very simple, since gas pressure and temperature can be easily and precisely measured. Moreover, the chamber headspace can be changed to consider the influence of different packaging configurations on CO₂ absorption. Various configurations can conveniently be achieved by adding inserts to change chamber volume, by varying gas composition, and by controlling temperature. Assuming chamber integrity can be maintained, the accuracy of CO₂ absorption estimation depends only on the measurements of gas pressure, temperature, and volume of the chamber. Based on the stated precision of the test chamber measurements, the maximum estimated error for CO₂ absorption measurement is approximately 5.1%.

ACKNOWLEDGMENT

The authors thank Mr. Tom McClure for the fabrication of the gas pressure monitoring chamber; Mr. Brian Smith and Mr. Henri Salman for their support through all the experiments.

REFERENCES

- BUSH, P. 1991. Packaging for fresh perceptions. *Prep. Foods*. 16(4), 104-106.
ENFORS, S.-O. and MOLIN, G. 1978. The influence of high concentrations of carbon dioxide on the germination of bacterial spores. *J. Appl. Bacteriol.* 45(2), 279-285.

- ENFORS, S.-O. and MOLIN, G. 1984. Carbon dioxide evolution of refrigerated meat. *Meat Sci.* 10(3), 197–206.
- FARBER, J.M. 1991. Microbiological aspects of modified-atmosphere packaging technology: a review. *J. Food Prot.* 54(1), 58–70.
- GILL, C.O. 1988. The solubility of carbon dioxide in meat. *Meat Sci.* 22(1), 65–71.
- GILL, C.O. and PENNY, N. 1988. The effect of the initial volume to meat weight ratio on the storage life of chilled beef packaged under carbon dioxide. *Meat Sci.* 26(1), 53–63.
- KLINE, S.J. and McCLINTOCK, F.A. 1953. Describing uncertainties in single-sample experiments. *Mechanical Eng.* 75(1), 3–8.
- PERRY, R.H. and CHILTON, K.H. 1973. Pressure measurements, In *Chemical Engineer's Handbook*, 5th Ed. pp. 22–38, McGraw-Hill, New York.
- SAS. 1988. SAS/STAT User's Guide, Release 6.03 Edition. SAS Institute Inc. Cary, NC.
- SEIDEMAN, S.C., SMITH, G.C., CARPENTER, Z.L., DUTSON, T.R. and DILL, C.W. 1979. Modified gas atmospheres and changes in beef during storage. *J. Food Sci.* 44(6), 1036–1040.
- TAYLOR, A.A. 1972. Gases in fresh meat packaging. *Meat World.* 5, 3–10.
- TOLEDO, R.T. 1991. Gases and vapor. In *Fundamental of Food Processing Engineering*. 2nd ed. Van Nostrand Reinhold, New York.
- ZHAO, Y., WELLS, J.H. and McMILLIN, K.W. 1994. Applications of dynamic modified atmosphere packaging for fresh red meat: a review. *J. Muscle Foods* 5(3), 299–328.
- ZHAO, Y., WELLS, J.H., and McMILLIN, K.W. 1995. Dynamic changes of headspace gasses in CO₂ and N₂ packaged fresh beef. *J. Food Sci.* 60(3), 571–575, 591.

MODELING THE POWER CONSUMPTION DURING SHEETING OF DOUGHS FOR TRADITIONAL INDIAN FOODS

C.V. RAGHAVAN¹, NAGIN CHAND^{2,3}, R. SRICHANDAN BABU and P.N. SRINIVASA RAO

*Departments of Process Engineering and Plant Design and
²Sensory Analysis and Statistical Services
Central Food Technological Research Institute
Mysore-570 013, India*

Accepted for Publication February 17, 1995

ABSTRACT

The model given by Levine has been extended to account for the effects of moisture, salt and fat through appropriate modifications based on theory and computational experience. Appropriate modifications to consistency index and flow behavior index as a function of moisture, salt and fat are given. The thickness of sheeted dough has been modeled as a function of gap, reduction ratio and the flow behavior index which constitutes an important contribution. The model so modified was fitted to experimental data on power consumption in sheeting dough prepared from two flour types, viz., whole wheat flour and resultant atta, respectively, at five combinations of gap and reduction ratios and three levels each of moisture, salt and fat (conforming to actual use ranges) using Nelder-Mead algorithm for nonlinear optimization. These models provided 12 constants for each flour type which gave fundamental information on the dough properties for each flour type. Three-dimensional graphics have been used to interpret the model. These models appear to be of much practical use.

INTRODUCTION

Sheeting is an important unit operation in the baking industry and it directly determines the power consumption. Consequently much work has been reported in the literature on sheeting and power requirements (Levine 1985; Kilborn and Tipples 1974). Most of the work is limited to the sheeting for bread making and

¹ Correspondence to: C.V. Raghavan, Scientist, Dept. Process Engineering and Plant Design, Central Food Technological Research Institute, Mysore-570 013, India.

³ Present Address: Scientist, CFTRI Regional Centre, Guru Nanak Engineering College P.O., Gill Road, Ludhiana-141 006, India.

generally related to single level of moisture (used in bread making). Commendable work on constructing a working model to predict power consumption based on theoretical considerations with imposition of certain assumptions has been reported by Levine (1985). In the simplified form also, this model is quite complex. The actual use of the model has been made after assumptions on key physical constants pertaining to dough rheology such as flow behavior index, the dimensionless point at which sheet separates from the roller and the final thickness of sheeted dough (only as a simple multiple of the gap). The model does not account for the effect of different levels of moisture, salt and fat, all of which profoundly modify dough rheology, and hence the power requirements. The purpose of this study is to extend the model reported by Levine (1985) to account for the effects of moisture, salt and fat and also to fit the model more realistically, principally without assumptions of the kind noted above. Two possible common approaches are:

- (1) incorporate such forms of relationship which describe the dough consistency as a function of water, salt and fat based on reported theory, where they exist, or propose appropriate models where the literature is scanty, or
- (2) exploratory modeling using suitable and economic designs offered by statistics under response surface methodology (RSM).

This paper elaborates on the first approach to account for the effects of gap, reduction ratio (RR), water, salt, and fat on power consumption in sheeting of dough prepared from whole wheat flour and resultant *atta*, respectively, covering a wide range in each variable.

Box-Behnken design (Box and Behnken 1960) was used to plan experiments for three factors, water, salt, and fat at each chosen levels of gap and reduction ratios. The design minimized number of experiments under the circumstances. The second approach has also been investigated and is being reported separately.

MATERIALS AND METHODS

Wheat Flours

Whole wheat flour was obtained from a local Chakki (disk mill) and resultant *atta* was produced on a roller flour mill from International School of Milling Technology, CFTRI, Mysore.

Sheeting and Power Consumption Measurements

Experiments were carried out on a dough sheeter developed at CFTRI, Mysore. The unit consists of two-teflon rollers of 50 mm diameter and 300 mm

length. The gap between the rollers can be adjusted by an eccentric shaft mechanism. The maximum clearance between the rollers is 5 mm. The two-teflon rollers are driven by a 0.25 HP motor through a compact reduction gear unit. The rollers rotate at 85 rpm. The power consumed was measured by a digital wattmeter. Dough was prepared under predetermined conditions as given in Table 1.

TABLE 1.
THE BOX-BEHNKEN DESIGN FOR 3 INDEPENDENT VARIABLES

Trial No.	Moisture	Salt	Fat
1	-1	-1	0
2	-1	0	-1
3	-1	1	0
4	-1	0	1
5	0	1	1
6	0	-1	1
7	0	0	0
8	0	0	0
9	0	0	0
10	0	-1	-1
11	0	1	-1
12	1	-1	0
13	1	1	0
14	1	0	-1
15	1	0	1

Coded Values Variable

Moisture,	for WWF (Moisture%-65)/5, for resultant <i>atta</i> (Moisture%-50)/5
Salt,	for WWF (Salt%-1.5)/0.5, for resultant <i>atta</i> (Salt%-4)/0.5
Fat,	for WWF (Fat% -4)/2, for resultant <i>atta</i> (Fat%-1.5)/0.5

METHODOLOGY

Experimental Design

Box-Behnken design (Box and Behnken 1960) was used to investigate the effects of three independent variables viz., water (W), salt (S) and fat (F) at certain discrete and achievable values for reduction ratio (RR) chosen for the purpose, and roll gap upon the power consumption. This statistical design is an

incomplete 3×3 factorial which leads to only 15 experiments for the determination of the linear, quadratic and first order interactions. The designs for the two types of wheat flours are given in Table 1. These designs were repeated at each of the combination of gap (and reduction ratio). Five levels of gap (4.4, 3.15, 1.9, 1.05 and 0.55 mm) were used requiring 5×15 , i.e., 75 experiments in total.

Model Development

The theoretical model (detailed later) was extended to reflect the effects of moisture, salt, and fat on power consumption in the sheeting and fitted using the flexible polyhedron search method published by Nelder and Mead (1965) wherein the values of all the parameters were determined, many of which were generally assumed in literature as reflected earlier. The data corresponding to the experiments (0, 0, 0) performed in identical conditions at central point of Box-Behnken experimental design allow appreciation of reproducibility of results.

RESULTS AND DISCUSSION

Theoretical Considerations

In the present analysis, wheat dough has been assumed to be pseudoplastic fluid material governed by power-law model for reduction of dough thickness from t_f to t_o as shown in Fig. 1.

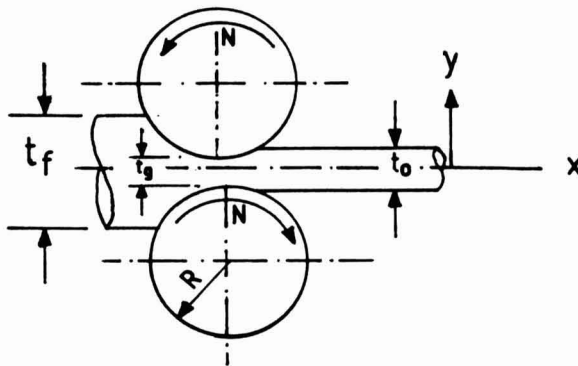


FIG. 1. SCHEMATIC REPRESENTATION OF ROLLS

$$(t_f = 2H_f; t_g = 2H_g; t_o = 2H_o)$$

The most common and simplest mathematical model to describe the power consumption with reference to different reduction ratios (Middleman 1977) is:

$$\tau_{xy} = \int_{y=0}^{y=h(x)} \frac{dp}{dx} \cdot dy \tag{1}$$

where

$$\tau_{xy} = 0 \text{ at } y = 0; h(x) = H_g \left(1 + \frac{x^2}{2H_g R} \right)$$

But the power consumption is given by:

$$P = 2WU \int_{\bar{x}_{feed}}^{\bar{x}_{discharge}} \tau_{xy}|_{y=h(x)} \cdot dx \tag{2}$$

Integrating Eq. (1), we have

$$\tau_{xy} = \frac{dp}{dx} \int_{y=0}^{y=H_g(1 + \frac{x^2}{2H_g R})} dy \tag{3}$$

or

$$\tau_{xy}|_{y=h(x)} = \frac{dp}{dx} \cdot H_g \left[1 + \frac{x^2}{2H_g R} \right] \tag{3}$$

where $\frac{dp}{dx}$ = pressure gradient, defined by (Levine 1985)

$$= - \left[\frac{2n+1}{n} \right]^2 \cdot \frac{m}{\sqrt{2RH_g}} \cdot \left[\frac{U}{H_g} \right]^n \cdot \sqrt{\frac{2R}{H_g}} \cdot \frac{(\bar{x}^2 - \lambda^2) |\lambda^2 - \bar{x}^2|^{n-1}}{(1 + \bar{x}^2)^{2n+1}} \tag{4}$$

where,

$$\lambda^2 = \left[\frac{H_o}{H_r} - 1 \right], \tag{5}$$

H_o = function of t_r , t_g and n

$$\bar{x} = \frac{x}{\sqrt{2RH_g}} \Rightarrow dx = \sqrt{2RH_g} \cdot d\bar{x} \tag{6}$$

$$H_o = \lambda_o H_g (RR)^{n \cdot \lambda_1} + \lambda_2 \tag{7}$$

where RR is Reduction Ratio, = H_f/H_g

Now substituting the value of dp/dx in Eq. (3), we get

$$\tau_{xy|y=kx} = \left(\frac{2n+1}{n} \right)^n \cdot \frac{m}{\sqrt{RH_g}} \cdot \left(\frac{U}{H_g} \right)^n \cdot \sqrt{\frac{2R}{H_g}} \cdot \frac{(\lambda^2 - \bar{x}^2) |\lambda^2 - \bar{x}^2|^{n-1}}{(1 + \bar{x}^2)^{2n+1}} \cdot H_g \left[1 + \frac{x^2}{2H_g R} \right]$$

But $\bar{x} = \frac{x}{\sqrt{2RH_g}}$. Therefore $x^2 = 2 \cdot R \cdot H_g \cdot \bar{x}^2$.

Substituting this in the above equation, we get

$$\tau_{xy|y=kx} = \left(\frac{2n+1}{n} \right)^n \cdot \frac{m}{\sqrt{RH_g}} \cdot \left(\frac{U}{H_g} \right)^n \cdot \sqrt{\frac{2R}{H_g}} \cdot \frac{|\lambda^2 - \bar{x}^2|^n}{(1 + \bar{x}^2)^{2n}} \cdot H_g \tag{8}$$

After considering several modifications and testing them, the following model best described the power consumption for sheeting as a function of fundamental parameters (as detailed earlier) as well as moisture, salt and fat.

$$P = 2WU \int_{\bar{x}_{feed}}^{\bar{x}_{discharge}} \tau_{xy|y=kx} dx$$

but $dx = \sqrt{2 \cdot R \cdot H_g} \cdot d\bar{x}$.

$$P = 2WU \left(\frac{2n+1}{n} \right)^n \cdot \frac{m}{\sqrt{RH_g}} \cdot \left(\frac{U}{H_g} \right)^n \cdot \sqrt{\frac{2R}{H_g}} \cdot H_g \sqrt{2RH_g} \int_{\bar{x}_{feed}}^{\bar{x}_{discharge}} \frac{|\lambda^2 - \bar{x}^2|^n}{(1 + \bar{x}^2)^{2n}} d\bar{x}$$

or

$$P = 2WU \sqrt{2RH_g} \cdot \left(\frac{2n+1}{n} \right)^n \cdot \left(\frac{U}{H_g} \right)^n \cdot m \cdot \int_{\bar{x}_{feed}}^{\bar{x}_{discharge}} \frac{|\lambda^2 - \bar{x}^2|^n}{(1 + \bar{x}^2)^{2n}} d\bar{x} \tag{9}$$

at feed, $\bar{x} = \sqrt{\frac{H_f}{H_o} - 1}$ and discharge, $x = \bar{x}_{dis}$ (not known)

$R = 5.0/2$, $U = 2\pi R.N/60$; where $N = 85$ rpm and $W = 13$ cm and where m , the consistency index, is a function of moisture, salt and fat and based on theory (Rao 1977), as well as experience (from actual computations) following functions were found suitable.

$$m = m_o \cdot \exp(k_1 \cdot \text{water} + k_2 \cdot \text{water}^2) \cdot (1 + k_3 \cdot \text{salt}^{k_4}) \cdot (1 + k_5 \cdot \text{fat}^{k_6}) \quad (10)$$

Similarly for the flow behavior index, n , the following equation appears to be reasonable

$$n = n_o (1 + k_7 \cdot \text{Salt}^{k_8} + k_9 \cdot \text{Fat}^{k_{10}}) \quad (11)$$

where

$$\begin{aligned} \text{Total Mass} &= 1 + (\text{Moisture\%/100}) + (\text{Salt\%/100}) + (\text{Fat\%/100}) \\ \text{water} &= (\text{Moisture\%/100})/\text{Total Mass}; \\ \text{salt} &= (\text{Salt\%/100})/\text{Total Mass}; \\ \text{fat} &= (\text{Fat\%/100})/\text{Total Mass}, \end{aligned}$$

Therefore m_o , n_o , λ_o , λ_1 , λ_2 , \bar{x}_{dis} and k_1 to k_{10} are constants to be determined; m decreased with water, may increase with salt, and decrease with fat, and n may be sensitive to salt and fat.

It was apparent from the examination of initial runs (results not presented) that k_2 was almost zero, and, therefore, for m quadratic term in water may not be necessary. On similar grounds, the effect of salt and fat on “ m ” were linear in nature while for n , the effect of salt was linear and that of fat, a power function. Therefore, in the modified form,

$$m = m_o \cdot \exp(k_1 \cdot \text{water}) \cdot (1 + k_2 \cdot \text{salt}) \cdot (1 + k_3 \cdot \text{fat}) \quad (12)$$

$$n = n_o \cdot (1 + k_4 \cdot \text{salt}) \cdot (1 + k_5 \cdot \text{fat}^{k_6}) \quad (13)$$

Equation (9) was integrated using Simpson’s quadratic formula using 40 intervals.

All the relevant parameters (12 in number, viz., m_o , n_o , λ_o , λ_1 , λ_2 , \bar{x}_{dis} , and k_1 to k_6) were computed by fitting the model to experimental data through the flexible polyhedron search algorithm of Nelder and Mead (1965), which was suitably extended to provide analysis of variance and multiple correlation (Table 2).

The Model Fit

Levine (1985) and Levine and Drew (1990) assumed values for certain constants, especially for the consistency index, the flow behavior index and the dimensionless distance at the discharge based on the values generally cited in literature and picking up the most probable ones for the first two constants,

while for the last, Levine (1985) derived the value with assumption of residual power gradients in the sheeted dough at the extremes of the sheeting process (equal to zero). They clearly indicated that the actual determination was rather difficult.

TABLE 2.
RESULTS OF ANOVA*

Source	df	Mean Square	
		Resultant <i>atta</i>	WWF
Model	12	5.70×10^3	2.16×10^3
Error	62	8.79×10^2	1.46×10^2
Multiple R		0.75	0.86
Mean Absolute Deviation		20.03	8.83

*Significant at 5% confidence level

However, certain numerical techniques are available which can compute (as contrast to experimental determination) such values of the unknown constants in a proposed model so as to give best fit to the experimental data on the final response of interest, which is power consumption in this particular case. The computed values of m_0 , n_0 , λ_0 , λ_1 , λ_2 , \bar{x}_{dis} , and k_1 to k_6 for the two flour types are given in Table 3. Table 4 shows the experimental and model predicted power consumption for sheeting of doughs prepared from WWF and Resultant *atta*. It is apparent from the values of m_0 that the WWF gave doughs of higher consistency as compared to those of Resultant *atta*, however, higher moisture levels used in WWF required lower Power consumption. The value of n_0 (Flow behavior index) gave values of 0.335 and 0.260 which conforms to the range reported for wheat flours. The value of λ_1 is important as it determines the ultimate thickness of the sheeted dough. The values were 2.328 and 2.036 for WWF and Resultant *atta* doughs, respectively, which particularly indicates that the sheet thickness at the discharge will be much greater at larger reduction ratios. Viscoelastic properties support such observations. Using the values of λ_0 , λ_1 and λ_2 , the thickness of sheeted doughs at given Hg and RR can be predicted. The discharge distances obtained were 0.7392 and 0.5722 for WWF and Resultant *atta*, respectively, which are much higher compared to the value given by Levine (1985) which was low at 0.224. The computation of the same has been illustrated by Levine elsewhere (Levine and Drew 1990). The magnitude of \bar{x}_{dis} reported in this paper for doughs prepared from WWF and resultant *atta* are much higher than can be explained so easily, and at least not by the

reasoning given by Levine and Drew (1990). Such high values indicate the discharge of sheeted dough by the rollers much later, and it may be due to stickiness exhibited by the sheeted doughs.

TABLE 3.
COEFFICIENTS DETERMINED USING 2ND ORDER EQUATION FOR
POWER CONSUMPTION

Parameter	Resultant <i>atta</i>	WWF
m_0	358	560
n_0	0.335	0.260
λ_0	0.597	0.613
λ_1	2.328	2.036
λ_2	0.078	0.082
\bar{x}_{dis}	0.5722	0.7392
k_1	-30.47	-26.32
k_2	0.078	0.034
k_3	-36.40	-14.40
k_4	-1.15	-7.45
k_5	-0.061	-0.038
k_6	0.360	0.380
Multiple R	0.75	0.86

The values of k_1 indicated that increasing water levels decreased the consistency of doughs prepared from resultant *atta* more than those from WWF. On the other hand, salt increased the consistency, and nearly twice as much for resultant *atta* as for WWF. Fat decreased the consistency of resultant *atta* much more than it did for doughs from WWF. It indicated that the effectiveness of fat (in decreasing consistency) increased with decreasing extraction rate (of flour). Contrary to this, salt decreased the flow behavior index of WWF nearly seven times more than it did for resultant *atta*.

The values of k_5 and k_6 indicated that fat decreased the flow behavior index of resultant *atta* much more than that for WWF. These results (with multiple correlations of 0.86 and 0.75 for WWF and resultant *atta*, respectively, Table 2) clearly reflect that the variation in rheological properties with water, salt and fat depended on the flour characteristics, such as the extraction rate (apart from the wheat type) and particle size may also play an important role. It becomes imperative to consider interaction between all the macro- and micro-constituents of wheats with water, salt and fat before concluding their effect of a visibly simple but a complex unit operation of sheeting and ultimately the power consumption.

TABLE 4.
EXPERIMENTAL AND PREDICTED POWER CONSUMPTION FOR SHEETING OF
DOUGHS FROM WWF AND RESULTANT ATTA

SN	RR ^b	Gap	X ₃ *	X ₄ *	X ₅ *	Power Consumption (Watts)			
						WWF ^a		Resultant <i>atta</i>	
						Obs	Pred	Obs	Pred
1	1.14	0.440	-1	-1	0	50	44	52	40
2	1.14	0.440	-1	0	-1	48	32	44	39
3	1.14	0.440	-1	1	0	38	39	36	40
4	1.14	0.440	-1	0	1	44	36	30	24
5	1.14	0.440	0	1	1	26	21	18	14
6	1.14	0.440	0	-1	1	12	17	12	14
7	1.14	0.440	0	0	0	20	17	16	9
8	1.14	0.440	0	0	0	8	17	10	9
9	1.14	0.440	0	0	0	12	15	4	9
10	1.14	0.440	0	-1	-1	12	15	24	22
11	1.14	0.440	0	1	-1	16	15	18	22
12	1.14	0.440	1	-1	0	28	18	24	13
13	1.14	0.440	1	1	0	20	17	8	13
14	1.14	0.440	1	0	-1	24	25	16	13
15	1.14	0.440	1	0	1	20	19	4	8
16	1.40	0.315	-1	-1	0	72	63	52	74
17	1.40	0.315	-1	0	-1	54	52	56	55
18	1.40	0.315	-1	1	0	56	57	56	74
19	1.40	0.315	-1	0	1	46	47	52	59
20	1.40	0.315	0	1	1	32	28	72	39
21	1.40	0.315	0	-1	1	22	22	40	39
22	1.40	0.315	0	0	0	24	27	34	20
23	1.40	0.315	0	0	0	30	28	8	20
24	1.40	0.315	0	0	0	14	22	16	20
25	1.40	0.315	0	-1	-1	14	22	30	36
26	1.40	0.315	0	1	-1	18	22	40	36
27	1.40	0.315	1	-1	0	30	27	38	32
28	1.40	0.315	1	1	0	34	27	46	32
29	1.40	0.315	1	0	-1	40	36	20	24
30	1.40	0.315	1	0	1	24	24	42	26
31	1.67	0.190	-1	-1	0	106	87	152	120
32	1.67	0.190	-1	0	-1	70	78	116	77
33	1.67	0.190	-1	1	0	70	78	106	120
34	1.67	0.190	-1	0	1	62	59	76	111
35	1.67	0.190	0	1	1	34	35	118	82
36	1.67	0.190	0	-1	1	26	28	106	82
37	1.67	0.190	0	0	0	48	40	56	36
38	1.67	0.190	0	0	0	54	12	62	36
39	1.67	0.190	0	0	0	32	30	26	36
40	1.67	0.190	0	-1	-1	22	30	52	57
41	1.67	0.190	0	1	-1	44	30	72	57
42	1.67	0.190	1	-1	0	32	37	72	65
43	1.67	0.190	1	1	0	42	41	58	65

TABLE 4. (Continued)

SN	RR ^b	Gap	X ₃ *	X ₄ *	X ₅ *	Power Consumption (Watts)			
						WWF ^a		Resultant <i>atta</i>	
						Obs	Pred	Obs	Pred
44	1.67	0.190	1	0	-1	44	50	44	42
45	1.67	0.190	1	0	1	28	31	58	60
46	1.80	0.105	-1	-1	0	92	100	154	136
47	1.80	0.105	-1	0	-1	80	193	122	95
48	1.80	0.105	-1	1	0	82	89	96	136
49	1.80	0.105	-1	0	1	66	65	72	115
50	1.80	0.105	0	1	1	40	30	76	89
51	1.80	0.105	0	-1	1	32	30	58	89
52	1.80	0.105	0	0	0	52	48	26	43
53	1.80	0.105	0	0	0	56	50	36	43
54	1.80	0.105	0	0	0	34	34	36	43
55	1.80	0.105	0	-1	-1	30	34	40	74
56	1.80	0.105	0	1	-1	48	34	62	74
57	1.80	0.105	1	-1	0	34	42	96	81
58	1.80	0.105	1	1	0	44	48	52	81
59	1.80	0.105	1	0	-1	48	57	64	57
60	1.80	0.105	1	0	1	32	34	68	69
61	1.90	0.055	-1	-1	0	96	110	172	142
62	1.90	0.055	-1	0	-1	82	106	194	116
63	1.90	0.055	-1	1	0	88	98	148	142
64	1.90	0.055	-1	0	1	68	70	82	103
65	1.90	0.055	0	1	1	44	42	130	82
66	1.90	0.055	0	-1	1	36	33	88	82
67	1.90	0.055	0	0	0	64	55	72	46
68	1.90	0.055	0	0	0	72	57	72	46
69	1.90	0.055	0	0	0	42	38	50	46
70	1.90	0.055	0	-1	-1	44	38	62	93
71	1.90	0.055	0	1	-1	52	38	84	93
72	1.90	0.055	1	-1	0	44	46	102	91
73	1.90	0.055	1	1	0	48	55	84	91
74	1.90	0.055	1	0	-1	48	63	58	74
75	1.90	0.055	1	0	1	46	36	64	66

*As under Table 1

^aWhole wheat flour^bReduction ratio

The approach detailed here reflects the need to actually determine or compute the constants governing the power consumptions during sheeting operation. The pressure gradient in the dough during sheeting does not appear to be zero, especially for large RR values as the material, that is, dough, is viscoelastic in nature. This may be a major reason for higher values of \bar{x}_{dis} reported in this paper. The differences in power consumption for the two doughs and comments on the trends of power consumption with the water, salt, fat, etc.,

will be explained through certain selected 3-D graphs.

Effect of Water and Salt on Power Consumption at RR of 1.9, Gap of 0.055 cm and 4% and 1.5 % Fat

The variation of power consumption for water and salt is given in Fig. 2(a) and 2(f). For both the flour types, power consumption decreased exponentially with water, the reduction was much more for resultant *atta* dough as compared to doughs prepared from WWF. With salt, power consumption increased marginally at all levels of water.

Effect of Water and Fat on Power Consumption

The 3-D graphs at 1.5 and 4% salt are given in Fig. 2(b) and 2(g) for WWF and resultant *atta*, respectively. For both the flour types the power consumption decreased with fat and the effect was more pronounced for dough prepared from resultant *atta*. The trend with water was similar to that explained earlier.

Effect of Fat and Salt on Power Consumption

The power consumption decreased with fat for both the dough types; however, for WWF doughs, it followed a decreasing convex curve while for the resultant *atta* it was almost a linear decrease. The two doughs also showed different patterns of power consumption with salt. For WWF, power consumption decreased with increasing salt while it increased for resultant *atta*. The effects of fat and salt (compared to that for water) on power consumption are also complicated due to their relation with the flow behavior index [Fig. 2(c) and 2(h)].

Effect of Gap and Fat on Power Consumption

Figures 2(d) and 2(i) show the variation of power consumption with gap and fat at constant levels of RR (1.9), water (65 and 50%), and salt (1.5 and 4%) for WWF and resultant *atta*, respectively. For both the flour types, the power consumption decreased sharply with increasing gaps (from 0.05 to 0.21 cm) and then stabilized at gaps of >0.21 cm requiring small power consumption. With increasing fat, as expected, the Power consumption decreased for both the flour types.

Effect of Water and RR on Power Consumption

At constant levels of gap, salt and fat, the power consumption as a function of water and RR are shown in Fig. 2(e) and 2(j) for WWF and resultant *atta*,

respectively. The power consumption increased with RR, for both the flour types, hyperbolically; however, at higher RR values, the power consumption increased slowly especially at higher moisture levels, while at lower moisture the power consumption kept increasing quite significantly but not as much as it did up to RR values of 1.2.

The variation in H_0 was related to the gap, RR and n and detailed under theoretical considerations. As it will be important to predict the thickness of the sheeted dough, the 3-D plots of $2H_0$ (output thickness) are shown in Fig. 3(a) and 3(b) for WWF and resultant *atta*, respectively, keeping water, salt and fat at constant levels as detailed earlier.

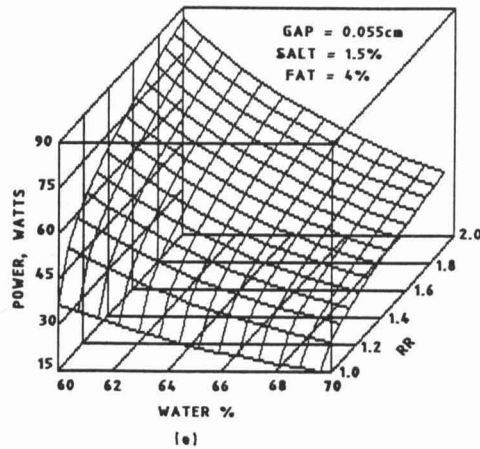
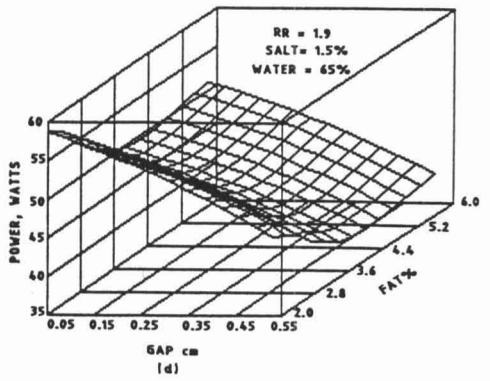
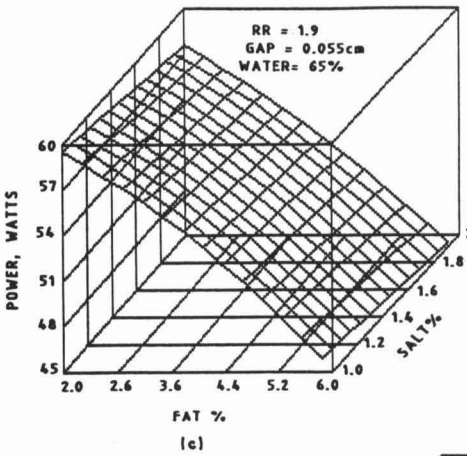
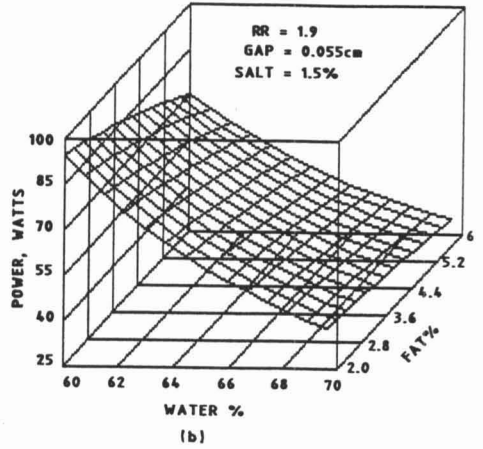
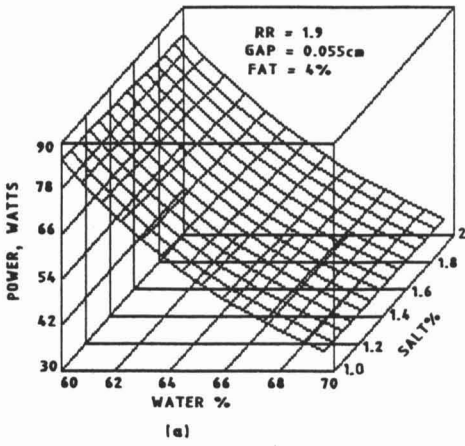
The latter two appear in the relationship developed between n and salt and fat. It is apparent from these figures that at higher RR values, with increasing gaps the output thickness could be more than 2–3 times the gap. However, at the lowest gap values tried in the reported experiments (0.055 cm), the predicted values of 0.15 and 0.2 cm appear to be on the higher side, and there is a scope to improve the model further.

Similarly Fig. 4(a) and 4(b) show variation of n , the flow behavior index, with salt and fat and show that n decreases with increasing salt levels and just marginally so with increasing fat levels. The latter is clear in Fig. 4(b) for resultant *atta*. These plots throw light on the influence of additives, such as salt and fat, on fundamental properties of doughs and justifies further research work in building more theoretically sound and practically supported models in future.

CONCLUSIONS

It is apparent from the results presented in this paper that the final sheet thickness depends on the gap, reduction ratio and flow behavior index and that actual quantitative relationship will be desirable rather than assume a flat constant determining the final thickness of the sheeted dough. As the material is viscoelastic in nature, the elastic energy retained in the material after sheeting will actually determine the final thickness. Reduction ratio has been identified as the single most important parameter determining the final thickness, along with the flow behavior index which is determined by the type of flour and ingredients, such as salt and fat, present in the dough. As a result, the relationship given for the predictions of sheet thickness, coupled with the determination of n as a function of salt and fat, is an important quantitative contribution detailed in this paper in the quest for building a model for power consumption.

The influence of water and salt on the consistency index, though known, has been given in quantitative terms, along with the effect of fat. These modifications increased the relevance and applicability of the model to actual use conditions for the preparation of various sheeted products such as chapathi, *nan* and other related products.



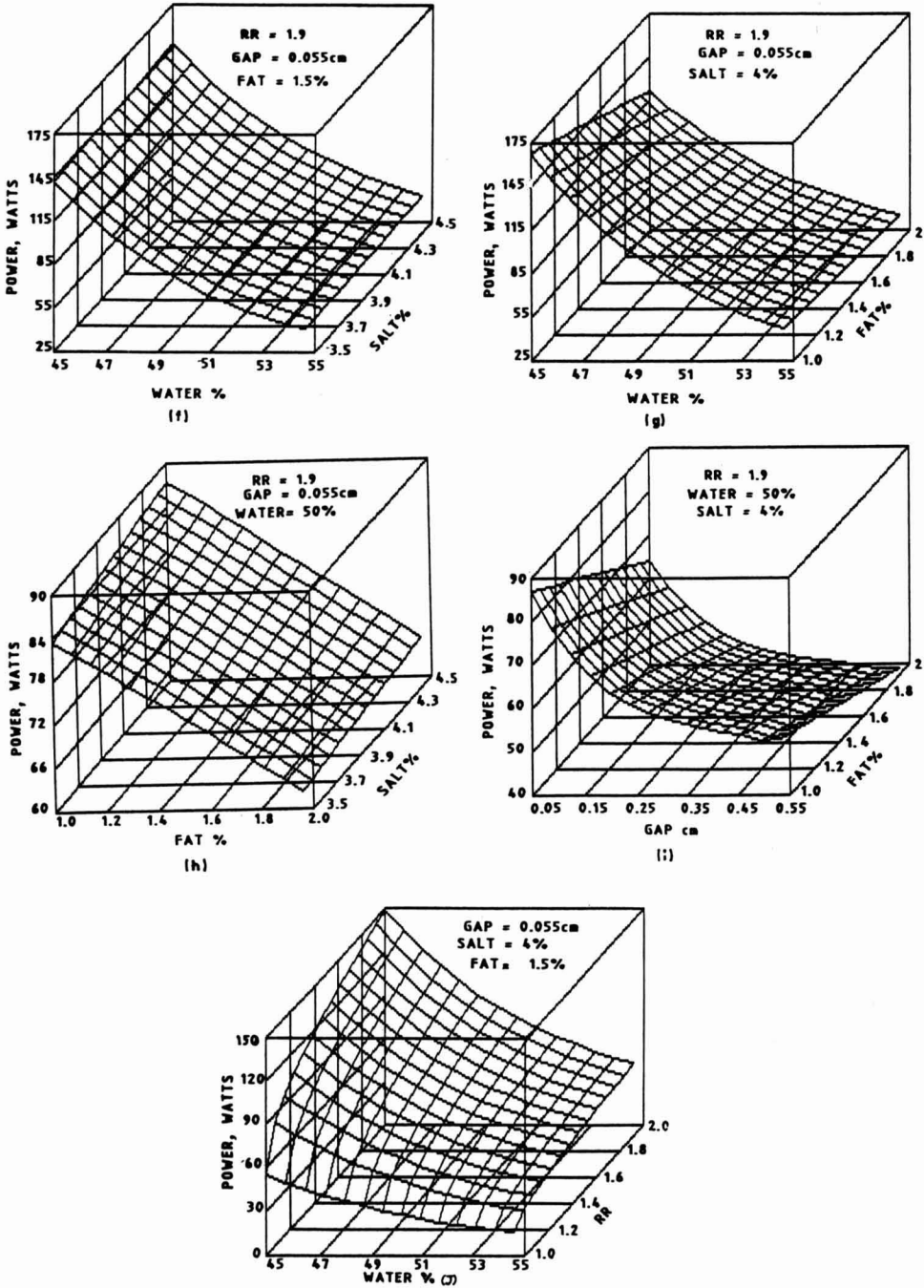


FIG. 2. RESPONSE SURFACES SHOWING THE EFFECTS OF DIFFERENT LEVELS OF MOISTURE, SALT, FAT, RR AND GAP ON POWER CONSUMPTION FOR TWO TYPES OF FLOURS (WWF AND RESULTANT ATTA, RESPECTIVELY)

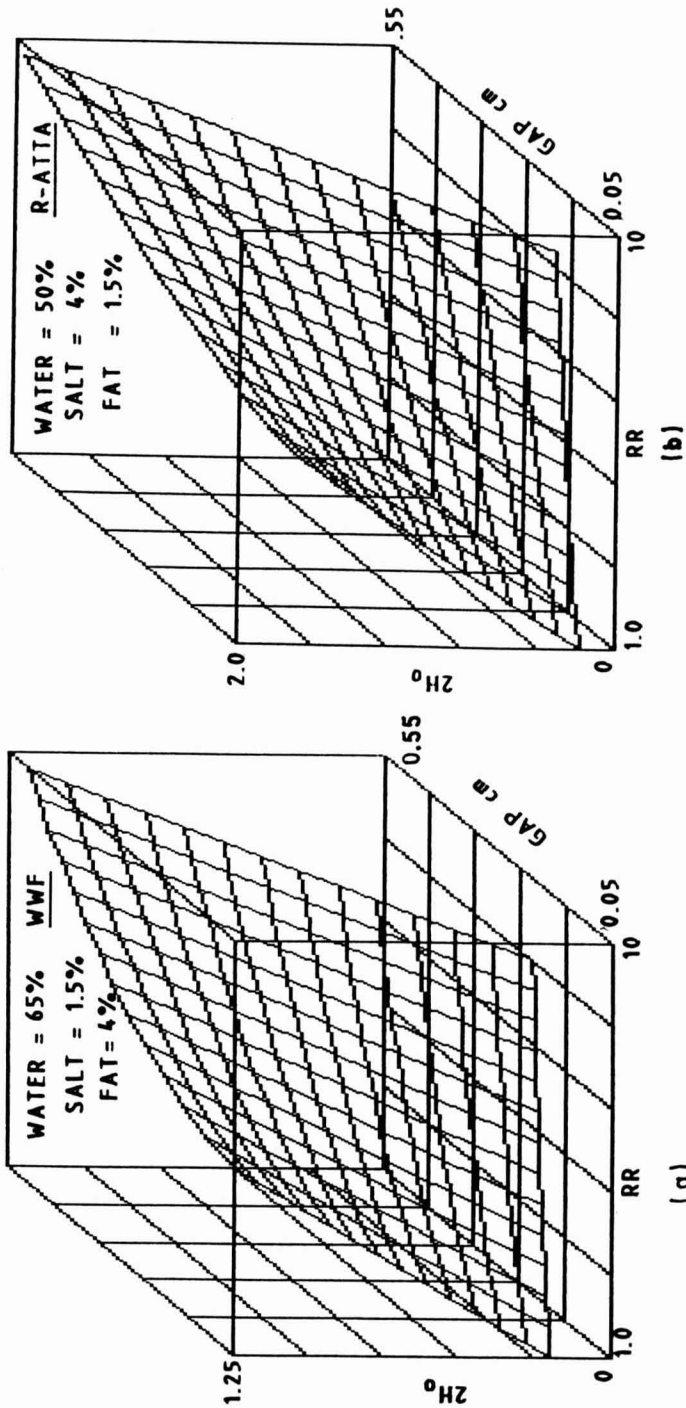


FIG. 3. RESPONSE SURFACES SHOWING THE EFFECT OF RR AND GAP ON 2H₀ (FINAL SHEET THICKNESS) FOR TWO TYPES OF FLOURS (WWF AND RESULTANT ATTA, RESPECTIVELY)

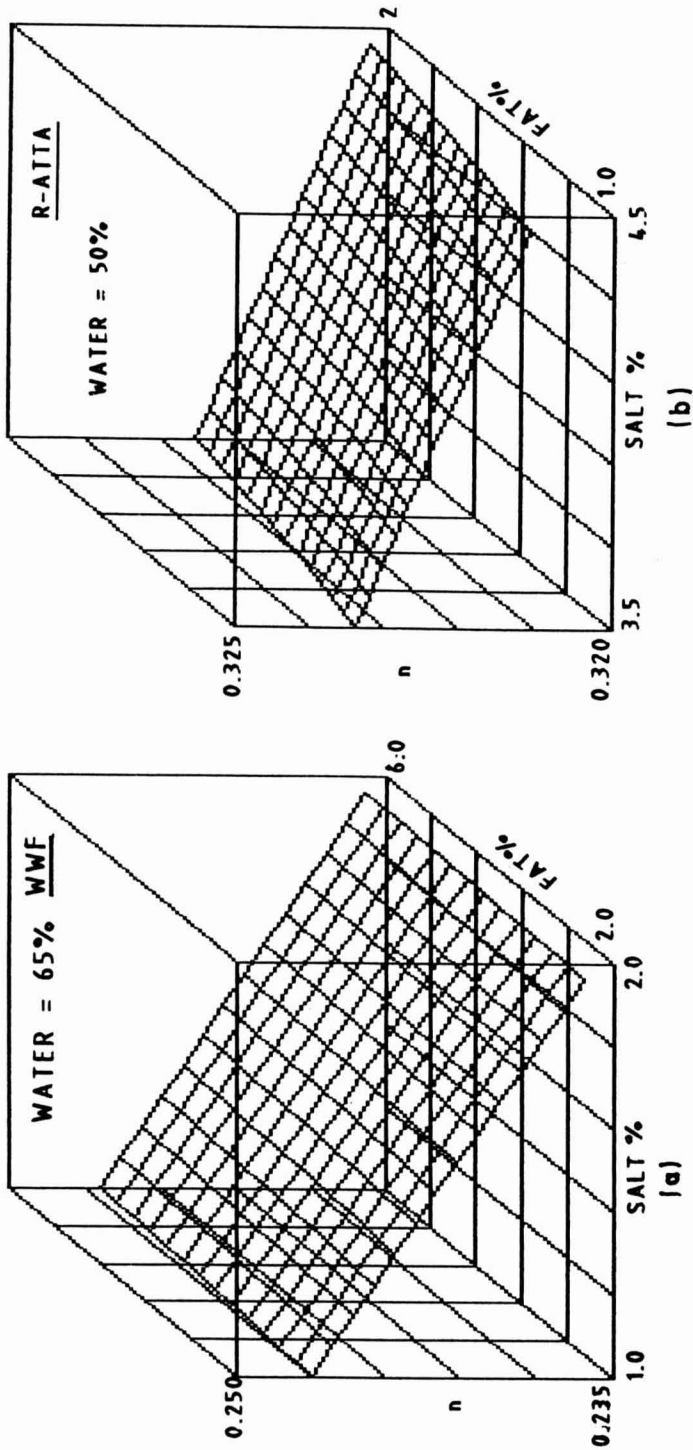


FIG. 4. RESPONSE SURFACES SHOWING THE EFFECT OF SALT AND FAT ON, n , FLOW BEHAVIOR INDEX FOR TWO TYPES OF FLOURS (WWF AND RESULTANT ATTA, RESPECTIVELY)

The magnitude of \bar{x}_{dis} as obtained for the two flour types indicates that a certain pressure gradient remained in the dough even at the extremes of the sheeting process; this requires further careful examination of the mathematical complexities involved, and from the mechanical engineering point of view. However, the approach adapted in this communication provides a practical approach to actually computing some of the important parameters governing power consumption.

NOMENCLATURE

English

D	=	Roll diameter
H	=	One half of sheet thickness
h(x)	=	Distance from center line to roll surface
m	=	Flow consistency
n	=	Power law flow index
N	=	Roll rotational speed
P	=	Power consumption, Watts
p	=	Pressure between rolls
R	=	Roll radius
t	=	Sheet thickness
U	=	Peripheral roll velocity
W	=	Roll width
x	=	Coordinate in direction of dough flow
\bar{x}	=	Dimensionless position = $x/\sqrt{2RHg}$
y	=	Coordinate in direction normal to dough flow M = Moisture, %
S	=	Salt, %
F	=	Fat, %
RR	=	Reduction Ration Subscriptions
dis	=	Discharge
f	=	Feed position
g	=	Nip
o	=	Output

Greek letters

λ	=	Dimensionless distance from nip to separation
τ_{xy}	=	Shear stress (dynes/cm ²)

REFERENCES

- BERGEN, J.T. and SCOTT, B.W. 1951. Pressure distribution in the calendering of plastic materials, *J. Appl. Mech.* 18, 101–106.
- BOX, G.E.P. and BEHNKEN, D.W. 1960. Some new three level designs for the study of quantitative variables. *Technometrics* 2, 455–475.
- CHONG, J.S. 1968. Calendering of thermosplastic materials. *J. Appl. Polym. Sci.* 12, 191–212.
- COCHRAN, W.G. and COX, G.M. 1957. *Experimental Designs*, John Wiley & Sons, New York.
- EHRMAN, G. and VLACHOPOULOS, J. 1975. Determination of power consumption in calendering. *Rheol. Acta* 14, 761–764.
- KILBORN, R.H. and TIPPLES, K.H. 1974. Implications of the mechanical development of bread dough by means of sheeting rolls. *Cereal Chem.* 51, 648–657.
- LEVINE, L. 1985. Throughput and power of dough sheeting rolls. *J. Food Proc. Eng.* 7, 223–228.
- LEVINE, L. and DREW, B.A. 1990. Rheological and engineering aspects of the sheeting and laminating of doughs. In *Dough Rheology and Baked Product Texture*, (H. Faridi and J.M. Faubion, eds.) pp. 513–556, Van Nostrand Reinhold, New York.
- MIDDLEMAN, S. 1977. *Fundamentals of Polymer Processing*, McGraw-Hill, New York.
- NELDER, J.A. and MEAD, R. 1965. A simplex programme for solving minimization problems. *Computer J.* 7, 308–313.
- TADMOR, Z. and GAGOS, C.G. 1979. *Principles of Polymer Processing*, John Wiley & Sons, New York.

EFFECT OF PLASTICIZER LEVEL AND TEMPERATURE ON WATER VAPOR TRANSMISSION OF CELLULOSE-BASED EDIBLE FILMS¹

MANJEET S. CHINNAN² and HYUN J. PARK³

²*Center for Food Safety and Quality Enhancement
Department of Food Science & Technology
University of Georgia, Agricultural Experiment Station
Griffin, GA 30223-17973*

and

³*Author Park was a graduate student in the
Department of Food Science & Technology,
University of Georgia and is now an
Assistant Professor with the Department of Food Engineering
Mokpo National University, Mokpo, Korea*

Accepted for Publication February 17, 1995

ABSTRACT

This study was conducted to determine water sorption isotherms of cellulose-based films made from methyl cellulose (MC) and hydroxypropyl cellulose (HPC), and to evaluate the effect of plasticizer concentration and temperature on water vapor permeability coefficient in those films. The equilibrium moisture contents of MC film and HPC film increased slowly with an increase in water activity (a_w) up to 0.75, but increased greatly after 0.75 a_w . The water vapor permeability coefficient of HPC film increased as the concentration of polyethylene glycol (PEG) increased; however, the water vapor permeability coefficient of MC film which contained 0.22 ml PEG/g cellulose was lower than of films which contained no or higher PEG. An Arrhenius-type relationship was fitted to examine temperature dependence of water vapor permeability coefficients of cellulose films. The edible films studied exhibited relatively low activation energies (14.56-16.43 kJ/mol) compared with typical food packaging materials.

¹ Department of Food Science and Technology, University of Georgia, Agricultural Experiment Station, Griffin, GA 30223.

² Send Correspondence to: Dr. Manjeet S. Chinnan, Professor Center of Food Safety and Quality Enhancement, Department of Food Science & Technology, University of Georgia, Griffin, GA 30223-1797, TEL: 770-228-7284, FAX 770-229-3216

INTRODUCTION

Controlling moisture exchange is a critical factor in extending the shelf-life of moisture sensitive foods (fresh fruits and vegetables), and processed products (frozen foods, candies, snacks and cookies). Edible coatings for fresh fruits and vegetables have been used to control moisture loss with the purpose of prolonging their shelf-life during storage (Erbil and Muftugil 1986; Risse *et al.* 1987; Smith and Stow 1984). Water loss in fresh fruits and vegetables can adversely affect their quality during the marketing period. Edible coatings can act as a moisture barrier. They can also create and allow the build-up of carbon dioxide level and reduction of oxygen level inside the fruit or vegetable tissue thus reducing respiration rate and potentially extending product shelf-life.

Concerns have been raised about transmigration of monomers from plastic films into foods when in contact (Park and Ashcraft 1989); for example, the monomer of polyvinyl chloride has been listed as a carcinogen. However, cellulose-based films are edible, biodegradable and fall under the GRAS (generally recognized as safe) category (Kester and Fennema 1986). The cellulose-based films may be used as packaging materials which come in contact with foods. Edible coatings for processed products also could be used as moisture barriers to extend product shelf-life during their marketing. Kester and Fennema (1989b) reported that the lipid-cellulose film placed at the interface of two components, bread and a tomato-based sauce, effectively retarded migration of moisture from sauce to bread during storage. Rico-Pena and Torres (1990a) used methyl cellulose-palmitic acid film in a simulated ice cream cone core as moisture-impermeable barrier and observed that the sample of sugar cone which contained this film showed no detectable moisture increase for 10 weeks at -23C and for 4 weeks at -12C.

Gas and water vapor permeation properties in edible films including cellulose are affected by several factors such as solvent type, plasticization, polymer material, and other film additives (Banker 1966; Banker *et al.* 1966; Pascat 1986). Gontard *et al.* (1993) recently published data on the effect of glycerin as a plasticizing agent on water vapor barrier properties of wheat gluten film and reported that the water vapor transmission rate increased as concentration of the plasticizer increased in the film. Park and Chinnan (1995) made cellulose-based films which contained two different concentrations of plasticizer and found that the gas and water vapor permeability coefficient increased with increasing plasticizer level. Overall, very limited work has been reported in the literature on the plasticizer effect on the water vapor barrier properties of cellulose-based films.

Several reports exist on determining the water vapor permeability coefficient and water vapor sorption isotherm in plastic films (Labuza and Contreras-Medellin 1981; Karel *et al.* 1959). Linear relationship between water

content and water activity (a_w) in the plastic films was observed (Karel *et al.* 1959). Water vapor permeation properties of cellulose-based films and protein-based films are different when compared with plastic films. The moisture isotherms of most edible films made from biopolymers are not linear over a wide range of a_w . Gontrad *et al.* (1993) reported that the slope of water vapor sorption isotherm of wheat gluten film increased linearly in the range of 0 to 0.68 a_w and then increased sharply beyond 0.68 a_w . However, data on water vapor sorption isotherm of cellulose-based films is not available.

Labuza and Contreras-Medellin (1981) found that water vapor gas permeability coefficients increased in plastic films as temperature increased. Temperature effect on oxygen permeability coefficients of protein-based films was reported by Gennadios *et al.* (1993), and Arrhenius plots were fitted by them in the temperature range of 7 to 35C. However, the authors of this study are not aware of any study reporting the effect of temperature on water vapor barrier properties of cellulose-based films.

The objectives of this study were to (1) determine the water vapor sorption isotherms of cellulose-based films, and (2) evaluate the effect of plasticizer concentration and temperature on water vapor permeability coefficients in those films.

THEORETICAL CONSIDERATION

Fick's first law can be applied to the water vapor permeation process when it is assumed that the diffusion is in a steady state and there is a linear concentration gradient through the film. Then, the flux (J) is given by

$$J = D \cdot \Delta C/X = Q/(A \cdot t) \quad (1)$$

where, J is flux ($\text{g}/\text{m}^2 \cdot \text{s}$), D is diffusion coefficient (m^2/s), ΔC is concentration difference across the film (g/m^3), X is thickness of the film (m), Q is amount of water diffusing through the film (g), A is area of the film (m^2) and t is time (s) (Crank 1975).

The driving force needs to be expressed in terms of partial pressure difference, rather than the concentration difference because it is easier to measure pressure difference and then correlate to concentration difference. Therefore, Henry's law, where the vapor pressure of the solute varies with concentration in a linear manner, could be applied. A rearrangement of terms yields the following equation in terms of permeability coefficient and partial pressure difference (Crank 1975).

$$D \cdot S \cdot (p_2 - p_1)/X = P \cdot (p_2 - p_1)/X = Q/(A \cdot t) \quad (2)$$

where, S is the Henry's law solubility coefficient ($\text{g}/\text{m}^3 \text{ Pa}$), p_2-p_1 is the partial pressure difference across the film (Pa) and P is the permeability coefficient ($\text{g}\cdot\text{m}/\text{m}^2\cdot\text{s}\cdot\text{Pa}$). It may be noted that Henry's law is not applicable in those packaging materials which exhibit nonlinear moisture sorption isotherm (Karel *et al.* 1959; DeLeiris 1986); however, it is often applied to such materials (e.g., edible films). In situations when Henry's law is applied for determining permeability coefficients, the resulting values are effective or average permeability coefficients and valid only for the conditions of the experiment.

MATERIALS AND METHODS

Materials

The materials used to prepare the cellulose films were: methyl cellulose (25 cp), hydroxypropyl cellulose (370,000 mw), polyethylene glycol (400 mw) (Aldrich Chemical Company, Inc., Milwaukee, WI); and ethanol, 95% (Fisher Scientific, Pittsburgh, PA). All the salts for saturated salt solutions to obtain moisture isotherms are listed in Table 1 and were acquired from Fisher Scientific (Pittsburgh, PA).

TABLE 1.
RELATIVE HUMIDITY (%) OF VARIOUS SALTS SOLUTIONS¹

Salts	Relative humidity ¹	
	5C	21C
Potassium acetate	25	23
Magnesium chloride	33	33
Magnesium nitrate	54	52
Cupric chloride	65	68
Sodium chloride	76	75
Ammonium sulfate	81	79
Lithium sulfate	84	85
Potassium sulfate	98	97

¹Rockland (1960).

Preparation of the Cellulose-Based Films

Methyl cellulose (MC) and hydroxypropyl cellulose (HPC) based film solutions were prepared by dissolving 9 g of each cellulose in a solvent mixture

containing 200 ml of ethanol and 100ml of distilled water (Kamper and Fennema 1984; Park and Chinnan 1995). Three solutions were prepared for each cellulose type containing polyethylene glycol (PEG) as plasticizer at levels of 0, 0.11, 0.22 and 0.33 ml PEG/g cellulose. Brinkmann homogenizer (Westbury, NY) was used to mix the film solution. For degassing, solution was heated until it started boiling. The degassed solution was poured onto a glass plate and dried. The film thus formed was carefully detached from the glass plate and used for determining moisture sorption isotherm and water vapor permeability coefficient properties.

Thickness Measurement

A micrometer was used to measure the film thickness to an accuracy of 0.0025 mm. Ten measurements were made at random positions on each film.

Moisture Sorption Isotherms

Dried HPC film and MC film were cut into small pieces (less than 0.015 g), weighed, and then placed over saturated salt solutions in desiccators at constant temperature (5C and 21C) to provide water activities in the range 0.23-0.97 (Table 1). Final moisture contents were determined after moisture had equilibrated which was verified by periodic weight measurements. Samples were dried overnight at 100C under vacuum to determine moisture content as described in AOAC (1980) method 23.002 for gelatin. Tests were conducted in triplicate.

Water Vapor Permeability Coefficient (WVP)

Three plastic cups of high density polyethylene (3 mm thick) filled with desiccant and covered with HPC film and MC film to be tested were placed individually in two desiccators, one was 33%RH (MgCl_2) and the other was 75%RH (NaCl), at 5, 13, 21C, respectively. The change in weight of the cups against time was recorded every two hours. The permeability coefficient was calculated from Eq. 2; where water vapor pressure (p_1) on the desiccant side of the film was assumed to be zero and the water vapor pressure (p_2) in the desiccator due to MgCl_2 or NaCl salt solution was calculated from the vapor pressure of pure water at respective selective humidities. It is to be noted that no forced air movement was provided and we did not specifically follow the ASTM E96-80 method for determination of WVP. However, we did follow the procedures published by other researchers and the authors of this study (Kamper and Fennema 1984; Aydt *et al.* 1991; Park and Chinnan 1995).

RESULTS

Moisture Sorption Isotherms

Sorption isotherms of the MC film and HPC film at 5 and 21C are shown in Fig. 1 and 2, where moisture content was plotted against water activity. At higher temperatures, less moisture was absorbed at a given water activity. This trend is well documented in literature for most food materials. The sorption isotherm curves of MC film and HPC film (Fig. 1 and 2) can be viewed as two distinct segments indicating that the equilibrium moisture increases slowly with an increase in water activity up to 0.75, beyond which there was a sharp increase in equilibrium moisture of the films tested. Linear regression analysis of moisture content and water activity (a_w) data for a_w from 0 to 0.75 yielded R^2 values greater than 0.98 (Table 2). Including a_w values beyond 0.75 drastically reduced R^2 values.

The shape of sorption isotherm of the MC film was similar to that of methyl cellulose-palmitic acid film, reported by Rico-Pena and Torres (1990b), which had weight ratio of 3:1 at 24C. The equilibrium moisture of MC film was slightly higher than that of HPC film at a given water activity. Moisture isotherms were not determined at 13C, although the water vapor permeability coefficients were measured at 13C in addition to 5 and 21C. Observing the similarity in shapes of 5 and 21C isotherms, it was not believed necessary to obtain 13C isotherm for our study.

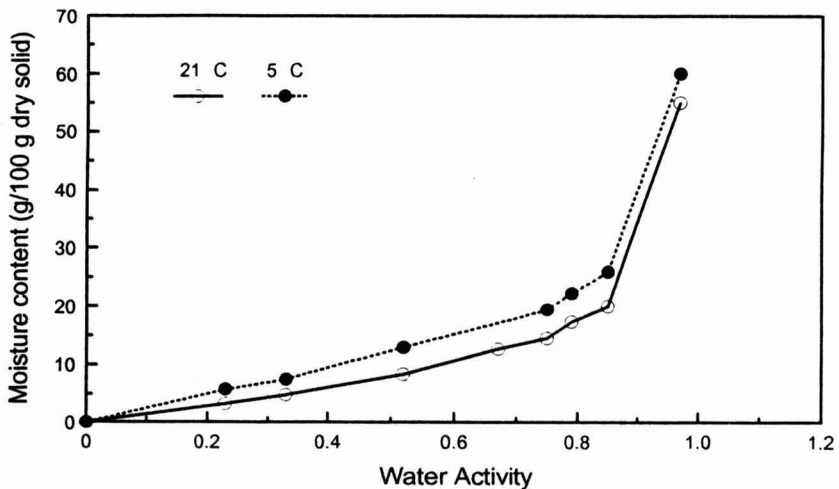


FIG. 1. MOISTURE SORPTION ISOTHERMS OF METHYL CELLULOSE FILM WITHOUT PLASTICIZER AT 5 AND 21C.

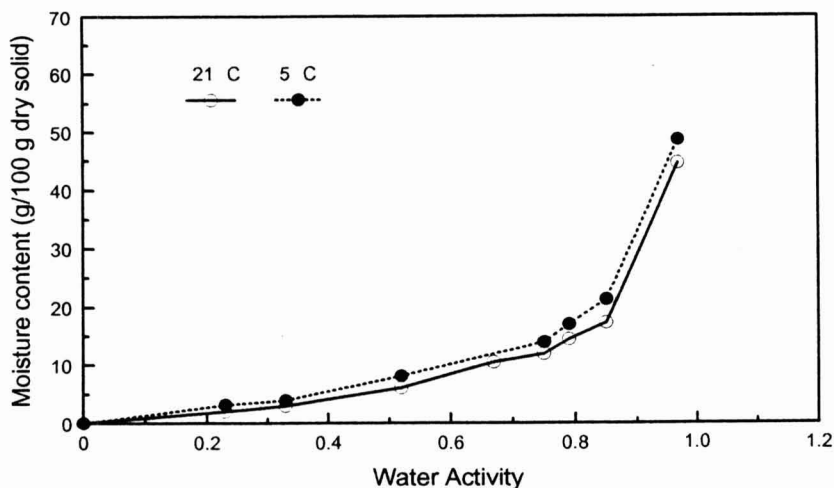


FIG. 2. MOISTURE SORPTION ISOTHERMS OF HYDROXYPROPYL CELLULOSE FILM WITHOUT PLASTICIZER AT 5 AND 21C

TABLE 2.
REGRESSION ANALYSIS OF MOISTURE ISOTHERM DATA OF METHYL CELLULOSE (MC) AND HYDROXYPROPYL CELLULOSE (HPC) FILMS

Film	Temperature (C)	Relative humidity-Data Range (%)	Regression analysis statistics	
			Slope	R ²
MC	5	0-33	23.1	0.995
		0-75	24.6	0.995
	21	0-33	14.4	0.999
		0-75	19.6	0.980
HPC	5	0-33	12.4	0.988
		0-75	15.3	0.973
	21	0-33	8.95	0.999
		0-75	16.5	0.949

Water Vapor Permeability Coefficient (WVP)

WVPs of cellulose films, MC and HPC, were considerably greater than those of commonly used plastic films such as polyethylene (PE) and polyvinyl chloride (PVC) in Table 3. Without any plasticizer, WVP of HPC film was expected higher than that of MC film because HPC has a hydroxyl group in hydroxypropyl functional groups. But WVP of HPC film was lower than that of methyl cellulose. Reduction of WVP of HPC film could be attributed to formation of hydrogen bond between HPC polymers (Banker *et al.* 1966).

TABLE 3.
WATER VAPOR PERMEABILITY COEFFICIENTS OF SELECTED FILMS

Film	Thickness (mm)	Relative humidity difference(%)	Permeability ^a
Cellulose film in this study ^b			
HPC	0.08	75	68.5 ± 2.7
		33	51.6 ± 4.4
MC	0.11	75	154.4 ± 4.1
		33	113.5 ± 5.7
Cellulose films from the literature			
C 18-C 16 HPMC ^c	0.04	97	4-22
C18-C16 MC/HPMC ^c	0.02	97	3-16
HPMC ^d	0.01-0.04	85	15-200
Other films from the literature			
PE ^c	-	100-90	0-7
PVC ^c	-	100-90	0.6

^a Unit of permeability is in $\text{pg}\cdot\text{m}/\text{m}^2\cdot\text{s}\cdot\text{Pa}$ at 21°C; p is an abbreviation of pico (10^{-12}).

^b Cellulose films without plasticizer.

^c Kester and Fennema (1989a); C18 (stearic acid), C16 (palmitic acid), MC (methyl cellulose), HPMC (hydroxypropylmethyl cellulose), PE (Polyethylene, low density) and PVC (Polyvinyl chloride).

^d Hagenmaier and Shaw (1990).

It may be noted that Eq. 2 can be used to calculate the WVP in linear portion of moisture sorption isotherm for hydrophilic films because of Henry's law (Karel *et al.* 1959; DeLeiris 1986). WVPs of MC and HPC films in this study were measured at a_w differences by 0-0.33 and 0-0.75 which are linear portions in moisture sorption isotherms curves of the films. Therefore, the permeability of the films are theoretically same if these are measured inside of linear portion of moisture sorption isotherms curves. However, slopes of moisture content and a_w data for a_w from 0 to 0.75 in moisture sorption isotherms curves were higher than those of a_w from 0 to 0.33, which can cause

higher WVPs in the films. Kester and Fennema (1989a) also reported that the WVPs of cellulose films measuring at 0-97% relative humidity (RH) gradient were lower than those of films measuring at 67-95% RH gradient in cellulose films. Higher slopes of moisture content and a_w data for a_w from 67-95 than those of the slopes for a_w from 0-95 in moisture sorption isotherms of methyl cellulose films (Rico-Pena and Torres 1990b) would contribute to higher WVPs of the cellulose films measuring at 67-95% RH gradient in Kester and Fennema work (1989a). Labuza and Contreras-Medellin (1981) also reported that many hydrophilic films show a change in WVP depending on vapor pressure conditions. The HPC film was more flexible than MC film, which is probably attributed to HPC polymer having longer side chains than MC. WVPs of cellulose films of Kester and Fennema (1989a) contained stearic and palmitic acids and were lower than those of cellulose films prepared in our laboratory, which could be attributed to fatty acids in the former films (Table 3). WVP of plastic films were 2 orders of magnitude lower than those of cellulose films.

Plasticizer Effect. The effect of plasticizer concentration on WVP of cellulose films is shown in Fig. 3. WVP of HPC film increased as the concentration of polyethylene glycol (PEG) increased from 0 to 0.33 ml PEG/g cellulose. However, the WVP of MC film showed a different trend compared to HPC film. The WVP of MC film containing 0.22 ml PEG/g cellulose was lower than those of MC films which contained 0, 0.11 and 0.33 ml PEG/g cellulose. Banker *et al.* (1966) observed that the plasticizer could enhance or retard moisture permeation of cellulose films, depending upon its concentration. Park and Chinnan (1995) reported that the WVP of HPC film and MC film increased as the concentration of PEG increased from 0.11 to 0.33 ml PEG/g cellulose. In wheat gluten film, WVP increased linearly as concentration of the plasticizer, glycerin, increased in the range of 16 to 33 g glycerin/100 g protein (Gontard *et al.* 1993). The surfaces of cellulose films containing higher level of plasticizer had smoother appearance than the films with low level of plasticizer.

Temperature Dependence. Temperature dependence of WVP of HPC and MC films is illustrated in Fig. 4. An Arrhenius-type relationship given below was fitted to data.

$$P = A \cdot \exp(-E_a/R \cdot T) \quad (3)$$

where P is permeability coefficient ($\text{g} \cdot \text{m} / \text{m}^2 \cdot \text{s} \cdot \text{Pa}$), A is constant, E_a is activation energy (J/mol), R is gas constant ($8.314 \text{ J/mol} \cdot \text{K}$) and T is absolute temperature (K). After logarithmic transformation, Eq. 3 is written as

$$\ln(P) = \ln(A) - (E_a/R) \cdot (1/T) \quad (4)$$

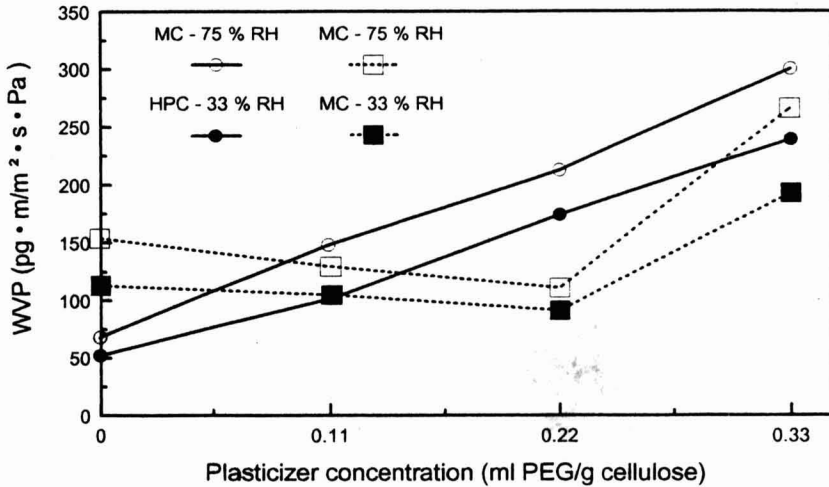


FIG. 3. PLASTICIZER EFFECT ON WATER VAPOR PERMEABILITY COEFFICIENT (WVP) OF HYDROXYPROPYL AND METHYL CELLULOSE FILMS
 HPC-75% RH (HPC film, WVP measured with 75% RH difference)
 HPC-33% RH (HPC film, WVP measured with 33% RH difference)
 MC-75% RH (MC film, WVP measured with 75% RH difference)
 MC-33% RH (MC film, WVP measured with 33% RH difference)
 PEG (polyethylene glycol), HPC (hydroxypropyl cellulose)
 and MC (methyl cellulose).

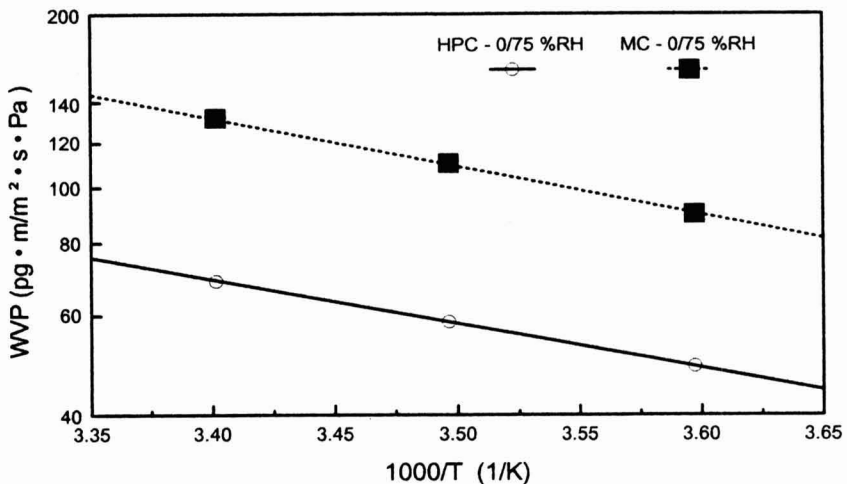


FIG. 4. TEMPERATURE DEPENDENCE OF THE WATER VAPOR PERMEABILITY COEFFICIENT (WVP) OF HYDROXYPROPYL AND METHYL CELLULOSE FILMS WITHOUT PLASTICIZER
 HPC-75% RH (HPC film, WVP measured with 75% difference)
 HPC (hydroxypropyl cellulose).

Slope of the fitted regression line allowed calculation of an apparent activation energy E_a . The same procedure described above was applied to calculate activation energy of MC film. The activation energies of HPC and MC films which had no plasticizer were 14.56 and 16.43 kJ/mol, respectively. These are relatively low activation energies, when compared with various packaging films such as polyvinylidene chloride, polypropylene, polyvinyl chloride and polyethylene (Labuza and Contreras-Medellin 1981; Myers *et al.* 1961). Kester and Fennema (1989a) observed a large value for activation energy (59.4 kJ/mol) in a waxed laminated cellulose film, this is probably due to heterogeneity of the laminated film. Gennadios *et al.* (1993) reported that activation energies of protein films such as corn-zein, wheat gluten and wheat and soy protein isolate films ranged from 46 to 50 kJ/mol (11 to 12 Kcal/mol), which is several fold greater than the cellulose films investigated here.

SUMMARY AND CONCLUSIONS

The sorption isotherm curves of MC film and HPC film indicated that the equilibrium moisture content increases slowly with an increase in water activity (a_w) up to 0.75, but increases sharply after a_w of 0.75. The equilibrium moisture of MC film was slightly higher than that of HPC film at a given water activity. The water vapor permeability coefficient of cellulose films were 2 orders of magnitude greater than those of typical plastic films, polyethylene and polyvinyl chloride. The water vapor permeability coefficient of HPC film increased as the concentration of polyethylene glycol (PEG) increased; however, the water vapor permeability coefficient of MC film which contained 0.22 ml PEG/g cellulose was lower than those of MC films which contained 0, 0.11 and 0.33 ml PEG/g cellulose. Temperature dependence of the water vapor permeability coefficient of HPC film and MC film followed an Arrhenius type relationship. The activation energies of HPC film and MC film containing no plasticizer were 14.56 and 16.43 kJ/mol, respectively; these are relatively low active energies compared with typical food packaging materials such as polyvinylidene chloride, polypropylene, polyvinyl chloride and polyethylene. Additional observations about these cellulose based films indicate that they have appearance and surface characteristics similar to those of plastic films. They are also transparent, without any odor and taste.

REFERENCES

- AOAC. 1980. *Official Methods of Analysis*, 13th ed. Association of Official Analytical Chemists, Washington, DC.
- AYDT, T.P., WELLER, C.L. and TESTIN, R.F. 1991. Mechanical and barrier properties of edible corn and wheat protein films. *Trans. ASAE* 34,

- 207—211.
- BANKER, G.S. 1966. Film coating theory and practice. *J. Pharm. Sci.* 55, 81–89.
- BANKER, G.S., GORE, A.Y. and SWARBRICK, J. 1966. Water vapor transmission properties of free polymer films. *J. Pharm. Pharmac.* 18, 457–466.
- CRANK, J. 1975. *The Mathematics of Diffusion*, pp. 44–68, Oxford University Press, London.
- DELEIRIS, J.P. 1986. Water activity and permeability. In *Food Packaging and Preservation. Theory and Practice*, (M. Mathlouthi, ed.) pp. 213–233, Elsevier Applied Science, London, England.
- ERBIL, H.Y. and MUFTUGIL, N. 1986. Lengthening the postharvest life of peaches by coating with hydrophobic emulsions. *J. Food Processing and Preservation* 10, 269–279.
- GENNADIOS, A., WELLER, C.L. and TESTIN, R.F. 1993. Temperature effect on oxygen permeability of edible protein-based films. *J. Food Sci.* 58, 212–219.
- GONTARD, N., GUILBERT, S. and CUQ, J. 1993. Water and glycerol as plasticizers affect mechanical and water vapor barrier properties of an edible wheat gluten film. *J. Food Sci.* 58, 206–211.
- HAGENMAIER, R.D. and SHAW, P.E. 1990. Moisture permeability of edible films made with fatty acid and hydroxypropyl methylcellulose. 38(9), 1799–1803.
- KAMPER, S.L. and FENNEMA, O. 1984. Water vapor permeability of edible bilayer films. *J. Food Sci.* 49, 1478–1485.
- KAREL, M., PROCTOR, B.E. and WISEMAN, G. 1959. Factors affecting water-vapor transfer through food packaging films. *Food Technol.* 13, 69–74.
- KESTER, J.J. and FENNEMA, O. 1986. Edible films and coatings: a review. *Food Technol.* 40, 47–59.
- KESTER, J.J. and FENNEMA, O. 1989a. An edible film of lipids and cellulose ethers: barrier properties to moisture vapor transmission and structural evaluation. *J. Food Sci.* 54, 1383–1389.
- KESTER, J.J. and FENNEMA, O. 1989b. An edible film of lipids and cellulose ethers: performance in a model frozen food system. *J. Food Sci.* 54, 1390–1406.
- LABUZA, T.P. and CONTRERAS-MEDELLIN, R. 1981. Prediction of moisture protection requirements for foods. *Cereal Food World* 26, 335–343.
- MYERS, A.W., MEYER, J.A., ROGERS, C.E., STANNETT, V. and SZWARC, M. 1961. Studies on the gas and vapor permeability of plastic films and coated papers. VI. The permeation of water vapor. *TAPPI* 44, 58–69.

- PARK, H.C. and ASHCRAFT, C.R. 1989. The use of polyacrylnitrile film in barrier food packaging. In *Plastic Film Technology*, (K.M. Finlayson, ed.) pp. 12–20, Techomic, Lancaster, PA.
- PARK, H.J. and CHINNAN, M.S. 1995. Gas and water vapor barrier properties of edible coatings for fruits and vegetables. *J. Food Eng.* 25, 497–507.
- PASCAT, B. 1986. Study of some factors affecting permeability. In *Food Packaging and Preservation: Theory and Practice*, (M. Mathlouthi, ed.) pp. 6–23, Elsevier Applied Science, London, England.
- RICO-PENA, D.C. and TORRES, J.A. 1990a. Edible methyl cellulose-based films as moisture impermeable barriers in Sundae Ice Cream cones. *J. Food Sci.* 55, 1468–1469.
- RICO-PENA, D.C. and TORRES, J.A. 1990b. Oxygen transmission rate of an edible methylcellulose-palmitic acid film. *J. Food Process Engineering* 13, 125–133.
- RISSE, L.A., CHUN, D., MCDOLAND, R.E. and MILLER, W.R. 1987. Volatile production and decay during storage of cucumbers waxed, imazalil-treated, and film-wrapped. *HortScience* 22, 274–276.
- ROCKLAND, L.B. 1960. Saturated salt solutions for static control of relative humidity between 5C and 40C. *Analytical Chemistry* 32, 1375–1376.
- SMITH, S.M. and STOW, J.R. 1984. The potential of a sucrose ester coating material for improving the storage and shelf-life qualities of Cox's orange Pippin apples. *Annu. Appl. Biol.* 104, 383–391.

HEAT TRANSFER TO AND TRANSPORT PROPERTIES OF WHEAT GLUTEN IN A TUBULAR REACTOR

T.D. STRECKER

Kellogg Company
235 Porter St./P.O. Box 3423
Battle Creek, MI 49016

R.P. CAVALIERI¹

Biological Systems Engineering Dept.
Washington State University
Pullman, WA 99164

and

R. ZOLLARS

Chemical Engineering Dept.
Washington State University
Pullman, WA 99164

Received for Publication March 20, 1995

ABSTRACT

The design and modeling of a tubular reactor, similar to an extrusion rheometer, which accounts for reacting flow is described. A numerical study (finite differences) of heat transfer to a flowing and reacting biopolymer melt (wheat gluten), similar to extrusion processing, is described and compared to experimental data. The cylindrical wall is nonisothermal in the axial direction, but is adequately characterized by a third-order polynomial determined experimentally. Convective and viscous dissipation terms are included in the energy equation. The rheological behavior of the melt is described by a power

law model, $\tau = m_0 e^{\left(\frac{-E}{RT}\right)} \dot{\gamma}^n$. The consistency coefficient pre-exponential, m_0 , is 530,000-2,100,000 Pa-secⁿ and the power law exponent or flow index, n , is 0.38-0.65 for a 25-30% moisture content range and a 110-209 C temperature range. The flow index decreases with increasing conversion due to polymerization reactions occurring at elevated temperatures. Flow curves, bulk temperatures, and temperature profiles are presented for a variety of cylinder wall temperatures and biopolymer moisture contents.

¹To whom correspondence should be sent; Phone (509) 335-1578.

INTRODUCTION

New texturized plant protein products are being developed each year. In recent years wheat flour and gluten have become more widely used in feedstock formulations for use in extrusion cooking (Barres *et al.* 1990; Lawton *et al.* 1985; Boyal and Phoolka 1989; Andersson and Hedlund 1990).

Extruders first became important to the food industry as a process to mix flour with steam or water and to pump this mixture at elevated pressures through extrusion dies to form a product (Harper 1981). They are now used extensively to form and/or cook product in a one-step unit operation.

Several groups have stated the research needs in food extrusion processing (Harper and Harmann 1973; Baird and Reed 1989). They said that the following areas of research are still needed to facilitate further application of food extrusion and, more importantly, understand the process more scientifically: (1) extruder modeling, (2) transport phenomena, (3) physical properties, (4) physical and chemical reactions, (5) process control, and (6) scale up.

Mathematical models of single-screw extruders have been developed and tested using polymer extrusion theory for plastics (Harper 1981; Wagner 1987; Baird and Reed 1989). Numerous extrusion flow equations have been developed by Biesenberger and Sebastian (1983), Fricke *et al.* (1977), Tadmor and Gogos (1979) that are readily applicable to food extrusion theory.

However, kinetic, thermodynamic, and rheological properties of food doughs during extrusion must be known before theoretical extruder equations can effectively be used for modeling. Since their properties are functions of operating variables such as temperature, shear rate, time-temperature history, and moisture content, mechanistic models describing kinetic and thermodynamic processes are needed for application to extrusion theory. The variability of temperature, shear rate, time-temperature history and pressure throughout an extruder renders them almost useless in kinetic, thermodynamic and rheological analysis. Only in the case of major simplifying assumptions, such as Newtonian flow and isothermal conditions, can a proximate analysis be done. Since it is known that plasticated doughs behave as non-Newtonian fluids (Baird and Reed 1989), considerable error is already introduced by the first assumption.

The extrusion rheometer, referred to most often as a capillary rheometer, has been used as a tool for measuring viscosity of molten polymers and doughs over a wide range of shear rates (Pezzin 1962; Morgan *et al.* 1978; Wagner 1987). Pezzin (1962) used an extrusion rheometer to obtain rheological data on polystyrene and other polymers and he concluded that such data could be correlated with flow behavior of polymers in commercial extrusion processing. Therefore, an extrusion rheometer should provide an adequate method of measuring rheological properties of food dough feedstocks operating at similar conditions found in extrusion processes. Lower viscous dissipation is adequately

compensated for by applying direct heat to the rheometer. Thus, an extrusion rheometer serves as a useful laboratory extruder for studying kinetic, thermodynamic, and rheological properties of dough feedstocks analyzed at typical extruder operating conditions.

Most often an extrusion rheometer is used to measure, in the case of dough materials, the viscosity of the material that has reached temperature equilibrium with the heated sample reservoir. Typically, the dough is placed in a heated sample reservoir, allowed to equilibrate, and then, using a plunger-ram system, extruded through a die. With this system no account is taken for the effect of time-dependent reaction on flow properties since the total reaction has been allowed to take place (equilibration time) before the interacting material is extruded. Transport processes in a food extruder are the result of a reacting flow, which is quite different from usual plastics extrusion processes involving no chemical reactions. A rheometer capable of simulating such flow would be of great utility in providing information on kinetic, thermodynamic, and rheological properties actually occurring during extrusion processing.

The objectives of this research were to: (1) design and construct a simple tubular reactor, similar to an extrusion rheometer, for studying kinetic and rheological properties of doughs during extrusion, (2) model the heat transfer to the biopolymer melt in the reactor, and (3) determine the rheological properties of a reacting and flowing system.

DESIGN OF THE TUBULAR REACTOR

Since no reaction was desired before entering the heated reaction region, the reactor, the apparatus was designed with two temperature regions. The sample reservoir needed to be cooled so that no thermally-induced reactions would occur. Therefore, one of the design criterion was to determine how to confine the heat to the reactor without heating the sample reservoir walls in the process. Another design criterion was to simulate the residence times in the melt-section of an extruder, i.e., 2-10 s (Harper 1981). Once the temperature profiles in the reactor were modeled, the time-temperature history of the biopolymer melt was predictable and kinetic information was, therefore, obtainable.

The sample reservoir with an inside diameter 1.27 cm and 10.2 cm long was constructed. An identical section was constructed for the reactor as is shown in Fig. 1. A 1.27 cm polyamide plastic spacer was constructed to fit between these two sections to provide thermal insulation. It was able to withstand the temperatures and pressures typically used in an extruder. A 500W band heater 5.08 cm in length was employed to heat the reactor. The die was 1.59 mm in diameter and 10.2 cm in length. A pressure vessel was constructed to pressurize the reactor outlet using nitrogen to prevent flashing as the extrudate exited the reactor. Two thermocouple wells (not shown in Fig. 1) were installed. One was

located just above the thermal insulator to monitor the cool zone temperature and the other one was located above the band heater for temperature monitoring and heater control. The barrel housing the reactor was wrapped with 6.0 cm thick insulation to prevent heat losses. The entire apparatus was bolted to a stand and an Instron universal testing machine was used to provide the force for the plunger and the force measurements needed to perform the experiments.

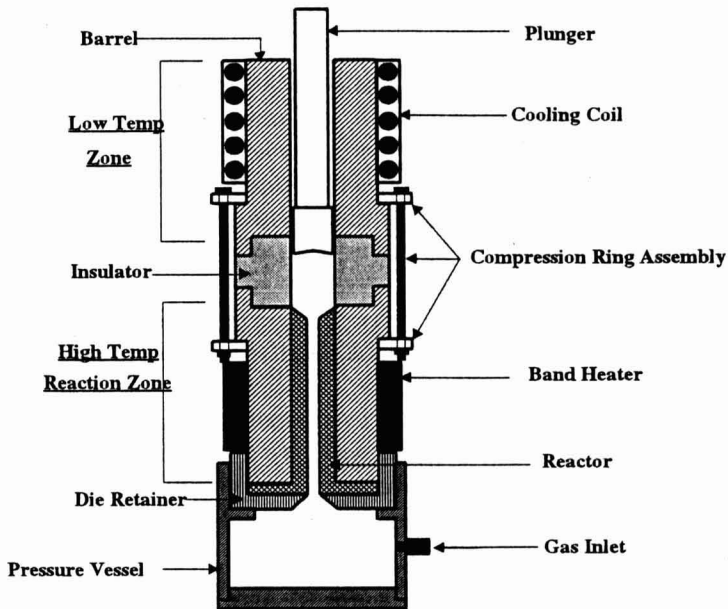


FIG. 1. TUBULAR REACTOR SHOWING LOCATION OF MAJOR COMPONENTS

MATHEMATICAL FORMULATION

The physical system for pressure flow through a cylindrical channel (extruder die) is illustrated in Fig. 2. It consists of flow through a cylinder with an inside radius, R , and wall temperatures characterized by third-order

polynomials. The reactor wall temperature profiles were determined experimentally by inserting a thermocouple probe into the reactor and taking measurements every 5.0 mm. The experimentally determined reactor wall temperature profiles are shown in Fig. 3. The average axial wall temperature, $T_{z,avg}$, was the arithmetic average temperature along the entire length of the reactor wall. Table 1 lists the equations for each curve in Fig. 3.

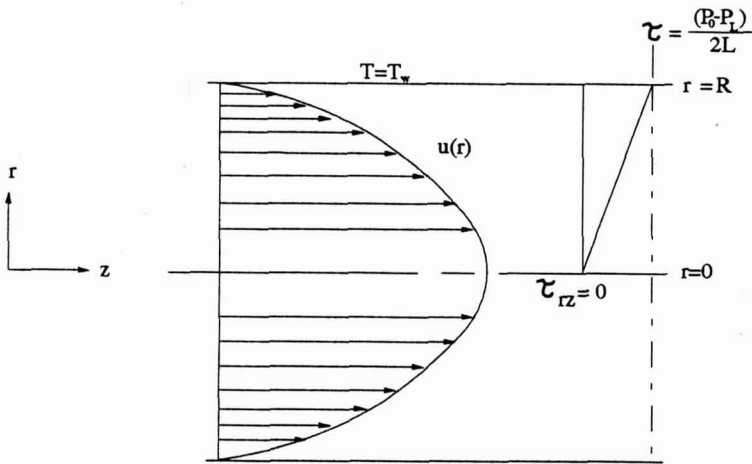


FIG. 2. NOTATION FOR PRESSURE FLOW THROUGH A CYLINDRICAL CHANNEL

TABLE 1.
AXIAL WALL TEMPERATURE PROFILE EQUATIONS FOR THE EXTRUDER DIE
USED FOR THE WALL BOUNDARY CONDITIONS IN SIMULATING HEAT TRANSFER
TO A FLOWING MOLTEN BIOPOLYMER.

$T_{z,avg}(C)$	$T_z = f(z)$
110	$3.21 \times 10^{-5} z^3 - 0.0174 z^2 + 1.74 z + 73.9$
167	$1.93 \times 10^{-5} z^3 - 0.0215 z^2 + 2.39 z + 115$
209	$8.43 \times 10^{-5} z^3 - 0.0391 z^2 + 3.51 z + 145$

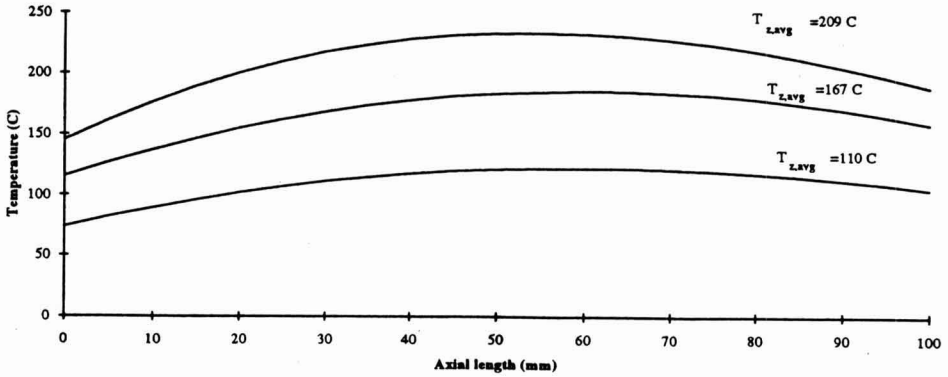


FIG. 3. AXIAL REACTOR WALL TEMPERATURE PROFILES WITH THE AVERAGE AXIAL WALL TEMPERATURE GIVEN FOR EACH PROFILE

The energy equation can be simplified by making the following assumptions:

- (1) Inertial forces are negligible in comparison with viscous and pressure forces.
- (2) Body forces (e.g., gravity) are also negligible.
- (3) Thermal conductivity, specific heat and density are constant.
- (4) Normal stresses are negligible.
- (5) Heat transfer by conduction in the direction of flow is negligible compared to both convection in the direction of flow and conduction perpendicular to the direction of flow.

The simplified energy equation is

$$\rho c_p u \frac{\partial T}{\partial z} = k \frac{\partial}{\partial r} \left[r \frac{\partial T}{\partial r} \right] + \tau_{rz} \left[-\frac{du}{dr} \right] \quad (1)$$

or

$$\rho c_p u \frac{\partial T}{\partial z} = k \frac{\partial^2 T}{\partial r^2} + \frac{k}{r} \frac{\partial T}{\partial r} + \tau_{rz} \left[-\frac{du}{dr} \right] \quad (2)$$

where u is the velocity in the z -direction.

A common constitutive equation for polymer melts is

$$\tau_{rz} = \eta \left[-\frac{du}{dr} \right] \quad (3)$$

where

$$\eta = m \left| \frac{du}{dr} \right|^{n-1} \quad (4)$$

Since non-isothermal conditions existed in the reactor, the Arrhenius form of η was used resulting in Eq. (4) becoming

$$\eta = m_0 e^{\left(\frac{-E}{RT}\right)} \left| \frac{du}{dr} \right|^{n-1} \quad (5)$$

Then, by substitution into the energy equation, we obtain

$$\rho c_p u \frac{\partial T}{\partial z} = k \frac{\partial^2 T}{\partial r^2} + \frac{k}{r} \frac{\partial T}{\partial r} + m_0 e^{\left(\frac{-E}{RT}\right)} \left[-\frac{du}{dr} \right]^{n+1} \quad (6)$$

From the continuity and momentum equations the velocity profile is

$$u = \left[\frac{\Delta P}{2Lm} \right]^{1/n} \left[\frac{R}{\nu} \right] \left[1 - \left(\frac{r}{R} \right)^\nu \right] \quad (7)$$

where $\nu = \frac{n+1}{n}$

From Eq. (7) we obtain an expression for $\frac{du}{dr}$

$$\frac{du}{dr} = - \left[\frac{\Delta P r}{2Lm} \right]^{1/n} \quad (8)$$

Substitution of Eq. (7) and (8) into Eq. (6) for u and du/dr results in the following energy equations as a function of r :

$$\rho C_p \left[\left(\frac{\Delta P}{2Lm} \right)^{1/n} \left(\frac{R}{\nu} \right) \left[1 - \left(\frac{r}{R} \right)^\nu \right] \right] \frac{\partial T}{\partial z} = k \frac{\partial^2 T}{\partial r^2} = m_0 e^{\left(\frac{-E}{RT} \right)} \left[\left(\frac{\Delta Pr}{2Lm} \right)^\nu \right]^{n+1} \quad (9)$$

The boundary conditions for the above equations are the following:

$$\begin{aligned} z = 0: & \quad T = T_0 \text{ (given in Table 3)} \\ r = R: & \quad T = f(z) \text{ (given in Table 1)} \end{aligned}$$

A finite difference scheme using an integration technique of the Adams-Moulton type was used to solve the previous equations. The finite difference method used ten elements in the radial direction and each element was subsequently integrated in the axial direction. Integration error criteria was 1×10^{-6} .

The local bulk temperature, T_{bulk} , was determined by calculating a weighted average of the temperatures at each element using the following definition:

$$T_{\text{bulk}} = \sum_{i=1}^n T_i \left(\frac{r_i^2 - r_{i-1}^2}{R^2} \right) \quad (10)$$

where i is the element used in the finite difference scheme.

MATERIALS AND METHODS

Fractionation

Commercial gluten, the unfractionated protein constituent of wheat feedstock, was purchased from Midwest Grain Company. Gluten was fractionated into ethanol soluble gliadin and ethanol insoluble glutenin using the Osborne procedure (Osborne 1907). Albumin and globulin, water soluble proteins, were solubilized using 0.5M NaCl. The 0.5M NaCl - gluten mixture was agitated for 2 h at 4C and subsequently centrifuged for 2 h at 2000 g. The supernatant was discarded and the residue was rinsed with 40 ml distilled water for 30 minutes to remove residual salt. The residue remaining after solubilization with salt solution was then solubilized with 70% ethanol. The ethanol insoluble fraction, glutenin, was freeze dried, milled and stored at 4C. Five gram samples were used in all experiments. All experiments were done in triplicate. Each powdered sample was mixed with water to achieve a 25% or 30% moisture content (w.b.) and stored overnight at 4C to reach equilibrium.

Biopolymer Rheology

The reactor was heated to 100, 155, or 195C depending on the temperature desired using a proportional controller. The sample reservoir was cooled by pumping ice water through the cooling coil and was maintained below 40C. An Instron testing instrument was employed to ram the plunger and measure the resulting force. The Instron was operated in the load control mode so that a constant load could be maintained independent of displacement. The pressure vessel was equipped with a viewing glass and light so that velocity measurements could be made. As soon as the extrudate started to exit the reactor, a timer recorded time of flow. The length of the extrudate was then measured and a resulting velocity could be calculated. The following expression was used to compute the apparent shear rate (Cogswell 1981):

$$\Gamma = \frac{4Q}{\pi R^3} \quad (11)$$

where Γ is the uncorrected shear rate (sec^{-1}), Q is the volumetric flow rate (m^3/s), and R is the reactor radius (m). The Rabinowitsch correction was used to calculate the wall shear rate (Cogswell 1981):

$$\dot{\gamma}^w = \left[\frac{3n+1}{4n} \right] \dot{\Gamma} \quad (12)$$

where n is the power law exponent.

Slippage at the reactor wall was considered negligible. Entrance and exit pressure losses were neglected due to the L/D ratio being greater than 10. Shear stress was calculated from the following expression (Cogswell 1981):

$$\tau_w = \frac{\Delta P D}{4L} \quad (13)$$

where ΔP is the axial pressure drop across the reactor axially (MPa), D is the reactor diameter (m), and L is the reactor length (m). The pressure drop through the reactor was calculated by taking the force measurement from the Instron, dividing it by the cross-sectional area of the reactor and subtracting the pressure in the pressure vessel (1.10 MPa) from it to get ΔP . The power law model was used as this has been shown to be highly correlated to shear rate and shear stress data of gluten doughs (Sharma and Hanna 1992). The equation used to determine the consistency coefficient, m , and the flow index, n , is shown below:

$$\tau = m_0 e^{\left(\frac{-E}{RT}\right)} \dot{\gamma}^n \quad (14)$$

where m_0 is the consistency coefficient pre-exponential ($\text{Pa}\cdot\text{sec}^n$), E is the

viscous activation energy and n is the power law exponent. Nonlinear regression was employed to determine the values of m_0 , E , and n since nonisothermal conditions existed in the tubular reactor. It should be noted that both shear stress, τ and temperature, T , in Eq. (14) varied with axial position in the tubular reactor at a given shear rate. Shear stress was assumed to decrease linearly from inlet to outlet based on Eq. (13) and temperature was nonlinear using experimental data represented in Fig. 3.

Extent of Reaction

A free thiol and total sulfhydryl assay according to the procedures of Chan and Wasserman (1993) was employed to determine disulfide concentration. It is hypothesized that gluten and glutenin crosslink via disulfide bonds (Ewart 1988; Graveland *et al.* 1978) Thus, disulfide bond concentration would give an indication of the extent of reaction.

RESULTS AND DISCUSSION

Rheological Properties

Values for m_0 , the consistency coefficient pre-exponential, n , the flow index, and E , the viscosity activation energy, resulting from nonlinear regression for gluten and glutenin are given in Table 2. The consistency coefficient gives an indication of the viscosity of a fluid. As Table 2 shows, it is evident that the viscosity of glutenin is almost twice the value as for gluten. Glutenin is the high molecular weight fraction of gluten, so the viscosity of this fraction would be expected to be greater in magnitude than that for the composite gluten. The flow index decreases with increasing extent of reaction at a constant moisture content. Our flow index values (n) of less than unity indicate pseudoplastic behavior, which is consistent with observations for cereal doughs (Sharma and Hanna 1992). No literature exists showing the flow index behavior for wheat flour doughs at elevated temperatures or for concentrated gluten doughs at any temperature. Studies on soy dough (Baird and Reed 1989) have shown the flow index to increase with temperature. This would indicate that as temperature increases the material approaches Newtonian behavior. But these studies were conducted on dough that had been allowed to react before extruding, so that viscosity changes were likely the result of temperature effects alone. The polymerization reactions are irreversible except for shear-induced chain scission. Thus, temperature effects would only influence chain mobility, not reactivity. In the present study, gluten and glutenin were reacting (see discussion below) and flowing simultaneously. As gluten polymerizes the flow behavior index should continue to decrease from unity since decreased chain mobility in a reacting polymer network should result in creating a less Newtonian fluid.

TABLE 2.
FLOW INDEX (N), CONSISTENCY COEFFICIENT PRE-EXPONENTIAL
(M_0) AND VISCOSITY ACTIVATION ENERGY (E) FOR WHEAT GLUTEN
AND GLUTENIN DOUGHS AT DIFFERENT MOISTURE CONTENTS (%MC)
AND EXTENT OF REACTION (X)

Sample	X	n	m_0 (Pa-sec ⁿ)	E (kcal/mol)	CV
Gluten:					
25% MC	0.17	0.52	1,100,000	0.62	12%
	0.63	0.45	980,000	0.95	17%
	0.79	0.39	1,200,000	1.20	10%
30% MC	0.20	0.65	530,000	0.62	16%
	0.90	0.55	550,000	0.95	14%
	1.00	0.48	680,000	1.20	17%
Glutenin:					
25% MC	0.18	0.54	2,100,000	0.62	19%
	0.35	0.49	1,500,000	0.95	20%
	0.43	0.38	2,000,000	1.20	15%
30% MC	0.18	0.57	1,300,000	0.62	11%
	0.50	0.50	1,100,000	0.95	10%

Viscosity flow curves for gluten are shown in Fig. 4. Glutenin showed similar behavior. Shear thinning, which is typical of pseudoplastic materials, is evident from the flow curves. In every case viscosity decreases with shear rate and temperature. Viscosity of 25% moisture content gluten at 110C is almost twice the viscosity of 30% moisture gluten at about the same temperature (data not shown). At higher temperatures moisture content has little affect on gluten viscosity. Viscosities for glutenin at different moisture contents show similar trends.

Extent of Reaction

Ewart (1968, 1972, 1979, 1988) has done extensive research in determining the role of disulfide bonds in gluten's viscoelastic properties and structure. He hypothesizes that glutenin is a trifunctional monomer capable of polymerizing via disulfide bond formation. Schofield *et al.* (1983) analyzed the effect of heat on sulfhydryl-disulfide interchange reactions and concluded they were the primary bonds responsible for network formation upon thermosetting. Numerous other researchers (Kaczowski and Mieszko 1980; Beckwith and Wall 1966; Graveland *et al.* 1978) have supported the disulfide bond hypothesis, but recent research (Ledward and Tester 1994) has shown that other reactions might also be important in network and crosslink formations.

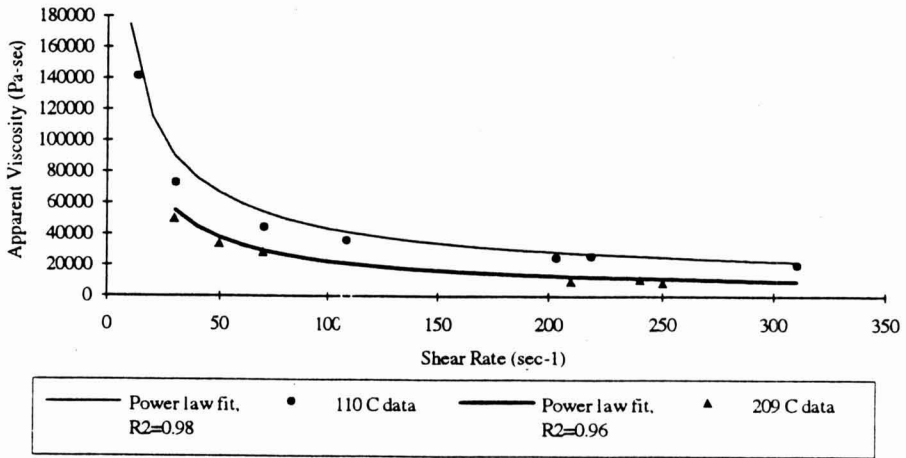


FIG. 4. VISCOSITY FLOW CURVES FOR 25% MOISTURE CONTENT GLUTEN

The extent of reaction, X , at different residence (process) times in the reactor is shown in Fig. 5 for gluten and glutenin. The extent of reaction is defined as the disulfide bond concentration (nmols) determined colorimetrically compared to the disulfide bond concentration at long residence times ($t = \infty$), not the total intrinsic disulfide bonds possible. Similar data were obtained for glutenin with the extent of reaction being lower due to mechanical degradation.

Heat Transfer Simulation Results

In order to obtain solutions for the energy equation in the tubular reactor a number of physical property data were needed. Thermal conductivity, density, and average velocity were determined through a separate set of experiments and are tabulated in Table 3. Rheological properties used in simulations are listed in Table 2. Specific heat was calculated using the following relation (Baird and Reed 1989):

$$c_p = 1.44 + 2.74X_w \quad (15)$$

A thermocouple probe, 1.02 mm in diameter and 30 cm in length, was inserted into the reactor to monitor the material temperature as it flowed through the reactor. The pressure vessel was equipped with a neoprene pressure seal that allowed the probe to be inserted into the reactor without losing pressure. Experimental data was collected and compared to simulation data as shown in Fig. 6. The agreement between data and simulation is acceptable considering the difficulty in maintaining the radial position of the thermocouple on the centerline and to visually determine the axial position with flowing extrudate.

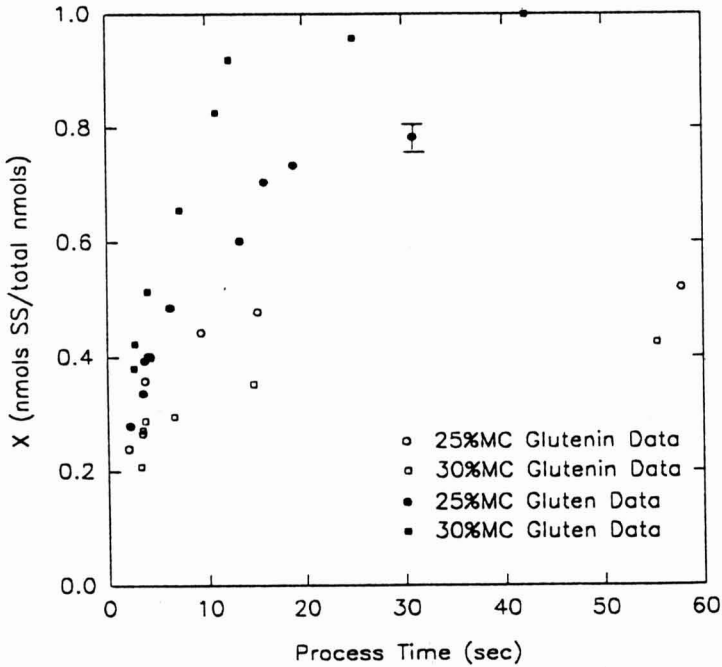


FIG. 5. EXTENT OF REACTION OF GLUTEN AND GLUTENIN AT 209C
 Error bar represents typical standard deviation for all data.

TABLE 3.

PHYSICAL PROPERTY DATA USED FOR SIMULATION ARE DENSITY, ρ , SPECIFIC HEAT, C_p , AND THERMAL CONDUCTIVITY, k

The average velocity in the z-direction is u_{avg} . Initial axial extrudate temperatures, T_0 is the extrudate temperature at $z=0$. The average die wall temperature, $T_{z,avg}$ is the average axial die wall temperature.

Sample	Die $T_{z,avg}$ (C)	T_0 (C)	u_{avg} (cm/s)	ρ (kg/m ³)	c_p (kJ/kgC)	k (W/mC)
Gluten:						
25% MC	110	45	2.94	1150	2.13	0.29
	167	55	2.89	1150	2.13	0.27
	209	62	2.85	1150	2.13	0.25
30% MC	110	45	2.72	1230	2.26	0.32
	167	55	2.67	1230	2.26	0.30
	209	62	2.57	1230	2.26	0.29
Glutenin:						
25% MC	110	45	2.61	1170	2.13	0.36
	167	55	2.57	1170	2.13	0.40
	209	62	2.16	1170	2.13	0.43
30% MC	110	45	3.14	1210	2.26	0.37
	167	55	2.77	1210	2.26	0.44
	209	62	2.77	1210	2.26	0.49

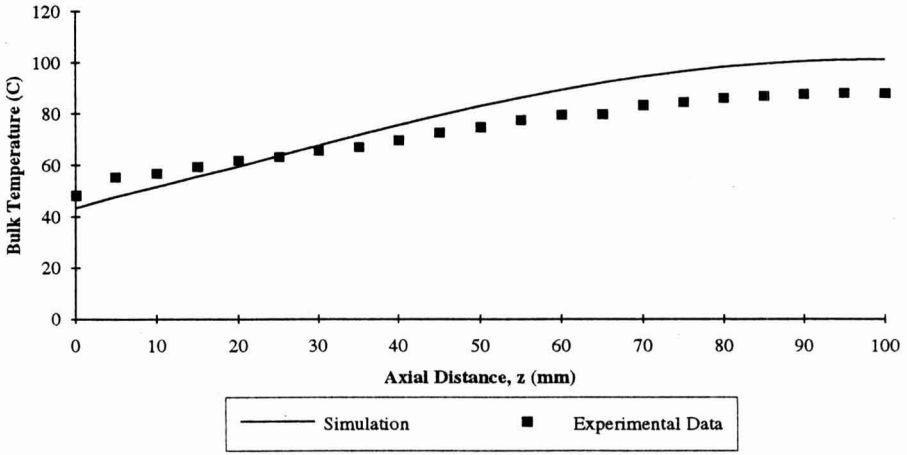


FIG. 6. COMPARISON OF EXPERIMENTAL VERSUS SIMULATED EXTRUDATE

Simulation results of temperature profiles for 25% moisture content gluten as a function of radial distance, r , at different axial locations are shown in Fig. 7. It can be seen that the temperature at the wall, $r=0.8$ mm, increases then decreases as axial distance increases. The simulation shows the expected behavior of increasing centerline temperature as a function of axial position. Likewise the temperature of the extrudate along the wall displays the increasing and decreasing behavior that the reactor wall boundary conditions require.

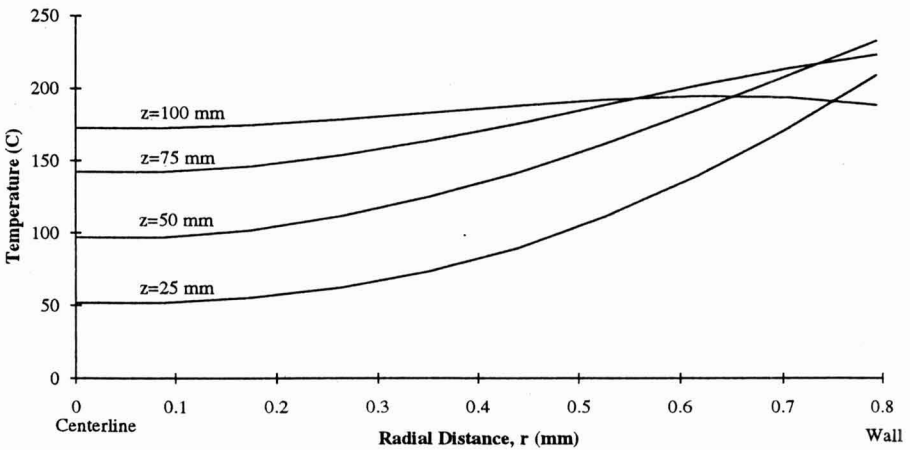


FIG. 7. PREDICTED RADIAL TEMPERATURE DISTRIBUTIONS AT DIFFERENT AXIAL LOCATIONS, Z

Plots of simulated bulk temperatures along the length of the reactor are shown in Fig. 8 for the power law viscosity model and for the inviscid model for 25% moisture content gluten. The bulk temperatures are shown for different reactor wall average temperatures. Plots for 30% moisture content gluten and for 25% and 30% moisture content glutenin are similar in shape and therefore, not shown here. The average axial bulk temperatures for these are shown in Table 3. The inlet temperatures are between 45-63C for the profiles shown in Fig. 8. The viscosity decreases with increasing temperature, i.e., increasing extent of reaction, and the bulk temperatures approach one another at increased axial lengths for the power law and inviscid fluid. The difference between the power law and inviscid fluids is greatest near the entrance where the viscosity is highest due to lowest temperature. This difference reflects the greater viscous dissipation under these conditions. Viscous dissipation increased the bulk temperature up to 16C more than that predicted for the inviscid fluid.

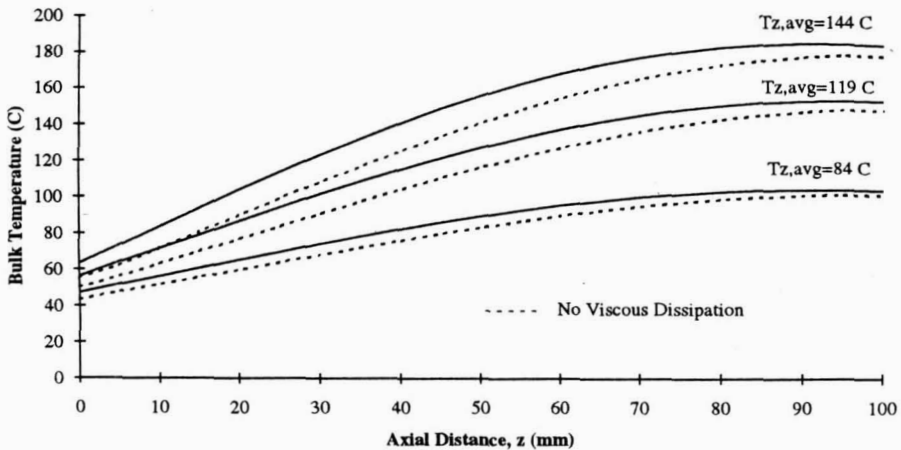


FIG. 8. BULK TEMPERATURES AS A FUNCTION OF AXIAL DISTANCE, Z, FOR (—) POWER LAW VISCOSITY FLUID AND (---) INVISCID FLUID
 $T_{z,avg}$ is the average axial temperature for the extrudate

CONCLUSIONS

The results for the power law viscosity model have been compared to the inviscid fluid model. Viscous dissipation accounted for a bulk temperature rise over the temperature experienced with no viscous effects. This simulation is

applicable for pressure flow in cylindrical coordinates only. Agur and Vlachopoulos (1981) have shown that flow in other geometries results in different viscosity requirements to adequately model heat transfer for the same fluid.

Rheological properties of gluten and glutenin have been determined for a reacting flow phenomena. Shear thinning pseudoplastic behavior was observed. The flow index decreased with increasing temperature which indicated further deviation from Newtonian behavior presumably due to crosslinking and polymerization. The rheological properties were subsequently used in simulation of heat transfer to the molten biopolymer. This research should prove helpful in modeling food extrusion of cereal doughs in general when the physical properties of the feedstock are known.

REFERENCES

- AGUR, E.E. and VLACHOPOULOS, J. 1981. Heat transfer to molten polymer flow in tubes. *J. Appl. Polym. Sci.* 26, 765.
- ANDERSSON, Y. and HEDLUND, B. 1990. Extruded wheat flour: correlation between processing and product quality parameters. *Food Qual. and Pref.* 2, 201.
- BAIRD, D.G. and REED, C.M.: 1989. Transport properties of food doughs. Ch. 7, In *Extrusion Cooking*, AACC, St. Paul, MN.
- BARRES, C., VERGNES, B., TAYEB, S. and VALLE, G. 1990. Transformation of wheat flour by extrusion cooking: influence of screw configuration and operating conditions. *Cereal Chem.* 62, 267.
- BECKWITH, A.C. and WALL, J.S. 1966. Reduction and reoxidation of wheat glutenin. *Biochim. Biophys. Acta* 130, 155.
- BIESENBERGER, J.A. and SEBASTIAN, D.H. 1983. Flow Phenomena. Ch. 5, In *Principles of Polymerization Engineering*. p. 516. John Wiley & Sons, New York.
- BOYAL, R.K. and PHOOLKA, M.K. 1989. Wheat based extruded products. *Indian Miller* 19, 54.
- CHAN, K.Y. and WASSERMAN, B.P. 1993. Direct colorimetric assay of free thiol groups and disulfide bonds in suspensions of solubilized and particulate cereal proteins. *Cereal Chem.* 70, 22.
- COGSWELL, F.N. 1981. *Polymer Melt Rheology*. pp. 25, 135. John Wiley & Sons, New York.
- EWART, J.A.D. 1968. A hypothesis for the structure and rheology of glutenin. *J. Sci. Fd. Agric.* 19, 617.
- EWART, J.A.D. 1972. A modified hypothesis for the structure and rheology of glutelins. *J. Sci. Fd. Agric.* 23, 687.
- EWART, J.A.D. 1979. Glutenin structure. *J. Sci. Fd. Agric.* 30, 482.

- EWART, J.A.D. 1988. Studies on disulfide bonds in glutenin. *Cereal Chem.* 65, 95.
- FRICKE, A.L., CLARK, J.P. and MASON, T.F. 1977. Cooking and drying of fortified cereal foods: extruder design. *Chem. Eng. Prog. Symp. Series 73*, 134.
- GRAVELAND, A., BOSVELD, P. and MARSEILLE, J.P. 1978. Determination of thiol groups and disulfide bonds in wheat flour and dough. *J. Sci. Fd. Agric.* 29, 53.
- HARPER, J.M. 1981. Food Extrusion. Ch. 1, In *Extrusion of Foods*, Vol. 1, p. 1. CRC Press, Boca Raton, FL.
- HARPER, J.M and Harmann, D.V. 1973. Effects of extruder geometry on torque and flow. *Trans. ASAE 16*, 1175.
- KACZKOWSKI, J. and MIELESZKO, T. 1980. The role of disulfide bonds and their localization in wheat protein molecules. *Ann. Tech. Agric.* 29, 377.
- LAWTON, J.W., DAVIS, A.B. and BEHNKE, K.C. 1985. High-temperature, short-time extrusion of wheat gluten and a bran-like fraction. *Cereal Chem.* 62, 267.
- LEDWARD, D.A. and TESTER, R.F. 1994. Molecular transformations of proteinaceous foods during extrusion processing. *Trends in Food Sci. and Tech.* 5(4), 117.
- MORGAN, R.G., SUTER D.A. and SWEAT, V.E. 1978. Design and modeling of a capillary food extruder. *J. Food Process Engineering* 2, 65.
- OSBORNE, T.B. 1907. The proteins of the wheat kernel. *Carnegie Inst., Publ.* No. 84.
- PEZZIN, G. 1962. Rheology of molten polymers. *Materie Plastiche Ed. Elastomeri* (Aug.).
- SCHOFIELD, J.D., BOTTOMLEY, R.C., TIMMS, M.F. and BOOTH, M.R. 1983. The effect of heat on wheat gluten and the involvement of sulphhydryl-disulfide interchange reactions. *J. Cereal Sci.* 1, 241.
- SHARMA, N. and HANNA, M. 1992. Assessing handling properties from flow parameters as influenced by dough water content. *Cer. Foods World* 37, 27.
- TADMOR, Z. and GOGOS, C.G. 1979. *Principles of Polymer Processing*, p. 353, John Wiley & Sons, New York.
- WAGNER, L.L. 1987. Numerical modeling of the cooking extrusion of a biopolymer. Ph.D. Dissertation, Virginia Polytechnic Inst., Blacksburg, VA.

AUTHOR INDEX

- AKKERMAN, J.C., DE GEE, M. and SCHENK, J. On Upscaling a Curd Particle Model to Batch Processing Scale 219
- BABU, R.S. *See* RAGHAVAN, C.V. *et al.*
- BALABAN, M.O. *See* BICHIER, J.G. *et al.*
- BHASKAR, A.R. *See* YU, Z.-R. *et al.*
- BICHIER, J.G., TEIXEIRA, A.A., BALABAN, M.O. and HEYLIGER, T.L. Thermal Process Simulation of Canned Foods Under Mechanical Agitation 17
- BRIGGS, J.L. and STEFFE, J.F. Kinetic Energy Correction Factor of a Herschel-Bulkley Fluid 115
- CAMERON, A.C. *See* TALASILA, P.C.
- CAVALIERI, R.P. *See* STRECKER, T.D. *et al.*
- CHAND, N. *See* RAGHAVAN, C.V. *et al.*
- CHINNAN, M.S. and PARK, H.J. Effect of Plasticizer Level and Temperature on Water Vapor Transmission of Cellulose-Based Edible Films 417
- CHIRUVELLA, R.V. *See* KARWE, M.V. *et al.*
- CLAYTON, J.T. *See* HICSASMAZ, Z.
- CRAPISTE, G.H. *See* RATTI, C.
- DE GEE, M. *See* AKKERMAN, J.C. *et al.*
- DESHPANDE, S.D. *See* THAKOR, N.J. *et al.*
- DURAL, N.H. *See* HUANG, C.-M.
- FALLER, J.F., HUFF, H.E. and HSIEH, F. Evaluation of Die Swell and Volumetric Expansion in Corn Meal Extrudates 287
- FRYER, P.J. *See* ZHANG, L.
- GRABOWSKI, S. and RAMASWAMY, H.S. Characterization of Single Particle Tube-Flow Behavior at Elevated Temperatures 343
- HEYLIGER, T.L. *See* BICHIER, J.G. *et al.*
- HICSASMAZ, Z. and CLAYTON, J.T. Mechanisms Involved in the Infusion of Starch Based Porous Food Materials by Oil Based Liquid Foods 267
- HSIEH, F. *See* FALLER, J.F. *et al.*
- HUANG, C.-M. and DURAL, N.H. Adsorption of Bile Acids on Cereal Type Food Fibers 243
- HUFF, H.E. *See* FALLER, J.F. *et al.*
- JALURIA, Y. *See* KARWE, M.V. *et al.*
- KARWE, M.V., CHIRUVELLA, R.V. and JALURIA, Y. Coordinate System Independence of Shear Rate During Isothermal Single-Screw Extrusion of a Newtonian Fluid 55

- LEE, J.H., SINGH, R.K. and LINEBACK, D.S. Particle Concentration Influence on Liquid Residence Time Distributions in a Model Aseptic Processing System 119
- LINEBACK, D.S. *See* LEE, J.H. *et al.*
- LIU, Y. and ZURITZ, C.A. Mathematical Modeling of Particulate Two-Phase Flow in a Helical Pipe 321
- LIU, Y. and ZURITZ, C.A. Mathematical Modeling of Solid-Liquid Two Phase Tube Flow: An Application to Aseptic Processing 135
- MALLIKARJUNAN, P. and MITTAL, G.S. Prediction of Beef Carcass Chilling Time and Mass Loss 1
- MERSON, R.L. *See* STOFOROS, N.G.
- MILES, J.J. and SWARTZEL, K.R. Evaluation of Continuous Thermal Processes Using Thermocouple Data and Calibrating Reactions 99
- MITTAL, G.S. *See* MALLIKARJUNAN, P.
- MOREIRA, R. PALAU, J. and SUN, X. Simultaneous Heat and Mass Transfer During the Deep Fat Frying of Tortilla Chips 307
- PATIL, R.T. *See* THAKOR, N.J. *et al.*
- PALAU, J. *See* MOREIRA, R. *et al.*
- PARK, H.J. *See* CHINNAN, M.S.
- RAGHAVAN, C.V., CHAND, N., BABU, R.S. and RAO, P.N.S. Modelling the Power Consumption During Sheeting of Doughs for Traditional Indian Foods 397
- RAGHAVARAO, K.S.M.S. *See* RASTOGI, N.K.
- RAMASWAMY, H.S. *See* GRABOWSKI, S.
- RAO, P.N.S. *See* RAGHAVAN, C.V. *et al.*
- RASTOGI, N.K. and RAGHAVARAO, K.S.M.S. Kinetics of Osmotic Dehydration of Coconut 187
- RATTI, C. and CRAPISTE, G.H. Determination of Heat Transfer Coefficients During Drying of Foodstuffs 41
- RIZVI, S.S.H. *See* YU, Z.-R. *et al.*
- SALENGKE, S. and SASTRY, S.K. Residence Time Distribution of Cylindrical Particles in a Curved Section of a Holding Tube: The Effect of Particle Size and Flow Rate 363
- SASTRY, S.K. *See* SALENGKE, S.
- SCHENK, J. *See* AKKERMAN, J.C. *et al.*
- SINGH, R.K. *See* LEE, J.H. *et al.*
- SOKHANSANJ, S. *See* THAKOR, N.J. *et al.*
- STEFFE, J.F. *See* BRIGGS, J.L.
- STOFOROS, N.G. and MERSON, R.L. A Solution to the Equations Governing Heat Transfer in Agitating Liquid/Particulate Canned Foods 165
- STRECKER, T.D., CAVALIERI, R.P. and ZOLLARS, R. Heat Transfer to and Transport Properties of Wheat Gluten in a Tubular Reactor 431

- SUN, X. *See* MOREIRA, R. *et al.*
- SWARTZEL, K.R. *See* MILES, J.J.
- TALASILA, P.C. and CAMERON, A.C. Modeling Frequency Distribution of Steady-State O₂ Partial Pressures in Modified-Atmosphere Packages 199
- TEIXEIRA, A.A. *See* BICHIER, J.G. *et al.*
- THAKOR, N.J., SOKHANSANJ, S., PATIL, R.T. and DESHPANDE, S.D. Moisture Sorption and Volumetric Changes of Canola During Hydrothermal Processing 233
- WELLS, J.H. *See* ZHAO, Y.
- YU, Z.-R., BHASKAR, A.R. and RIZVI, S.S.H. Modeling of Triglyceride Distribution and Yield of Anhydrous Milk Fat in a Continuous Supercritical Carbon Dioxide Extraction System 71
- ZHANG, L. and FRYER, P.J. A Comparison of Alternative Formulations for the Prediction of Electrical Heating Rates of Solid-Liquid Food Materials 85
- ZHAO, Y. and WELLS, J.H. Method for Measuring CO₂ Absorption in CO₂ and N₂ Packaged Fresh Meat 383
- ZOLLARS, R. *See* STRECKER, T.D. *et al.*
- ZURITZ, C.A. *See* LIU, Y.

SUBJECT INDEX

- Adsorption of bile acids, 243
Agitating liquid/particulate foods, 165
Aseptic processing system, 119, 135

Beef, 1
Bile acids, 243

Canned foods, 17
Canola, 233
Carcass chilling, 1
Cellulose-based edible film, 417
Chilling, 1
CO₂ absorption by fresh meat, 383
Coconut, 187
Corn meal extrudates, 287
Curd particles, 219
Cylindrical shaped particles, 363

Deep fat frying of Tortilla chips, 307
Die swell in extrusion, 287
Drainage of curd, 219
Drying, 41

Edible film, 417
Electrical heating, 86
Electrical heating rates, 85
Equivalent Point Method, 100
Extraction, 71
Extruder die design, 293
Extrusion, 55

Flow in a helical pipe, 321
Frying, 307

Heat and mass transfer in frying, 307
Heat transfer coefficient, 41
Heat transfer in wheat gluten, 431
Helical pipe, 321
Herschel-Bulkley fluid, 115

Infusion of oil into foods, 267
Isothermal extrusion, 55

Kinetic energy corrections, 115
Kinetics of osmotic drying, 187

Magnus lift force, 142
Mass loss in beef chilling, 1
Meat packaging, 383
Mechanical agitation, 17
Modified atmosphere packaging, 199, 383
Moisture sorption in canola, 233

Newtonian fluid extrusion, 55

Oil infusion, 267
Osmotic dehydration of coconut, 187

Particulate two-phase flow, 321
Plasticizer level in edible film, 417
Potato, drying, 44
Power consumption in dough sheeting, 397

Residence time distribution, 119, 363

Saffman lift force, 142
Shear rate in extrusion, 55

Single particle tube-flow behavior,
343
Single-screw extrusion, 55
Solid-Liquid tube flow, 135
Supercritical CO₂ extraction, 71
Terzaghi theory, 221
Thermal process calculations, 17

Thermal process evaluation, 99
Transport properties of wheat
gluten, 431
Triglycerides in milk fat, 71
Water vapor transmission of edible
film, 417
Wheat gluten, 431

F N P PUBLICATIONS IN FOOD SCIENCE AND NUTRITION

Journals

JOURNAL OF FOOD LIPIDS, F. Shahidi
JOURNAL OF RAPID METHODS AND AUTOMATION IN MICROBIOLOGY,
D.Y.C. Fung and M.C. Goldschmidt
JOURNAL OF MUSCLE FOODS, N.G. Marriott, G.J. Flick, Jr. and J.R. Claus
JOURNAL OF SENSORY STUDIES, M.C. Gacula, Jr.
JOURNAL OF FOODSERVICE SYSTEMS, C.A. Sawyer
JOURNAL OF FOOD BIOCHEMISTRY, J.R. Whitaker, N.F. Haard and H. Swaisgood
JOURNAL OF FOOD PROCESS ENGINEERING, D.R. Heldman and R.P. Singh
JOURNAL OF FOOD PROCESSING AND PRESERVATION, D.B. Lund
JOURNAL OF FOOD QUALITY, J.J. Powers
JOURNAL OF FOOD SAFETY, T.J. Montville
JOURNAL OF TEXTURE STUDIES, M.C. Bourne and M.A. Rao

Books

OF MICROBES AND MOLECULES: FOOD TECHNOLOGY AT M.I.T., S.A. Goldblith
MEAT PRESERVATION: PREVENTING LOSSES AND ASSURING SAFETY,
R.G. Cassens
S.C. PRESCOTT, M.I.T. DEAN AND PIONEER FOOD TECHNOLOGIST,
S.A. Goldblith
FOOD CONCEPTS AND PRODUCTS: JUST-IN-TIME DEVELOPMENT, H.R. Moskowitz
MICROWAVE FOODS: NEW PRODUCT DEVELOPMENT, R.V. Decareau
DESIGN AND ANALYSIS OF SENSORY OPTIMIZATION, M.C. Gacula, Jr.
NUTRIENT ADDITIONS TO FOOD, J.C. Bauernfeind and P.A. Lachance
NITRITE-CURED MEAT, R.G. Cassens
POTENTIAL FOR NUTRITIONAL MODULATION OF AGING, D.K. Ingram *et al.*
CONTROLLED/MODIFIED ATMOSPHERE/VACUUM PACKAGING OF
FOODS, A.L. Brody
NUTRITIONAL STATUS ASSESSMENT OF THE INDIVIDUAL, G.E. Livingston
QUALITY ASSURANCE OF FOODS, J.E. Stauffer
THE SCIENCE OF MEAT AND MEAT PRODUCTS, 3RD ED., J.F. Price and
B.S. Schweigert
HANDBOOK OF FOOD COLORANT PATENTS, F.J. Francis
ROLE OF CHEMISTRY IN PROCESSED FOODS, O.R. Fennema, *et al.*
NEW DIRECTIONS FOR PRODUCT TESTING OF FOODS, H.R. Moskowitz
PRODUCT TESTING AND SENSORY EVALUATION OF FOODS, H.R. Moskowitz
ENVIRONMENTAL ASPECTS OF CANCER: ROLE OF FOODS, E.L. Wynder *et al.*
FOOD PRODUCT DEVELOPMENT AND DIETARY GUIDELINES, G.E. Livingston, R.J.
Moshy, and C.M. Chang
SHELF-LIFE DATING OF FOODS, T.P. Labuza
ANTINUTRIENTS AND NATURAL TOXICANTS IN FOOD, R.L. Ory
UTILIZATION OF PROTEIN RESOURCES, D.W. Stanley *et al.*
VITAMIN B₆: METABOLISM AND ROLE IN GROWTH, G.P. Tryfiates
POSTHARVEST BIOLOGY AND BIOTECHNOLOGY, H.O. Hultin and M. Milner

Newsletters

MICROWAVES AND FOOD, R.V. Decareau
FOOD INDUSTRY REPORT, G.C. Melson
FOOD, NUTRITION AND HEALTH, P.A. Lachance and M.C. Fisher
FOOD PACKAGING AND LABELING, S. Sacharow



Statement of Ownership, Management, and Circulation
(Required by 39 U.S.C. 3685)

1. Publication Title: **Journal of Food Process Engineering**

2. Publication No.:

0	1	4	5	7	8	8	7	6
---	---	---	---	---	---	---	---	---

3. Filing Date: **October 1, 1995**

4. Issue Frequency: **Quarterly**

5. No. of Issues Published Annually: **4**

6. Annual Subscription Price: **\$142.00**

7. Complete Mailing Address of Known Office of Publication (Street, City, County, State, and ZIP+4) (Not Printer):
**6527 Main St. POB 374
 Trumbull, Fairfield, Connecticut 06611-0374**

8. Complete Mailing Address of Headquarters or General Business Office of Publisher (Not Printer):
**6527 Main St. POB 374
 Trumbull, Connecticut 06611-0374**

9. Full Name and Complete Mailing Address of Publisher, Editor, and Managing Editor (Do Not Leave Blank)

Publsher (Name and Complete Mailing Address):
 John J. O'Neill
 6527 Main Street, POB 374
 Trumbull, CT 06611

Editor (Name and Complete Mailing Address):
 Dr. Dennis K. Heldman
 253 Agricultural Engineering, Missouri University
 Columbia, MO 65211

Managing Editor (Name and Complete Mailing Address):
 Dr. R. Paul Singh
 Dept. of Agricultural Engineering
 University of California, Davis, CA 95616

10. Owner (If owned by a corporation, its name and address must be stated and also immediately thereunder the names and addresses of stockholders owning or holding 1 percent or more of the total amount of stock. If not owned by a corporation, the names and addresses of the individual owner must be given. If owned by a partnership or other unincorporated firm, its name and address as well as that of each individual must be given. If the publication is published by a nonprofit organization, its name and address must be stated.) (Do Not Leave Blank.)

Full Name	Complete Mailing Address
Food & Nutrition Press, Inc	6527 Main St. POB 374, Trumbull, CT 06611
John J. O'Neill	53 Stonehouse Road, Trumbull, CT 06611
Michael J. Tully	3 N. Slope, Union Gap, Clinton, NJ 08809
Kathryn & Christopher Ziko	8 Maria Alicia Dr., Huntington, CT 06484
John J. O'Neill, Jr.	115 Maureen St., Stratford, CT 06497

11. Known Bondholders, Mortgagees, and Other Security Holders Owning or Holding 1 Percent or More of Total Amount of Bonds, Mortgages, or Other Securities. If none, check here None

Full Name	Complete Mailing Address

12. For completion by nonprofit organizations authorized to mail at special rates. The purpose, function, and nonprofit status of the organization and the exempt status for federal income tax purposes. (Check one) Has Not Changed During Preceding 12 Months Has Changed During Preceding 12 Months (If changed, publisher must submit explanation of change with this statement)

13. Publication Name: **Journal of Food Process Engineering**

14. Issue Date for Circulation Data Below: **12/14/94, 4/11/95, 7/11/95, 9/19/95**

15. Extent and Nature of Circulation	Average No. Copies Each Issue During Preceding 12 Months	Actual No. Copies of Single Issue Published Nearest to Filing Date
a. Total No. Copies (Net Press Run)	400	400
b. Paid and/or Requested Circulation (1) Sales Through Dealers and Carriers, Street Vendors, and Counter Sales (Net amount)	0	0
(2) Paid or Requested Mail Subscriptions (Include Advertisers' Proof Copies/Exchange Copies)	244	249
c. Total Paid and/or Requested Circulation (Sum of 15b(1) and 15b(2))	244	249
d. Free Distribution by Mail (Borrowers, Complimentary, and Other Free)	53	54
e. Free Distribution Outside the Mail (Carriers or Other Means)	0	0
f. Total Free Distribution (Sum of 15d and 15e)	53	54
g. Total Distribution (Sum of 15c and 15f)	297	303
h. Copies Not Distributed (1) Office Use, Leftovers, Spoiled (2) Return from News Agents	103	97
i. Total (Sum of 15g, 15h(1), and 15h(2))	400	400
Percent Paid and/or Requested Circulation (15c / 15g x 100)	82%	82%

16. This Statement of Ownership will be printed in the Vol. 18, No. 6 issue of the publication. Check box if not required to publish.

17. Signature and Title of Editor, Publisher, Business Manager, or Owner: **Kathryn Ziko, Owner** Date: **October 1, 1995**

I certify that all information furnished on this form is true and complete. I understand that anyone who furnishes false or misleading information on this form or who omits material or information requested on the form may be subject to criminal sanctions (including fines and imprisonment) and/or civil sanctions (including multiple damages and civil penalties).

GUIDE FOR AUTHORS

Typewritten manuscripts in triplicate should be submitted to the editorial office. The typing should be double-spaced throughout with one-inch margins on all sides.

Page one should contain: the title, which should be concise and informative; the complete name(s) of the author(s); affiliation of the author(s); a running title of 40 characters or less; and the name and mail address to whom correspondence should be sent.

Page two should contain an abstract of not more than 150 words. This abstract should be intelligible by itself.

The main text should begin on page three and will ordinarily have the following arrangement:

Introduction: This should be brief and state the reason for the work in relation to the field. It should indicate what new contribution is made by the work described.

Materials and Methods: Enough information should be provided to allow other investigators to repeat the work. Avoid repeating the details of procedures that have already been published elsewhere.

Results: The results should be presented as concisely as possible. Do not use tables and figures for presentation of the same data.

Discussion: The discussion section should be used for the interpretation of results. The results should not be repeated.

In some cases it might be desirable to combine results and discussion sections.

References: References should be given in the text by the surname of the authors and the year. *Et al.* should be used in the text when there are more than two authors. All authors should be given in the Reference section. In the Reference section the references should be listed alphabetically. See below for style to be used.

RIZVI, S.S.H. 1986. Thermodynamic properties of foods in dehydration. In *Engineering Properties of Foods*, (M.A. Rao and S.S.H. Rizvi, eds.) pp. 133-214, Marcel Dekker, New York.

MICHAELS, S.L. 1989. Crossflow microfilters ins and outs. *Chem. Eng.* 96, 84-91.

LABUZA, T.P. 1982. *Shelf-Life Dating of Foods*, pp. 66-120, Food & Nutrition Press, Trumbull, CT.

Journal abbreviations should follow those used in *Chemical Abstracts*. Responsibility for the accuracy of citations rests entirely with the author(s). References to papers in press should indicate the name of the journal and should only be used for papers that have been accepted for publication. Submitted papers should be referred to by such terms as "unpublished observations" or "private communication." However, these last should be used only when absolutely necessary.

Tables should be numbered consecutively with Arabic numerals. The title of the table should appear as below:

TABLE 1.

ACTIVITY OF POTATO ACYL-HYDROLASES ON NEUTRAL LIPIDS, GALACTOLIPIDS AND PHOSPHOLIPIDS

Description of experimental work or explanation of symbols should go below the table proper. Type tables neatly and correctly as tables are considered art and are not typeset. Single-space tables.

Figures should be listed in order in the text using Arabic numbers. Figure legends should be typed on a separate page. Figures and tables should be intelligible without reference to the text. Authors should indicate where the tables and figures should be placed in the text. Photographs must be supplied as glossy black and white prints. Line diagrams should be drawn with black waterproof ink on white paper or board. The lettering should be of such a size that it is easily legible after reduction. Each diagram and photograph should be clearly labeled on the reverse side with the name(s) of author(s), and title of paper. When not obvious, each photograph and diagram should be labeled on the back to show the top of the photograph or diagram.

Acknowledgments: Acknowledgments should be listed on a separate page.

Short notes will be published where the information is deemed sufficiently important to warrant rapid publication. The format for short papers may be similar to that for regular papers but more concisely written. Short notes may be of a less general nature and written principally for specialists in the particular area with which the manuscript is dealing. Manuscripts that do not meet the requirement of importance and necessity for rapid publication will, after notification of the author(s), be treated as regular papers. Regular papers may be very short.

Standard nomenclature as used in the engineering literature should be followed. Avoid laboratory jargon. If abbreviations or trade names are used, define the material or compound the first time that it is mentioned.

EDITORIAL OFFICE: DR. D.R. HELDMAN, COEDITOR, *Journal of Food Process Engineering*, Food Science/Engineering Unit, University of Missouri-Columbia, 235 Agricultural/Engineering Bldg., Columbia, MO 65211 USA; or DR. R.P. SINGH, COEDITOR, *Journal of Food Process Engineering*, University of California, Davis, Department of Agricultural Engineering, Davis, CA 95616 USA.

CONTENTS

Characterization of Single Particle Tube-Flow Behavior at Elevated Temperatures S. GRABOWSKI and H.S. RAMASWAMY	343
Residence Time Distribution of Cylindrical Particles in a Curved Section of a Holding Tube: The Effect of Particle Size and Flow Rate S. SALENGKE and S.K. SASTRY	363
Method for Measuring CO ₂ Absorption in CO ₂ and N ₂ Packaged Fresh Meat Y. ZHAO and J.H. WELLS	383
Modeling the Power Consumption During Sheetting of Doughs for Traditional Indian Foods C.V. RAGHAVAN, N. CHAND, R.S. BABU and P.N.S. RAO	397
Effect of Plasticizer Level and Temperature on Water Vapor Transmission of Cellulose-Based Edible Films M.S. CHINNAN and H.J. PARK	417
Heat Transfer to and Transport Properties of Wheat Gluten in a Tubular Reactor T.D. STRECKER, R.P. CAVALIERI and R. ZOLLARS . . .	431
Author Index	449
Subject Index	45

